CANADA
DEPARTMENT OF ENERGY, MINES AND RESOURCES
OBSERVATORIES BRANCH

PUBLICATIONS

OF THE

Dominion Observatory

OTTAWA

Volume XXXVII

THE QUEEN'S PRINTER
OTTAWA, 1970

TABLE OF CONTENTS

		PAGE
No. 1	A Temperature Control System for the Canadian Pendulum Apparatus, by H.D. Valliant, I.R. Grant and J.W. Geuer	1
No. 2	An Electronic System for Measuring Pendulum Periods, by Herbert D. Valliant	11
No. 3	Record of Observations at Victoria Magnetic Observatory, 1966, by D.R. Auld and P.H. Andersen	21
No. 4	Polynomial Estimation of Certain Geomagnetic Quantities, Applied to a Survey of Scandinavia, by G.V. Haines	75
No. 5	A Three-Component Aeromagnetic Survey of the Nordic Countries and the Greenland Sea, by W. Hannaford and G.V. Haines	113
No. 6	The Effect of the Solar Cycle on Magnetic Activity at High Latitudes, by E.I. Loomer and G. Jansen van Beek	165
No. 7	A Symposium on Processes in the Focal Region, by Keichi Kasahara and Anne E. Stevens, *Editors*	181
No. 8	Record of Observations at Fort Churchill Magnetic Variometer Station, 1964-1965, by G. Jansen van Beek	237
No. 9	Record of Observations at Great Whale Magnetic Observatory, 1967, by E.I. Loomer	335
No. 10	Record of Observations at Agincourt Magnetic Observatory, 1967, by W.R. Darker and D.L. McKeown	411

CONTENTS

Page

Foreword 183

Focal Processes, and Various Approaches to their Mechanism by K. Kasahara, *Earthquake Research Institute, University of Tokyo, Japan* 187

Study of Earthquake Sources from the Seismic Spectrum by K. Aki, *Department of Geology and Geophysics, Massachusetts Institute of Technology, Cambridge, Mass., U.S.A.* 190

The Stress State in Earthquake Foci and the Elastic Stress Field of the Earth by L. M. Balakina, L. A. Misharina, E. I. Shirokova and A. V. Vvedenskaya, *Institute of Earth Physics, Academy of Sciences, Moscow, U.S.S.R.* 194

Dislocation Field Dynamics as an Approach to the Physics of Earthquake Processes by R. Teisseyre, *Institute of Geophysics, Polish Academy of Sciences, Warsaw, Poland* 199

Theoretical Fault Models by M. A. Chinnery, *Department of Geological Sciences, Brown University, Providence, R. I., U.S.A.* 211

A Physical Basis for Earthquake Statistics by L. Knopoff and C. –Y. King, *Institute of Geophysics and Planetary Physics, University of California, Los Angeles, California, U.S.A.*, and R. Burridge, *Department of Applied Mathematics and Theoretical Physics, Cambridge University, Cambridge, England* 224

Earthquake Mechanisms (abstract only) by D. T. Griggs, *Institute of Geophysics and Planetary Physics, University of California, Los Angeles, California, U.S.A.* 235

FOREWORD

A Symposium on Processes in the Focal Region was held at Zürich, Switzerland, October 5, 1967, during the Fourteenth General Assembly of the International Union of Geodesy and Geophysics. The idea for this Symposium originated with the thirteenth Council of the International Association of Seismology and Physics of the Earth's Interior (IASPEI). As President of the Association, Dr. J. H. Hodgson of Canada circulated letters to the council members seeking their advice on the form of future meetings and on possible subjects for symposia. The suggestion for the present topic was made by Dr. R. Teisseyre of Poland; some Canadian geophysicists made similar suggestions. With the concurrence of the Bureau of the Association, Dr. Hodgson included it among the IASPEI Symposia at Zürich, and asked one of the editors (Kasahara) to convene it.

The proposed subject might remind one of the so-called fault-plane work, a name familiar to all seismologists. However, Dr. Hodgson did not intend this field to be covered by the Symposium, although the concepts of faulting and dislocations might be included. During the past twenty or more years, outstanding progress has been achieved in seismology in clarifying our knowledge of seismic origins. However, it should be noted that the fault-plane work, in the traditional sense, is mainly concerned with seismic disturbances on and outside a 'focal sphere', which represents the origin in the first-order approximation.

Many other approaches must be introduced to study the nature of an earthquake origin in more detail, that is, to clarify what really occurs inside the focal region. For example, new methods for analyzing teleseismic signals have been developed since the late 1950's and are used to derive more information about source mechanisms, often called source parameters. We also note the studies on surface faulting, which have progressed in the past ten years. In addition, the physical theory of dislocations has been introduced to seismology and this theory has supported theoretical progress in the above-stated research. The coupling of earthquake seismology to physics, or to material science, is more evident in studies of rock mechanics which are being developed to clarify rupturing processes at a source. From all this evidence, it may safely be said that the study on the nature of earthquakes has entered its second phase. Thus the proposal for the present Symposium was quite timely.

Processes in the focal region are typical interfield problems as are many other problems in solid-earth science. The Symposium's subject is closely related to one of the ultimate problems in seismology, the causes of earthquakes. This problem concerns so many branches in the earth sciences that intimate cooperation is urgently needed for further progress.

Several major topics were chosen for the Symposium on the basis of these considerations, and they were discussed successfully by seven speakers, as well as by the participants. Unfortunately, Prof. A. Ben-Menahem was absent and his paper on "A Global Study of Deep Shocks" was not read nor available for publication. Dr. A. V. Vvedenskaya and her collaborators were also unable to attend, but, fortunately, their paper was presented by Prof. Yu. V. Riznichenko.

This volume presents six of the seven Symposium papers, in the same order in which they were read. Their purpose, of course, is not to provide final answers to the subjects, but rather to review the current status of their respective fields and to survey problems for which solutions are urgently needed to further progress in these fields. (We regret that Dr. Griggs' paper was not available for publication. However, we have reprinted his abstract as it appeared in the program of the Symposium.)

The editors are grateful to Dr. J. H. Hodgson, Director of the Observatories Branch, Department of Energy, Mines and Resources, Canada, and to Dr. K. Whitham, Chief of the Division of Seismology, Observatories Branch, for kindly offering the *Publications of the Dominion Observatory* for the present Symposium.

Keichi Kasahara and Anne Stevens, Editors

FOCAL PROCESSES, AND VARIOUS APPROACHES TO THEIR MECHANISM

Keichi Kasahara

Earthquake Research Institute
University of Tokyo
Japan

ABSTRACT: Wave radiation due to an abrupt change in the physical state of a certain earth volume – this is widely accepted as a concept of earthquake occurrence. A direct approach to focal processes is, therefore, to specify the 'state' as a function of various physical quantities and clarify the mode of its change in time and space with respect to each of the quantities. To further understand the processes, however, we need to know its background well, e.g., mechanism of trigger and rupture, mutual interaction with adjacent space, tectonic history, and source of energy. Co-operation of various branches in geoscience is urgently needed for successful approaches to the mechanism of focal processes.

Problems for future progress in this research field are discussed from this point of view as introductory remarks to the following papers in this Symposium.

RÉSUMÉ: Il est généralement admis que les tremblements de terre peuvent être dus à la propagation d'ondes causées par un changement brusque de l'état physique d'une certaine masse de la terre. Une manière directe d'aborder les phénomènes focaux consiste donc à définir cet 'état' comme une fonction de diverses quantités physiques, et à éclaircir ses variations dans le temps et dans l'espace en fonction de chacune de ces variables. Cependant, afin de mieux comprendre ce processus, il importe de bien connaître ses données de base, par exemple le mécanisme du déclenchement et de la rupture, l'interaction avec les masses avoisinantes, l'histoire tectonique et la source d'énergie. La coopération entre les diverses branches des sciences de la terre devient impérieusement nécessaire au succès de l'étude du mécanisme des phénomènes au foyer.

Enfin, en guise d'introduction aux travaux qui seront présentés au cours de cette conférence, l'auteur procède à un exposé des problèmes rattachés au progrès dans ce domaine de recherche.

The function of an earthquake source is often compared to that of a machine which accumulates energy from a deeper source to convert it instantaneously into kinetic energy, or seismic disturbances. Figure 1 illustrates schematically the structure of the earthquake machine.

An earthquake field, which is located at the centre of the figure, corresponds to the principal part of the machine. Let S denote its physical state at time t. Then, an earthquake occurrence may be represented by an abrupt change of S into S'. From this point of view, correct understanding of the transition, $S \rightarrow S'$, must be the cardinal point in the focal process studies. In principle, the transition is to be specified with respect to all of the physical quantities at every part of the field. Some of them will be quantities of the primary order, such as pressure σ, and temperature T. And some others may be second-order quantities, such as deviatoric pressure $\Delta\sigma$, and dissipation factor Q. Practically, however, we may omit from our discussion those quantities that are insensitively related to the present process. Studies to determine which of them are essential are urgently needed.

The earthquake field is subject to energy supplied by a deeper source, resulting in the accumulation of potential energy until it reaches the critical state. It is easy to imagine that the mode of energy supply is not that of action at a distance but that of action in a medium, so that we need to know about the structure with respect to density ρ, elasticity c, nonelasticity η, electrical properties r, etc., as well as to materials, if possible. Also, we need to understand the background of the accumulation process, that is to say, mutual interaction with the neighbours and tectonic history with respect to space and time.

The physical state of the field is checked always by the rupture criterion, which is dependent on the external (or internal) triggering perturbation. These conditions will be affected by the rupture itself, to control the earthquake sequences and other events in the postseismic stage.

The time relation of these processes and events may be conveniently understood by introducing three stages in a seismic cycle. Figure 2 illustrates schematically the states occurring in the three neighbouring fields at various phases.

The preseismic stage is characterized by accumulation of potential energy as stated previously. Energy source(s), accumulation mechanism including time rate and spatial distribution, and associated changes in the physical state must be clarified for an understanding of the mechanism of the preseismic stage.

Next is the principal stage, or the stage of rupture, which is characterized by conversion of potential energy into kinetic energy. There are a number of problems related to this stage, but the triggering mechanism, including the influences of faults from old catastrophes; the rupture mechanism, including type, geometry, development (velocity of rupture propagation), wave radiation, and the stopping mechanism of the rupture; and changes in state and properties at the focal region are considered essential.

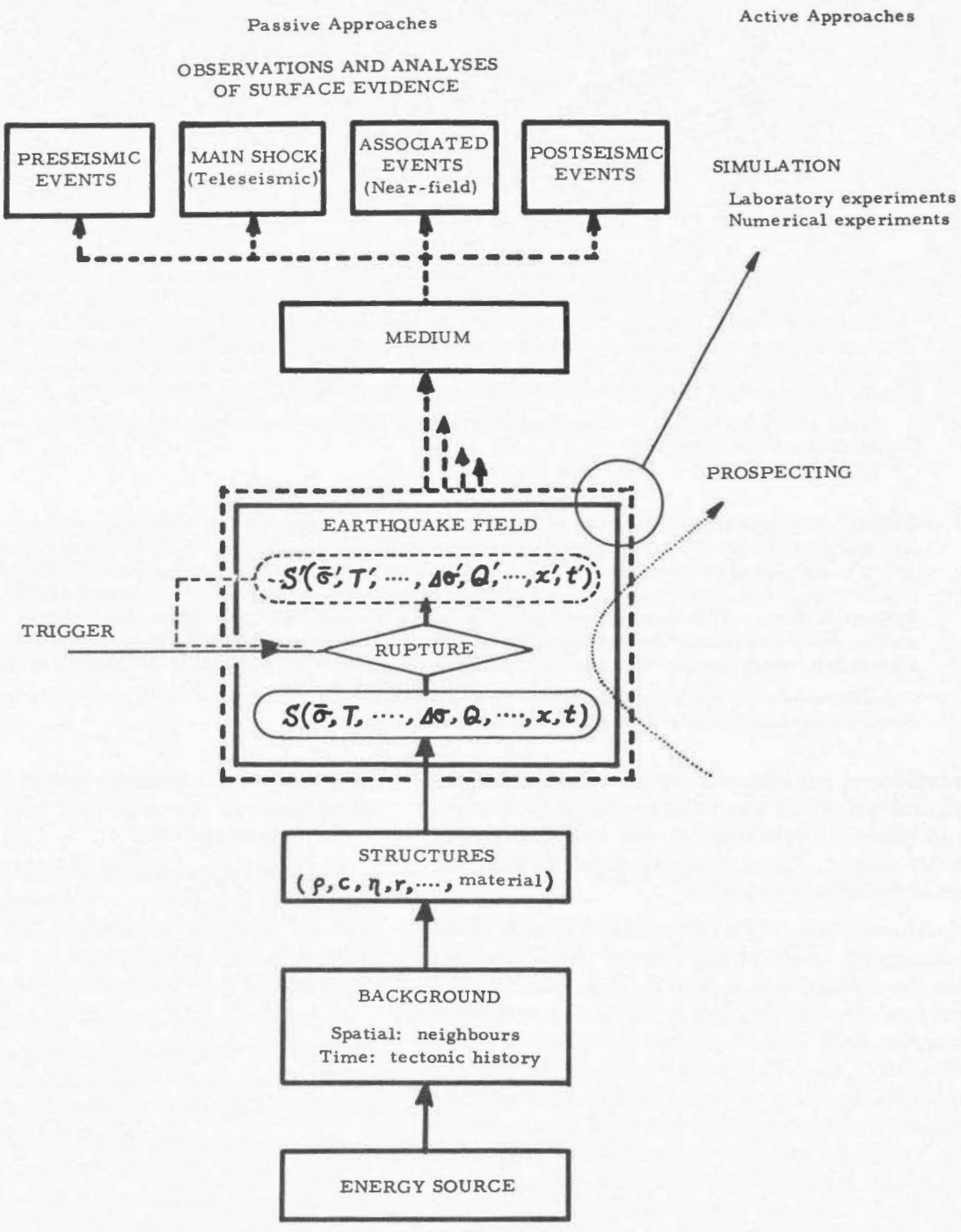

Figure 1. An earthquake machine and the associated phenomena.

The transition to a new equilibrium will occur in the postseismic stage. Mechanisms of aftershocks and other postseismic events, recovery of the changed state and properties, and hysteresis are examples of interesting problems. This is the last of the three stages, but this does not mean the end of the seismic event. Tectonic evidence and historical records of earthquakes in some regions seem to suggest the cyclic repetition of seismic activity. In this sense, the postseismic state itself is the very beginning of the preseismic stage in the next cycle.

Balance and partition of energy are the most fundamental problems in the physics of focal processes. Efficiency of energy conversion, energy loss in the various stages, coupling to the neighbours and to the other crustal phenomena are examples of the problems. The relation of seismic events to tectonic history is another basic problem.

Rupture and other sorts of changes in the field's state are transmitted through the medium to the surface, providing us with valuable sources of information about the focal processes. There have been, and are being, proposed many useful

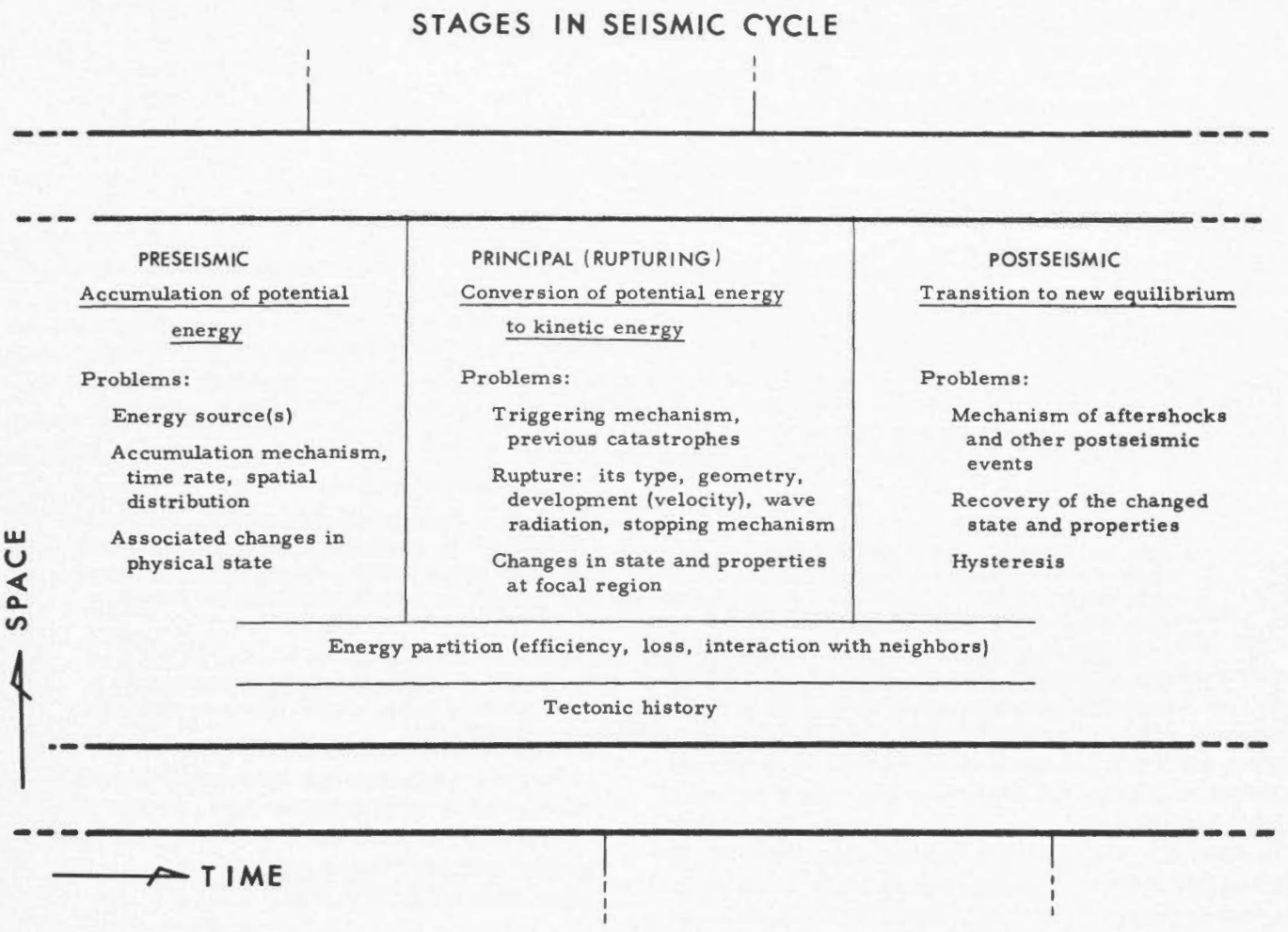

Figure 2. Three stages in a seismic cycle and various problems related to them.

techniques for this purpose, in which the surface evidence is corrected for propagation effects to derive what happened at the source. We shall see many examples of them in the following reviews.

From a logical point of view, the foregoing analyses may be placed in the group of passive approaches. In contrast, another type of research technique, say the active approach, may also be useful. Rock mechanics experiments on ruptures are a good example. If a laboratory experiment is planned carefully in the future, we shall be able to simulate the possible physical conditions in the focal region sufficiently well that we may test some of the fundamental processes of ruptures at a given depth under the controlled conditions. In this respect, numerical experiments on a computer may be added to the present group, although their development is rather a future problem. Geophysical prospecting with controlled signal sources has not often been planned for the present purpose, but the author would like to point it out as another example. It does not mean that we should use artificial energy sources, necessarily. Earthquakes occurring in and around the region of interest will provide us with convenient signal sources to study the state and properties in the focal region. S.Suyehiro, for instance, studied wave propagation through the Matsushiro swarm area, central Japan, and discovered the outstanding increase of wave dissipation in the area (high-frequency *P*-waves) associated with the swarm activity.

Perhaps the above discussion has been concerned too much with shallow (dèstructive) earthquakes. Processes at intermediate and deep foci must, of course, be equally interesting. In the case of these earthquakes, however, we naturally miss some sources of information, particularly near-field evidence. It is still not clear whether the processes at a deep focus are quite similar to those at shallower depths. This question must be answered before a successful approach to the mechanism at great depth can be made.

STUDY OF EARTHQUAKE SOURCES FROM THE SEISMIC SPECTRUM

Keiiti Aki

Department of Geology and Geophysics
Massachusetts Institute of Technology
Cambridge, Mass., U.S.A.

ABSTRACT: Earthquake sources have been primarily studied at two extreme frequencies, zero-frequency (static deformation) and infinite-frequency (first motions). Recent developments in long-period seismology have made it possible to use the spectral density of surface waves at long period for estimating the source parameters. We have now several examples in which all these three methods give consistent results with the assumption that an earthquake is a moving dislocation.

In principle, it should be possible to use the entire spectrum range for obtaining the source parameters. In practice, however, it is difficult to eliminate the effect of propagation media from the spectrum at short periods to isolate the source function. One way of avoiding this difficulty is to measure the spectrum near the source. Problems involved in such a study are discussed, taking the Parkfield earthquake as an example.

RÉSUMÉ: L'étude des sources de tremblements de terre a principalement porté sur deux fréquences extrêmes, c'est-à-dire nulle (déformation statique) et infinie (premiers mouvements). Les progrès récents de la séismologie à longue période ont rendu possible l'utilisation de la densité spectrale des ondes superficielles à longue période pour estimer les paramètres de la source. Plusieurs exemples montrent que ces trois méthodes donnent des résultats compatibles avec l'hypothèse qu'un séisme est une dislocation en mouvement.

Il devrait être possible, en principe, d'utiliser le spectre entier pour obtenir les paramètres de la source. En fait, il est difficile d'éliminer l'effet du milieu de propagation du spectre aux courtes périodes pour isoler le comportement de la source. On peut contourner cette difficulté en mesurant le spectre près de la source. L'auteur discute des problèmes que pose une telle étude, utilisant comme exemple le tremblement de terre de Parkfield.

Introduction

Earthquake sources have been primarily studied at two extreme seismic frequencies, zero-frequency (static deformation) and infinite-frequency (first motions). Recent developments in long-period seismology have made it possible to use the spectral density of surface waves at long periods for estimating the source parameters. We have now several examples, in which all three methods give consistent results with the assumption that an earthquake is a moving dislocation (Aki, 1966; Brune and Allen, 1967).

In principle, it should be possible to use the entire spectrum range for obtaining the source parameters. In practice, however, it is difficult to eliminate the effect of propagation media from the spectrum at short periods to isolate the source function. One way of avoiding this difficulty is to make observations near the source, minimizing the propagation effect. Then, an exact wave-theory for a simplified medium may be applied to interpret the observation. The present paper describes one result of the application of the above four methods to the Parkfield, California, earthquake of June 1966.

This earthquake offers a rather rigid test of available methods, because the data are nearly complete from detailed near-field and far-field observations.

Data from Near-Field Studies

The Parkfield earthquake took place along the main San Andreas fault north of Cholame. The surface breaks extended over 23 1/2 miles (37 km) (Brown, *et al.*, 1967). A preliminary investigation indicated that the aftershock zone roughly concides with the zone of surface breaks (McEvilly, 1966). Careful studies of the data from temporary stations of the U.S. Geological Survey revealed that the aftershocks were taking place in a very narrow zone within 1 or 2 km of the fault surface at depths of 0 to about 15 km (Eaton, 1967a, 1967b).

The main shock was located near the northwest end of the rupture zone (McEvilly, 1966). The fault must have propagated from there towards the southeast. Eaton (1967a) estimated the fault propagation velocity as 2.2 km/sec from the motion of a radio-time recorder operated at Gold Hill station, which was located very close to the fault at about 20 km from the northwest end of the fault.

The observed surface breaks indicated consistently a right-lateral strike slip of a few inches (Brown, *et al.*, 1967). Allen and Smith (1966) observed, 10 hours following the main shock, that the white line on the highway near the southeast end of the fault had been offset 4.5 cm in a right-lateral sense.

The displacement increased during successive hours and days, and reached about 11 cm a month later (Wallace and Roth, 1967).

The California Department of Water Resources had established in October 1965 a pentagon in the Parkfield area across the fault, and repeated distance measurements using a Model 2A geodimeter. The earthquake resulted in about 20 cm displacement, parallel to the fault strike, in a right-lateral sense (R. Hofmann, personal communication). The discrepancy between the measurements made by the geodimeter and those by the observation of surface breaks may be due either to the long time length between the successive geodimeter measurements or to a possible decoupling of soft surface layers (where the surface breaks are measured) from the basement rocks.

According to a detailed refraction study done by the U.S. Geological Survey, the fault area is characterized by a low-velocity sediment (V_p ~3km/sec) of thickness 1 to 2 km, overlying the basement rock with velocity 5 ~ 6 km/sec (Eaton, personal communication).

Love and Rayleigh Waves

Tsai and Aki (in preparation) measured the spectra of both Love and Rayleigh waves from this earthquake, observed at many WWSS stations. Their radiation patterns indicate the strike of the fault is N43°W, which better fits the trend of surface breaks than the direction derived from first motions (McEvilly, 1966). The latter gives N33°W, and this difference of 10° seems to be significant.

Nulls of the spectra due to finiteness of the source are identified at some stations which lie at relatively short distances and along paths of nearly uniform crustal structure. They are consistent with the fault length of 37 km and the rupture velocity of 2.2 km/sec obtained from near-field observations. A similar result was obtained by Filson and McEvilly (1967) from the record at Berkeley, where they found the fault length 30 km and the rupture velocity 2.2 km/sec. Tsai and Aki estimated the seismic moment (Aki, 1966) from both Love and Rayleigh waves, and obtained a consistent value of 2.0×10^{25} dyne cm. The moment may be expressed in terms of fault parameters as $M_0 = \mu \bar{D} S$ where μ is the rigidity, $\bar{D}$ is the average dislocation, and S is the area of the fault surface.

We may calculate the value of the seismic moment entirely from the near-field observation. As described previously, the offset observed 10 hours after the earthquake is about 5 cm. The fault length is about 37 km. Aftershock depths indicate the fault depth at about 15 km. The value of μ averaged over 15 km depth may be estimated as 3×10^{11} dyne/cm^2. These numbers give

$$M_0 = \mu \bar{D} L h$$
$$= 3 \times 10^{11} \times 5 \times 35 \times 10^5 \times 15 \times 10^5$$
$$= 0.9 \times 10^{25} \text{ dyne cm.}$$

This number coincides exactly with a previously reported number obtained from $G2$ waves of periods around 70 sec recorded at a few stations with sensitive instruments (Aki, 1967). A revised value of the seismic moment requires some modification of source parameters. The most ~~unreliable~~ parameter may be the average dislocation. If we double this, we get a complete agreement between near-field data and surface wave data.

Using these values, we may calculate the stress drop σ (Knopoff, 1958):

$$\sigma = \mu D_0 / 2h = 1.3 \times 10^6 \text{ dyne/cm}^2$$

where $D_0 = 4\bar{D}/\pi = 13$ cm. Thus, we get an extremely low stress drop value of about 1 bar. This value seems too low, even if the process is 'stick-slip' on the existing fault plane suggested by Brace and Byerlee (1966).

Seismic Displacement near the Fault

The Parkfield earthquake offers a rare opportunity for precise source mechanism study. For the first time in the history of seismology, we have records of seismic motions obtained almost exactly on the fault. In June 1965, the Coast and Geodetic Survey had installed a strong motion instrument array across the fault near its southeast end. One of the stations is located at about 80 m from the fault trace (Cloud, 1966). Housner and Trifunac (1967) reported an interesting feature of the seismogram recorded at this station. The horizontal displacement perpendicular to the fault strike, obtained by twice-integration of corresponding accelerograms, showed an impulse form with 1.5 seconds duration and 10 inches height. We did the integrations by ourselves and obtained a similar result, the pulse height being about 30 cm. Unfortunately the parallel component accelerometer was not in proper operation.

To explain the observed wave form, Aki (in preparation) computed a theoretical seismogram based on a moving dislocation model with source parameters obtained from field observations and surface wave studies. The procedure of computation is as follows.

Dividing the fault into small elements, the contribution from each element (its size is varied with the distance from the station, the smallest being $10^m \times 10^m$) is calculated from the formula for an infinitesimal dislocation (Maruyama, 1963). All the near-field terms, which vary with distance r, according to r^{-2}, r^{-3} and r^{-4}, as well as the far-field terms are included. The source function was assumed as a smoothed step function, with cut-off frequency at 3 cps. As far as the displacement is concerned, the synthesized seismogram did not show much dependence on the choice of the cut-off frequency.

The synthesized seismogram for components parallel to the fault showed a form of roughly the step function. This was expected because the station is so close to the fault that the displacement should be nearly the same as prescribed by the boundary condition.

The synthesized seismogram for perpendicular components showed an impulse form in good agreement with observation. It was found, however, that the dislocation must be about 60 cm to explain the observed impulse height of 30 cm.

Large dislocation estimated from the accelerometer record is inconsistent with the observation on surface cracks, but is consistent with the geodimeter observation, because the points where relative displacement of 20 cm was measured by the geodimeter are located at some distance (6∿9 km) from the fault and the relative displacement is expected to decrease with distance from the fault.

Since the value of seismic moment is fixed by the surface wave data, we must modify the source parameters again, if we accept large dislocation estimated from the accelerometer record.

We cannot change the fault length, because one end of the fault is close to the instrumental epicentre of the earthquake and the other end is near the accelerometer station where large dislocation is observed.

The only parameter left is the depth of the fault. We assumed that the depth of the aftershock zone represents the fault depth. This assumption seems not to be applicable to the Parkfield earthquake. The effective fault depth contributed to seismic radiation at the time of the main shock seems much smaller than the depth of the aftershock zone. This is, at least, more reasonable than the opposite case. Assuming that the average dislocation $\bar{D}$ is about 50 cm, we can calculate the moment carried by the sedimentary layer where the rigidity is about 0.8×10^{11} dyne/cm^2. For a thickness of 2 km, we get

$$M_0 \text{ (sediment)} = 3 \times 10^{24} \text{ dyne cm}$$

The total moment less the above value must have been carried by the basement rock. Assuming again $\bar{D} \sim 50$ cm, the depth within the basement is obtained as 3 km, the total depth of the fault being about 5 km.

The stress drop in the basement is no longer unusually low. It is still low, but of the order of 20 bars.

Conclusion

By a combined use of near-field and far-field data, the following conclusions may be drawn on the Parkfield earthquake.

1. Both seismological and geological evidences indicate the fault length of 30 ∿ 37 km.

2. A rupture velocity about 2.2 km/sec is supported by both near-field and far-field seismic observations.

3. An average dislocation of about 50 cm was estimated from the accelerometer record. This is consistent with the geodimeter measurement but not with the observations on the surface cracks.

4. The fault depth of about 5 km was estimated by combining the results from accelerometer records and surface wave spectra. This is about one third of the depth of the aftershock zone.

5. The stress drop in the basement rocks is estimated to be about 20 bars. Use of the dislocation measured on the surface and the depth inferred from the aftershock distribution leads to an extremely low stress drop, of the order of 1 bar.

We were very fortunate with the Parkfield earthquake in having data from so many sources. The accelerometer array of the Coast and Geodetic Survey was set up in June 1965, and both the geodimeter network of the California Department of Water Resources and the Gold Hill station of the Geological Survey were set up in October 1965, only eight months before the earthquake. In the next earthquake, we may not be as lucky as in this case.

In view of many important conclusions drawn from such combined analyses of data, we propose that many other fault zones be constantly monitored by strong motion accelerometer arrays (preferably on the basement rock), standard seismograph stations and geodimeter networks.

Acknowledgement

This research was supported by the Advanced Research Projects Agency and was monitored by the Air Force Office of Scientific Research under contract AF 49 (638) - 1632.

References

Aki, K., 1966. Generation and propagation of G waves from the Niigata earthquake of June 16, 1964. Part 2. Estimation of earthquake moment, released energy, and stress-strain drop from the G wave spectrum. *Bull. Earthq. Res. Inst.*, 44, 73-88.

Aki, K., 1967. Scaling law of seismic spectrum. *J. Geophys. Res.*, 72, 1217-1231.

Aki, K. Seismic displacement near the fault (in preparation).

Allen, C.R., and S.W. Smith, 1966. Pre-earthquake and post-earthquake surficial displacements, Parkfield earthquakes of June 27-29, 1966. *Bull. Seism. Soc. Am.*, 56, 966-967.

Brace, W.F., and J.D. Byerlee, 1966. Stick-slip as a mechanism for earthquakes. *Science*, 153, 990-992.

Brown, R.D., J.G. Vedder, R.E. Wallace, E.F. Roth, R.F. Yerkes, R.O. Castle, A.O. Waananen, R.W. Page, and J.P. Eaton, 1967. The Parkfield-Cholame, California, earthquakes of June-August 1966 – Surface geologic effects, water-resources aspects, and preliminary seismic data. *U.S. Geol. Survey Prof. Paper*, 579, 66 p.

Brune, J.N., and C.R. Allen, 1967. A low-stress-drop, low-magnitude earthquake with surface faulting: The Imperial, California, earthquake of March 4, 1966. *Bull. Seism. Soc. Am.*, 57, 501-514.

Cloud, W.K., 1966. The Parkfield, California, earthquake of June 27, 1966 – preliminary engineering seismological report. *U.S. Coast and Geodetic Survey.*

Eaton, J.P., 1967a. Instrumental seismic studies. In: The Parkfield-Cholame, California, earthquakes of June-August 1966. *U.S. Geol. Survey Prof. Paper*, 579, 57-65.

Eaton, J.P., 1967b. Dependence of hypocentre determinations on the distribution of recording stations and the precision of the seismic velocity model of the earth's crust in the Parkfield-Cholame area, read at the Conference on Geologic Problems of the San Andreas fault system, Stanford University, Palo Alto, California.

Filson, J., and T.V. McEvilly, 1967. Love wave spectra and the mechanism of the 1966 Parkfield sequence, read at the Conference on Geologic Problems of the San Andreas fault system, Stanford University, Palo Alto, California.

Housner, G.W., and M.D. Trifunac, 1967. Analysis of accelerograms – Parkfield earthquake, read at the 63rd annual meeting, Seismological Society of America, Santa Barbara, California.

Knopoff, L., 1958. Energy release in earthquakes. *Geophys. J.*, 1, 44-52.

Maruyama, T., 1963. On the force equivalents of dynamical elastic dislocations with reference to the earthquake mechanism. *Bull. Earthq. Res. Inst.*, 41, 467-486.

McEvilly, T.V., 1966. Preliminary seismic data, June-July, 1966, Parkfield earthquakes of June 27-29, 1966. *Bull. Seism. Soc. Am.*, 56, 967-971.

Tsai, Y.B., and K. Aki. Love and Rayleigh waves from the Parkfield earthquake of June 27, 1966 (in preparation).

Wallace, R.E., and E.F. Roth, 1967. Rates and patterns of progressive deformation, In: The Parkfield-Cholame, California, earthquakes of June-August, 1966. *U.S. Geol. Survey Prof. Paper*, 579, 23-39.

THE STRESS STATE IN EARTHQUAKE FOCI AND THE ELASTIC STRESS FIELD OF THE EARTH

L. M. Balakina, L.A. Misharina, E.I. Shirokova and A.V. Vvedenskaya

Institute of Earth Physics
Academy of Sciences
Moscow, U.S.S.R.

ABSTRACT: The stress state in earthquake foci and the Earth's elastic stress field with which earthquakes are associated are investigated by means of the analysis of the established regularities in the orientation of the principal axes of stresses active in the propagation of faults in the foci. The investigation has shown that in every investigated seismic region of the Earth either the greatest relative pressure or the greatest relative tension is horizontal and in the majority of regions normal to the trend of tectonic structures.

RÉSUMÉ: L'étude de la nature des contraintes dans les foyers des séismes, et du champ des contraintes élastiques terrestres qui les accompagne, consiste à analyser les régularités connues de l'orientation des axes principaux des contraintes auxquelles est due la propagation des failles aux foyers. Dans toutes les régions séismiques examinées la plus grande pression relative, ou la plus grande tension relative est horizontale, et dans la plupart des régions est perpendiculaire à la direction des structures tectoniques.

Introduction

The total accumulated experience of instrumental observations shows that the mechanism of the majority of foci irrespective of their depth is a shear caused by the sliding of one of the fault faces relative to another. The appearance and the spread of the slip surface in the deformed medium occur due to shear stresses at the points of this surface. The shear stresses at each point of the slip surface are equivalent to two principal stresses of tension and pressure acting on two mutually perpendicular areas which form angles of 45° with the slip surface. The third principal stress—the intermediate one—is equal to zero.

In the process of an earthquake the release of shear stresses (which we call the stresses acting in the foci) takes place at the points of the slip area. The directions of the principal axes of these stresses are connected in a certain way with the position of the nodal surfaces of the displacement fields in *P*, *SV* and *SH* waves which are generated in the process of the slip area growth (Vvedenskaya, 1956, 1960). The position of the nodal surfaces of the wave field does not depend on the rate nor the duration of the growth of the slip region in a source (Vvedenskaya, 1965, 1967). Hence the observations of the displacements in seismic waves may serve as the basis for the determination of the directions of the three principal stresses in the focus of the earthquake under consideration.

The peculiarities of the space distribution of the principal axes of stresses acting in earthquake foci of various seismic zones of the earth were discussed in some papers (Balakina, 1959, 1960, 1962; Shirokova, 1959, 1961, 1962, 1963, 1967; Rustanovich and Shirokova, 1964; Misharina, 1964a, 1964b; Lazareva and Misharina, 1965; Misharina and Pshennikov, 1965; Vvedenskaya and Balakina, 1960; Vvedensdaya, 1961; Vvedenskaya and Ruprekhtova, 1961). The authors found definite regularities in the orientation of these axes characteristic for each seismic region. The analysis of the established regularities provided the basis for the determination of the character of the stress state in corresponding zones and also for some conclusions concerning the Earth's elastic stress field with which earthquakes are associated. The detailed discussion of the results obtained can be found in the paper by Balakina, Vvedenskaya, Misharina and Shirokova (1967).

Regularities in the Orientation of Stresses Acting in Earthquake Foci

Let us consider the regularities in the orientation of stresses acting in the earthquake foci of some seismic belts.

The Mediterranean-Asiatic Belt

According to the type of stress orientation, this belt is divided into several regions (Shirokova, 1959, 1961, 1962, 1963, 1967; Rustanovich and Shirokova, 1964; Vvedenskaya and Ruprekhtova, 1961).

In the eastern Mediterranean the tension in the investigated earthquake foci, which are not systematically distributed, has a clear horizontal orientation (Shirokova, 1963). The intermediate (zero) stress as well as the pressure has various orientations. The regularities in the orientation of the stress axes relative to the surface structures are not established.

In the earthquake foci near the bend of the Carpathian arc, the pressure is oriented nearly parallel to the horizontal plane and normal to the arc's bend (Vvedenskaya and Ruprekhtova, 1961). The tension and the intermediate stress lie in the plane

whose intersection line with the Earth's surface serves as tangent to the arc. Along the strike the plane coincides with the axes of the observed folds in this region.

In the central part of the belt (the Caucasus and Asia up to 90°E), the pressure is directed approximately horizontally and is normal to the trend of the surface structures (Shirokova, 1959, 1961, 1962). The predominant orientation of tension is nearly vertical. The direction of the intermediate stress is close to horizontal and coincides with the strike of structures. Thus the eastern Mediterranean and the central part of the belt differ sharply as to the character of the orientation of stresses. If tension appears to be horizontal in the Mediterranean zone, then pressure becomes horizontal in the adjacent region to the east, and no area with mixed orientation is observed. The boundary separating the regions with different stress orientations is near 40°E.

In the eastern Asiatic part of the belt (to the east of 90°E), the orientation of pressure is the same as in the central part of the belt (Shirokova, 1967). The tension and the intermediate stresses have no distinct predominant orientation.

On the Sunda Islands (Shirokova, 1967), the pressure is directed approximately horizontally and across the strike of the island arc, i.e., the orientation character of these stresses is the same as within the greater part of the belt (the Caucasus and Asia). The tension is characterized by a slight predominance of the horizontal orientation. The intermediate stress is not marked by any predominant orientation.

The earthquakes with a focal depth about 150 km (the Carpathian mountains) and about 200 km (the Hindu-Kush mountains) reveal the same regularities in the stress orientation as those with foci located in the crust.

The Mongolian-Baikal Zone

Within the Mongolian-Baikal seismic zone, two distinct regions are established according to the stress peculiarities in the earthquake foci (Vvedenskaya and Balakina, 1960; Vvedenskaya, 1961; Misharina, 1964b; Misharina and Pshennikov, 1965). One of them, including the Baikal depression and extending further to the northeast along the system of ranges and depressions up to the Stanovoy ridge, is characterized by the near-horizontal tension oriented across the strike of structures and by the near-vertical pressure. In the other region situated to the west of Baikal, the direction of tension is close to vertical, while the pressure is practically horizontal and normal to the trend of structures. In both regions the direction of the intermediate stress is close to horizontal.

To the south and southwest of Baikal, a third region can be distinguished where the directions of the pressure and tension make angles not greater than 40° with the horizontal plane, while the intermediate stress is characterized by various orientations. Because of the lack of observational data, the boundaries of this region can be established only approximately. It seems to include the seismic zones of central and western Mongolia and is bordered by the Gobi-Altai mountain system to the south. The earthquake foci of the Gobi-Altai reveal nearly horizontal pressure normal to the structures and almost vertical tension, while the orientation of the intermediate stress is close to horizontal.

The Arctic-Atlantic Belt

The earthquake foci of the Arctic-Atlantic seismic belt are almost everywhere characterized by the near-horizontal orientation of pressure and tension and near-vertical orientation of the intermediate stress (Misharina, 1964a; Lazareva and Misharina, 1965).

In the Atlantic Ocean the tension is generally oriented across the trend of structures, while the direction of the pressure is along the axis of the oceanic ridges that is traced by means of the locations of earthquake epicentres. The same orientation of the stress axes seems to be typical for the earthquake foci of eastern Africa.

In the arctic part of the Arctic-Atlantic belt the orientation of stresses for different regions varies. In the region of the Norwegian and Greenland seas the nearly horizontal tension is normal to the strike of the sea ridge that is the extension of the Atlantic ocean ridge, while the direction of the near-horizontal pressure is along the strike of the sea structures. In the eastern part of the Arctic seismic belt (in the region of the Lomonosov ridge, Laptev sea and the delta of the Lena river), the predominant directions of pressure and tension also remain almost horizontal, but the belt trend is pursued only by the tension orientation while the pressure is generally normal to the line of epicentres. The tentative results show that in the region of the Verkhoyansk and Chersky ranges the pressure is horizontal and approximately normal to the trend of surface structures. The orientation of the tension and intermediate stress in the earthquake foci of this region is not definite.

The Pacific Belt

In the majority of the investigated foci in the marginal Pacific zone (excluding the California shore and probably the shore of Central America), the direction of pressure is close to horizontal and normal to the trend of the earthquake zones and the main surface structures (Balakina, 1959, 1960, 1962). Such relations between the orientation of pressure and the trend of structures are observed in the foci of both surface and deep earthquakes down to depths of 600 to 700 km. The orientation of tension and intermediate stress is not constant and varies from focus to focus.

Features of the Stress State in the Main Seismic Regions of the Earth

The established regularities in the orientation of the principal stresses acting in earthquake foci permit the character of the stress state in the investigated seismic regions to be outlined.

The stress state at each point of the deformed medium is determined by the position of the three principal axes and the three values of principal stresses. We find the position of the principal axes of the stress state in a certain seismic zone as a whole and determine the condition connecting its principal values. We assume that the location of the planes of maximum tangential stresses in this zone is determined by the established direction of the released shear stresses in the entire system of earthquake foci.

First, let us consider this condition in those seismic regions where the position of the principal axes of the released stresses for the entire system of foci remains constant (for instance, in Central Asia and Prybaikalye). The space directions of the pressure, intermediate and tension axes will be given the indices i, j and k, respectively. Then the following relations must be given for the values of the principal stresses σ_i, σ_j, σ_k of the stress state in the foci:

$$\left|\frac{\sigma_i-\sigma_k}{2}\right| > \left|\frac{\sigma_k-\sigma_j}{2}\right| , \left|\frac{\sigma_i-\sigma_k}{2}\right| > \left|\frac{\sigma_j-\sigma_i}{2}\right| , \left|\sigma_i-\sigma_k\right| = 2\tau_{\max}$$

These relations show that the stress tangents amount to the greatest absolute values $\tau_{\max}$ on the areas making angles of 45° with the axes with subscripts i and k. Proceeding from these conditions, or from the following ones equivalent to them,

$$|\sigma_i-\sigma_k| > |\sigma_k-\sigma_j| , |\sigma_i-\sigma_k| > |\sigma_j-\sigma_i|$$

we establish the following two relations between the values of the principal stresses of the stress state in the region under consideration: $\sigma_i < \sigma_j < \sigma_k$ and $\sigma_i > \sigma_j > \sigma_k$, only the first of which is valid, as is easily seen.

Now let us determine the relationship between the principal values of the total stress state in those seismic regions where successive earthquakes show that the position of only one principal axis of stresses acting in the foci remains constant, while the directions of the other two principal stresses change from focus to focus (for instance, the Mediterranean Sea, the Carpathian Mountains, the Pacific belt). We assume that the constant axis is the axis of pressure. The axis of the total stress state coinciding with the latter will be given the subscript i. The subscripts j and k will refer to the other two axes of the stress state whose orientation corresponds to the other two principal axes of the acting stresses. The following relations must be written for the principal values σ_i, σ_j, σ_k of the total stress state:

$$|\sigma_i-\sigma_k| > |\sigma_k-\sigma_j| , |\sigma_i-\sigma_k| \approx |\sigma_j-\sigma_i| , |\sigma_i-\sigma_k| = 2\tau_{\max}$$

They show that the tangential stresses τ_{ik} and τ_{ij}, where $\tau_{ik} = \frac{\sigma_i-\sigma_k}{2}$ and $\tau_{ij} = \frac{\sigma_j-\sigma_i}{2}$, have the greatest absolute values in the total stress state and are equal. In this case the principal values of the total stress state are related by $\sigma_i < \sigma_j \approx \sigma_k$, and the two orthogonal principal axes corresponding to the two mutually equal principal stresses can be arbitrarily oriented in the plane normal to σ_i.

If, in the entire system of earthquakes of a seismic region, the direction of the tension axis appears to be constant, the principal values of the total stress state will be related as $\sigma_i \approx \sigma_j < \sigma_k$, where the subscript k refers now to the principal axis of the stress state that coincides with the direction of the axis of the released tension in the foci.

TABLE 1

Stress States in Seismically Active Regions of the Earth

Seismic Regions	Condition Connecting the Principal Values of the Stress State	The Correlation between the Values of the Ellipsoid Axes of Stress	Type of Stress State near the Earth's Surface and Relative to σ_3 in the Deep Parts
The Pacific belt, the Sunda Islands, southeastern Asia, the region of the Chersky and Verkhoyansk ridges, the Carpathian Mountains	$\sigma_k \approx \sigma_j > \sigma_i$	$\sigma_3 \approx \sigma_2 > \sigma_1$	One-sided horizontal pressure normal to structures
Eastern Arctic region	$\sigma_k > \sigma_j > \sigma_i$	$\sigma_2 > \sigma_3 > \sigma_1$	Horizontal tension and pressure along and normal to structures
The central part of the Mediterranean-Asiatic belt (from $\lambda=40°$E to $\lambda=90°$E)	$\sigma_k > \sigma_j > \sigma_i$	$\sigma_3 > \sigma_2 > \sigma_1$	Horizontal uneven pressure, predominantly normal to structures
Mediterranean	$\sigma_k > \sigma_j \approx \sigma_i$	$\sigma_k > \sigma_j \approx \sigma_i = \sigma_3$	One-sided horizontal tension whose orientation relative to structures is unknown
Western Arctic, the Atlantic ridge, eastern Africa	$\sigma_k > \sigma_j > \sigma_i$	$\sigma_1 > \sigma_3 > \sigma_2$	Horizontal pressure and tension, respectively along and normal to structures
Prybaikalye	$\sigma_k > \sigma_j > \sigma_i$	$\sigma_1 > \sigma_2 > \sigma_3$	Horizontal uneven tension predominantly normal to structures

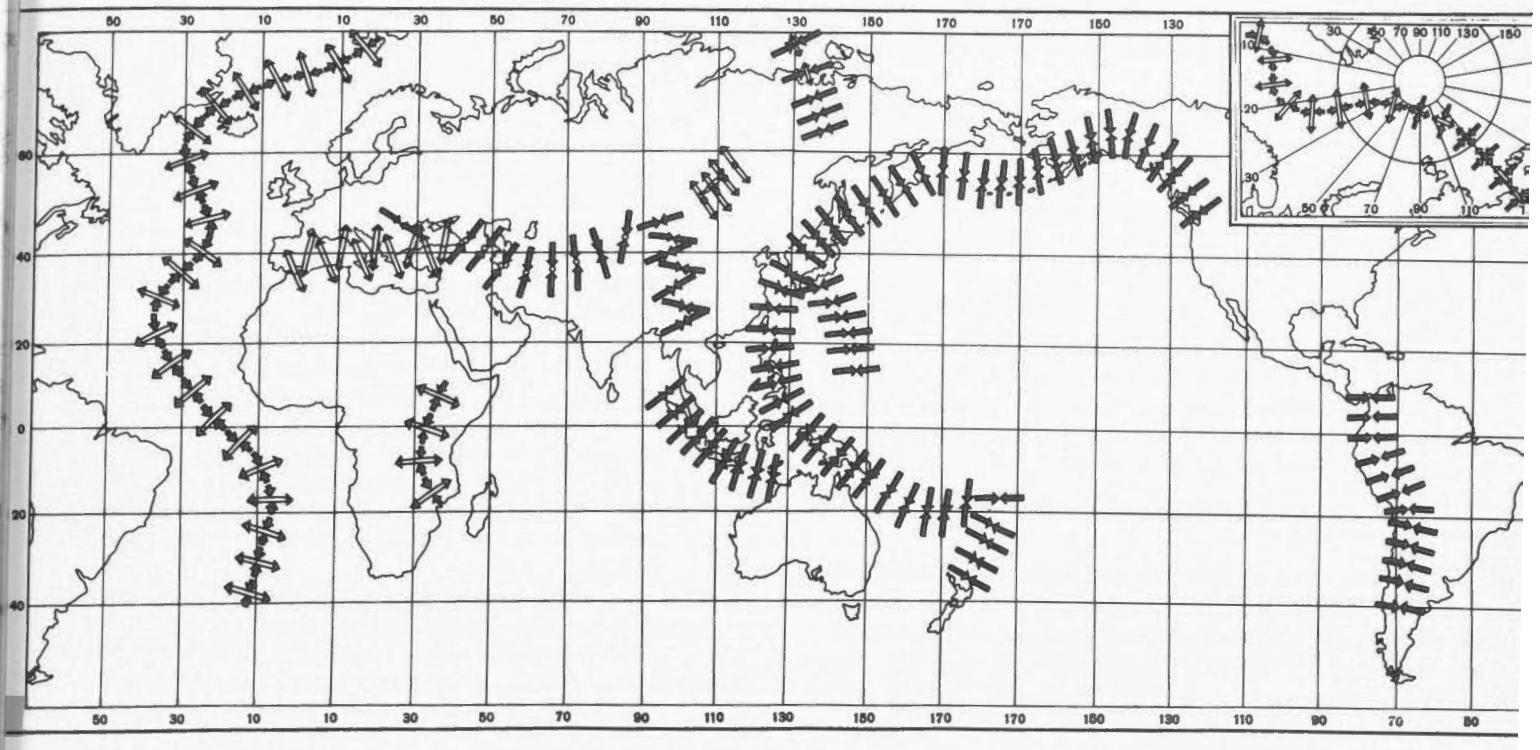

Figure 1. The field of the elastic stresses of the Earth.

Each of the relations $\sigma_i < \sigma_j < \sigma_k$, $\sigma_i < \sigma_j \approx \sigma_k$, $\sigma_i \approx \sigma_j < \sigma_k$ is characterized by a variety of stress states; hence the total stress state cannot be unambiguously determined proceeding from the known orientation of the principal axes of stress acting in the foci.

Here we introduce one more system of subscripts which will be referred to the principal axes of the stress state and which depend on the orientation of the axes relative to the Earth's surface and the trend of the structures. The subscript 1 will refer to that principal axis which lies in the horizontal plane normal to the trend of structures, 2 to the axis located in the same plane along the structures and 3 to the vertical axis. If we apply this system of subscripts to the established relations between the values of the principal stresses and give the same sign to all the three stresses, then the values of the ellipsoid axes of stresses for different seismic regions of the Earth will be related in the way shown in Table 1.

Among the variety of stress states which can be assumed on the basis of the established relation between the values of the principal stresses, we find one interesting system of possible states for which the value σ_3, i.e., the stress along the vertical axis, becomes zero. This additional condition to one of the principal values of stress is possible near the Earth's surface. Its introduction into the relationship between the principal values of the stress state in a certain seismic region permits one to determine the signs of the values σ_1 and σ_2 and thus to establish the type of stress state near the Earth's surface in this region. In general the positive principal stress corresponds to tension, the negative one to pressure.

The value σ_3 in the deep parts of the seismic regions is not equal to zero and remains unknown. But the established dependence between the principal values of stresses in the stress state of a seismic region as a whole can give us values for σ_1 and σ_2 relative to σ_3 which are algebraically greater or smaller than σ_3 or equal to σ_3. Let us consider that the principal stress with an algebraically greater value than σ_3 is a relative tension while the principal stress with the value less than σ_3 is a relative pressure. Then the type of the established stress state near the Earth's surface can be generalized and extrapolated to the deep parts of the seismic region, considering it relative to the vertically oriented principal stress.

The results of the determination of the type of stress states in different seismic regions are presented in the last column of the table.

On the Field of Elastic Stresses of the Earth

We call the field of elastic stresses of the Earth with which earthquakes are associated the space distribution of stress states in the entire system of seismic regions. The table shows that the type of stress state changes from one seismic region to another, i.e., the field of the elastic stresses of the Earth is heterogeneous.

In each seismic region of the Earth either the greatest relative pressure or the greatest relative tension is parallel to the horizontal plane. In most regions a certain relation is observed between the trend of surface structures and the direction of the principal axes of the stress state: either the

axis of the greatest relative pressure or the axis of the greatest relative tension is in the horizontal plane normal to the trend of structures.

Figure 1 illustrates the orientation of the principal stress axes in the field of the elastic stresses of the Earth. On the map the greatest relative pressure acting in the horizontal plane across the structures is shown by large converging black arrows, while the greatest relative tension is shown by large diverging white arrows. The white and black circles near these signs show, respectively, that another of the principal stresses, which makes the maximum difference with the greatest relative pressure or tension acting across the structures, is vertical. The small white and black arrows near the large ones show that the second principal stress is horizontal and acts along the structures. The one-sided pressure or tension is not represented by any additional sign near the large converging or diverging arrows, respectively.

The connections between the seismic zones and the regions of modern tectonic processes, as well as the relations between the direction of the principal axes of stress acting in the foci and the trend of tectonic structures imply that both the modern development of tectonic structures and the local release of stresses in earthquake foci are due to the field of elastic stresses of the Earth that is demonstrated on the map. Both the processes are maintained by the continuous generation of stresses in this field because of processes occurring in the interior of the Earth.

References

Balakina, L.M., 1959. On the distribution of stresses acting in earthquake foci in the northwestern Pacific. *Izv. AN SSSR, ser. geophys.*, 11, 1599-1604; in the Eng. ed. 1131-1135.

Balakina, L.M., 1960. Some results of the study of earthquake foci of May 4 and June 18, 1959, according to the instrumental data. *Bull. Soveta po Seismol.*, 11, 25-31.

Balakina, L.M., 1962. General regularities in the direction of the main stresses acting in the earthquake foci of the Pacific seismic belt. *Izv. AN SSSR, ser. geophys.*, 11, 1471-1483; in the Eng. ed. 918-926.

Balakina, L.M., A.V. Vvedenskaya, L.A. Misharina, and E.I. Shirokova, 1967. The stressed state in the earthquake foci and the field of the Earth's elastic stresses. *Izv. AN SSSR, Fizika Zemli*, 6, 3-15; in the Eng. ed. 333-342.

Lazareva, A.P., and L.A. Misharina, 1965. On the stresses in the earthquake foci of the Arctic seismic belt. *Izv. AN SSSR, Fizika Zemli*, 2, 5-10; in the Eng. ed. 84-87.

Misharina, L.A., 1964a. On the stresses in the earthquake foci of the Atlantic ocean. *Izv. AN SSSR, ser. geophys.*, 10, 1527-1534; in the Eng. ed. 924-928.

Misharina, L.A., 1964b. On the problem of stresses in the earthquake foci of Prybaikalye and Mongolia. In: The problems of the seismicity of Siberia. *Trudy Inst. Zemnoy Kory, Sibir. Otdel., AN SSSR*, Novosibirsk, 18, 50-69.

Misharina, L.A., and K.V. Pshennikov, 1965. The process of the discharge of stresses in the Earth's crust from the data of the Prybaikal and Mongolian earthquakes. *In the collected papers: Geological results of applied geophysics*, 22nd Intern. Geol. Congress, Izd. Nedra, Moscow, 75-84.

Rustanovich, D.N., and E.I. Shirokova, 1964. Some results of the study of the Ashkhabad earthquake of 1948. *Izv. AN SSSR, ser. geophys.*, 12, 1782-1788; in the Eng. ed. 1077-1080.

Shirokova, E.I., 1959. Determination of stresses acting in the foci of the Hindu-Kush earthquakes. *Izv. AN SSSR, ser. geophys.*, 12, 1739-1744; in the Eng. ed. 1224-1227.

Shirokova, E.I., 1961. On the stresses acting in the foci of Central Asia earthquakes. *Izv. AN SSSR, ser. geophys.*, 6, 876-881; in the Eng. ed. 572-576.

Shirokova, E.I., 1962. On the stresses acting in the foci of the earthquakes of the Caucasus and the adjacent regions. *Izv. AN SSSR, ser. geophys.*, 10, 1297-1306; in the Eng. ed. 809-815.

Shirokova, E.I., 1963. On the stresses acting in the foci of the earthquakes of the northwestern part of the Mediterranean-Asiatic seismic belt. *Bull. Soveta po Seismol.*, 15, 72-80.

Shirokova, E.I., 1967. General regularities in the orientation of the main stresses in the earthquake foci of the Mediterranean-Asiatic seismic belt. *Izv. AN SSSR, Fizika Zemli*, 1, 22-36; in the Eng. ed. 12-22.

Vvedenskaya, A.V., 1956. The determination of displacement fields in earthquakes by means of the dislocation theory. *Izv. AN SSSR, ser. geophys.*, 3, 277-284.

Vvedenskaya, A.V., 1960. The determination of stresses acting in earthquake foci from the observations of seismic stations. *Izv. AN SSSR, ser. geophys.*, 4, 513-519; in the Eng. ed. 341-344.

Vvedenskaya, A.V., 1961. The peculiarities of the stressed state in the foci of the Prybaikal earthquakes. *Izv. AN SSSR, ser. geophys.*, 5, 666-669; in the Eng. ed. 432-434.

Vvedenskaya, A.V., 1965. The determination of the displacements in body waves depending on the rate and the duration of the spread of dislocation. *Izv. AN SSSR, Fizika Zemli*, 1, 3-11; in the Eng. ed. 1-5.

Vvedenskaya, A.V., 1967. The possibilities of the determination of stress values acting in earthquake foci. *Izv. AN SSSR, Fizika Zemli*, 7, 14-19; in the Eng. ed. 428-431.

Vvedenskaya, A.V., and L.M. Balakina, 1960. The technique and results of the determination of stresses acting in earthquake foci of Prybaikalye and Mongolia. *Bull. Soveta po Seismol.*, 10, 73-84.

Vvedenskaya, A.V., and L.A. Ruprekhtova, 1961. The peculiarities of the stressed state in the earthquake foci near the bend of the Carpathian arc. *Izv. AN SSSR, ser. geophys.*, 7, 953-965; in the Eng. ed. 629-636.

DISLOCATION FIELD DYNAMICS AS AN APPROACH TO THE PHYSICS OF EARTHQUAKE PROCESSES

Roman Teisseyre

Institute of Geophysics
Polish Academy of Sciences
Warsaw, Poland

ABSTRACT: A series of discussions on earthquakes leads to the assumption that physical conditions prior to earthquake occurrences are described by some energy accumulation units. These units of energy accumulation are connected with interior inhomogeneities of the earth and from a stress point of view could be described by dislocations, cracks or other stress singularities.

The discussion of energy release in earthquakes is especially convenient in terms of dislocation dynamics. The main process of internal energy release is described by annihilation of two dislocation lines of opposite sign. Energy release can thus occur when two dislocation elements join, when a dislocation reaches the Earth's surface or any internal discontinuity and also in the process of thermal stress removal by a dislocation field. It is stressed that generation of dislocations corresponds rather to an internal stress concentration process. Some argumentation for the use of dislocations follows from the $1/r$ interaction type between neighbouring stress accumulation units, corresponding to a kind of superlattice.

It is also emphasized that cracks or other stress singularities can be approximated by a dislocation distribution. There follows a general approach to a unified theory by means of a dislocation density field. Thus, applications to the problem of the Earth's internal processes are discussed in terms of a dislocation density field. In this paper the relation between stresses of the thermal convection and a dislocation density is especially studied. Further, dislocation flow is assumed and related to the large-scale tectonic process. In this way the stress rates in the Earth's interior can be determined.

RÉSUMÉ: L'étude de séries de tremblements de terre amène à envisager les conditions physiques existantes avant les séismes comme des unités d'accumulation d'énergie rattachées aux hétérogénéites internes de la terre. Sous ce rapport de la contrainte, ces unités peuvent être identifiées comme des dislocations, des fissures ou d'autres singularités de contrainte.

La dynamique de la dislocation s'applique particulièrement bien à l'étude de l'émission de l'énergie dans les tremblements de terre. La phase principale de l'émission de l'énergie interne s'explique par l'annihilation de deux lignes de dislocation de signes opposés. L'émission de l'énergie peut ainsi se produire quand deux éléments de dislocation se joignent, quand une dislocation atteint la surface de la terre ou n'importe quelle discontinuité interne, et aussi quand un champ de dislocation annule une contrainte thermique. Il est à remarquer que la génération des dislocations correspond surtout au développement d'une concentration de la contrainte interne. Le type d'interaction $1/r$ produisant entre des unités voisines d'accumulation de contrainte correspond à une sorte de super-réseau et donne lieu à l'étude de l'utilité des dislocations.

L'auteur met aussi l'accent sur la possibilité de rapprocher les fissures et autres singularités de contrainte d'une répartition des dislocations. Suit l'élaboration générale d'une théorie unifiée basée sur le principe d'un champ de densité de dislocation. Ses applications au problème des processus internes de la terre s'expriment donc en fonction de ce champ. La relation entre les contraintes dues à la convection thermique et la densité de dislocation fait ici l'objet d'une étude particulière. De plus, après avoir admis le principe de la propagation des dislocations, celle-ci est rattachée au processus tectonique dans son ensemble. Il est possible de déterminer, de cette manière, le taux de contrainte à l'intérieur de la terre.

Introduction

Some physical properties of earthquake processes can be established by comparing the patterns of different types of earthquake series, which leads to the assumption that there are interrelations between different shocks forming part of one and the same earthquake series (Miyamura, *et al.*, 1965). The physical conditions can be explained by assuming that the particular shock, previous to its occurrence, forms a dynamic unit of internal energy storage in a confined volume and that its energy is afterwards released in the earthquake process. The concept of so-called earthquake volume (Tsuboi, 1958), defined on the basis of the infinitesimal elastic theory, should, however, be revised in the sense that energy storage is confined to a rather small volume whose self-strains exceed the standard value of ultimate strain. This would correspond to the situation in an overstrained material and it could be imagined that the interaction of forces maintains in balance the different, but adjacent, units of internal energy storage. This argumentation follows logically from the above-mentioned assumptions since otherwise, to understand energy releases in an earthquake series, we would have to assume incredibly rapid strain recovery.

The dynamic development of internal strain processes, revealed in separate shocks, is conditioned by two main factors (Teisseyre, 1961a). The general stress field, especially one of shearing character, governs the regional seismic activity and has to be considered as a factor varying in time at a rather slow rate. Inhomogeneities of the Earth's interior, all kinds of internal failures, intrusions and fractures combine with the general stress field to form local stress concentrations and

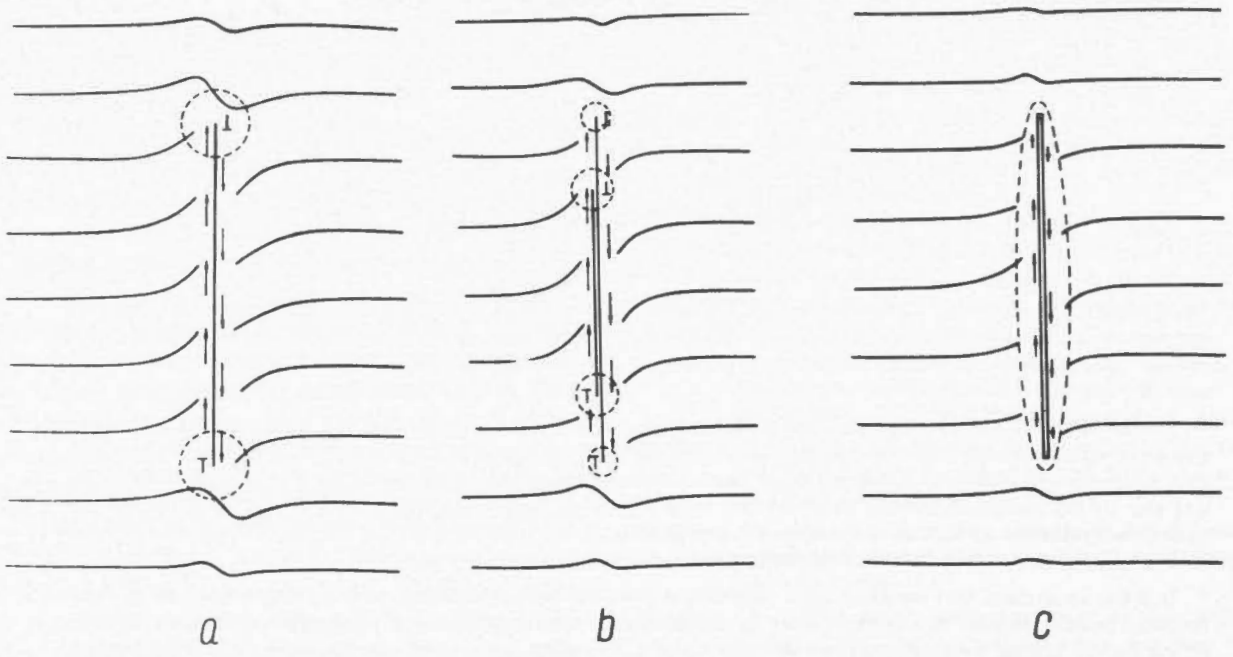

Figure 1. Cross-section along a discontinuity surface. (a) constant discontinuity along the dislocation surface, (b) displacement field of the superimposed dislocations – two dislocation pairs, (c) crack – continuous change of displacement discontinuity.

nuclei of dynamic processes. Thus it is assumed that the units of internal energy storage are originally connected with internal inhomogeneities, but it is also possible that further dynamic developments may spread out from those internal sources (Kasahara and Teisseyre, 1966). The role of heterogeneity of the material is distinctly emphasized in Mogi's papers on classification of shock sequences (Mogi, 1963a, 1963b).

The units of internal strain concentration defined in the foregoing can be described with methods similar to those used in solid-state physics, but only for the theory of a continuous medium. Thus, we may consider such stress singularities as dislocations, cracks, or the general field of dislocation density. The dislocations constitute here somewhat idealized forms determined by jumpwise discontinuities in displacement along a dislocation surface. In cracks (Griffith, 1921), the displacement discontinuity varies from near zero at its edges to a maximum value at the centre of the crack. Unlike the dislocations, the stresses are also discontinuous when intersecting the crack surface.

For dislocations, the theorem holds that a displacement discontinuity, constant along the dislocation surface, produces considerable stress concentration but usually along the boundaries of the dislocation (Figure 1). Those boundaries form singularity lines limiting the dislocation surface element, so that the dynamic characteristics of the dislocation can all be deduced from considerations regarding those dislocation lines. By grouping of the dislocations (lines) it becomes, however, possible to approach the real state of stress and strain conditions in the medium and, particularly, to describe the crack field (Figure 1). Formal mathematical equivalence is achieved by using a continuous dislocation distribution along a given surface (Eshelby, *et al.*, 1951).

Finally, we may infer that the simple form of mathematical interpretation and the possibility of grouping dislocations in various combinations argue in favour of applying the dislocation theory to earthquake processes. More complex strain patterns as well as plastic deformations or semiplastic ones (distortions due to laminar stratification) can be described by means of the field of dislocation density (Teisseyre, 1966).

The earthquake dislocation theory was studied by a number of authors, but some of them treated the problem from the static viewpoint only. Among them, the papers by J.A. Steketee (1958) present clearly the advantages obtained by application of the dislocation theory to seismology. Another approach was selected by G.W. Housner (1955) in his statistical studies on earthquakes in the frame of the dislocation theory. A.V. Vvedenskaya (1956, 1958) achieved a description of earthquake processes by treating the formation of dislocations as a seismic event in a focal region. Her considerations, including the dynamic process of dislocation appearance, were originally based on F.R.N. Nabarro's method of dislocation synthesis (Nabarro, 1951).

S. Droste and R. Teisseyre (1959), and later Teisseyre (1961b), also examined the dislocation mechanism of earthquakes, assuming, however, *a priori* some distribution of dislocations in the Earth's interior. Thus, the dislocations are treated by those authors as units of internal energy storage, only those dislocation processes being considered which lead to release of internal energy. Effective energy release occurs when two dislocation lines of opposite sign mutually approach and annihilate. This process, called pair annihilation, takes place when two dislocation elements join, or when a dislocation reaches the Earth's surface (in this case the dislocation

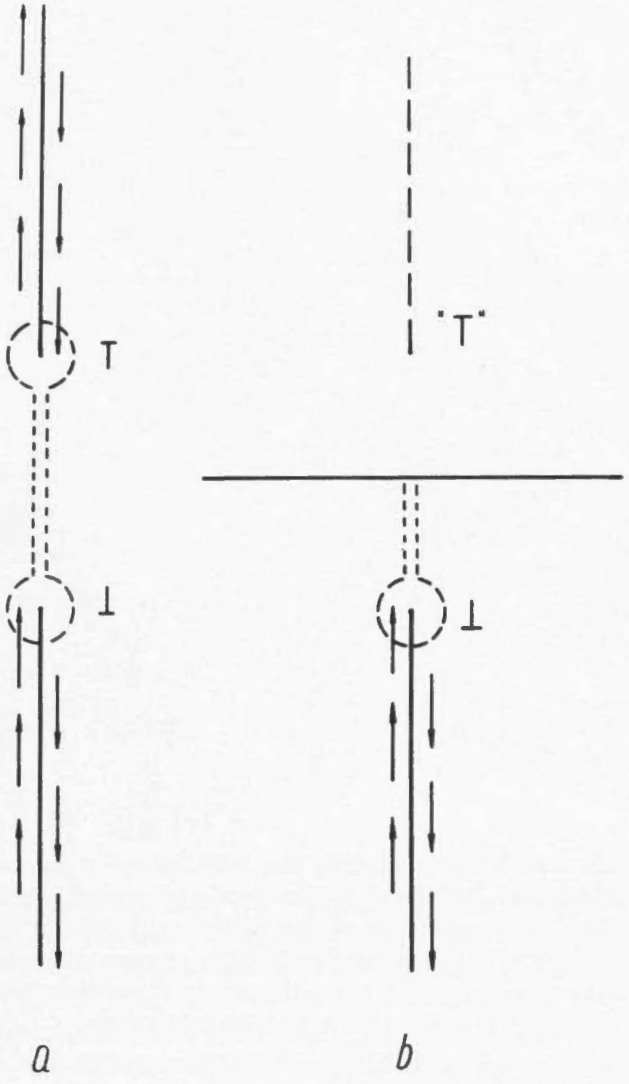

Figure 2. Mechanism of dislocation pair annihilation. (a) joining of two dislocation elements – (⊥,T) pair annihilation, (b) effect of free surface – image dislocation.

annihilates with its image), or when a dislocation intersects an internal discontinuity (Figure 2).

The simplest form of a dislocation element is a strip bounded by two parallel lines, that is, by two dislocations (lines) of opposite sign. Appearance of a dislocation element is thus equivalent to creation of a dislocation pair. A similar equivalence holds for the annihilation process of a pair. From the dynamic viewpoint, which is commonly applied to the earthquake mechanism, both processes are equivalent and correspond to a model of two dipoles with moments (Figure 3). From the energy point of view, the creation of a dislocation corresponds to some kind of internal energy transformation, revealed by its concentration around the dislocation lines. Nevertheless, part of the internal energy will be spent on seismic radiation owing to the rapid dynamic mass shift. In the annihilation process, the release of internal energy accumulated in dislocations produces an earthquake and causes an effective decrease of strains in a given confined region. As a result, the total stress system and the interaction pattern between adjacent accumulation units will change and may produce further energy releases (Figure 4). This event may be described in the following manner. After the earthquake, the balance of stress interaction between accumulation units is destroyed, which may lead to some rearrangements of their positions so that further energy releases may be expected (Teisseyre, 1964).

The main difficulty in theory concerns the dislocation sources. The simplest procedure would be to assume *a priori* some pattern of dislocation distribution in the highly inhomogeneous interior of the Earth, or at least to assume some sources as the nuclei in which dislocations have to be created. The latter assumption was adopted by K. Kasahara and R. Teisseyre (1966) to explain earthquake swarm activity.

Figure 3. Equivalence of the Love forces with the dislocations. (a) dislocation element and two dipoles, (b) an elongated dislocation surface and two dipoles – total zero moment.

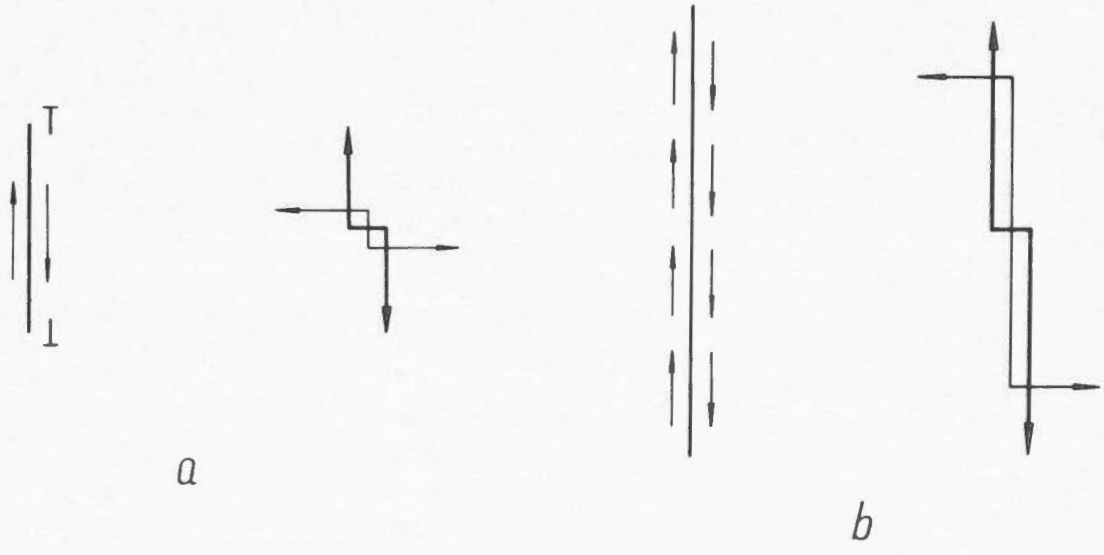

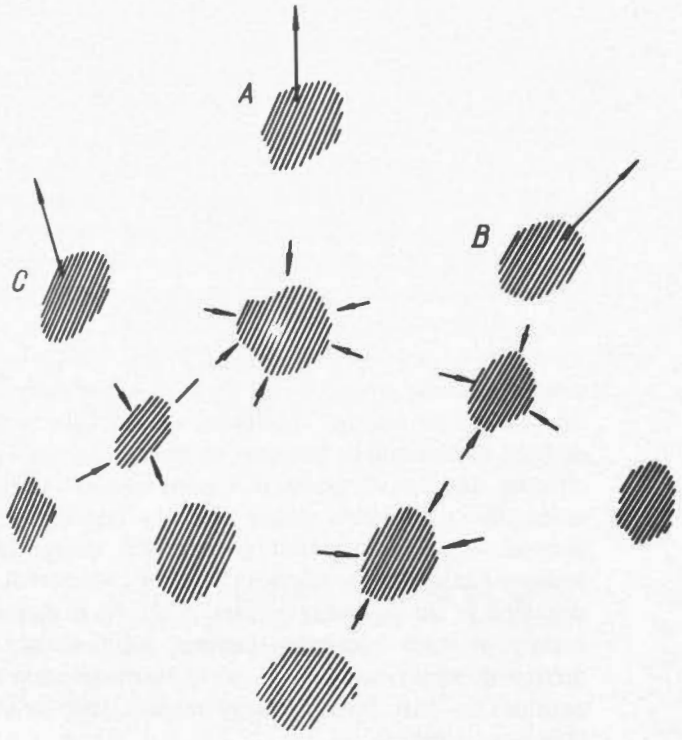

Figure 4. Interaction pattern – A,B,C, outer energy accumulation units.

As was mentioned, the dislocation theory allows one to imagine and calculate stress conditions and displacements prior to the earthquake and also their subsequent changes resulting from energy release. Comparison of energy data and displacement values on the Earth's surface obtained from observation and the dislocation theory shows quite satisfactory agreement (Alpan and Teisseyre, 1966). Even static solutions in the frame of the dislocation theory permit calculation of the surface displacements originating from various types of sources. The respective results yield a theoretical explanation of the geodetically measured deformations on the Earth's surface (Chinnery, 1961; Teisseyre, 1961a; Weertman, 1965).

The occurrence of earthquake sequences could be investigated theoretically in terms of the interaction between energy-accumulation units (Miyamura, *et al.*, 1965). The interactions between accumulation units could form a physical basis for constructing some models of dynamic development of an internal system. The time-course of a dynamic process in the focus was investigated by several authors (Vvedenskaya, 1959, 1965; Ben-Menahem, 1961; Savage, 1965) and can thus be theoretically estimated.

There are a great number of papers dealing with detailed problems of dynamic displacements due to dislocations, cracks or other stress singularities, which, from the viewpoint presented in this study, belong in a general sense to the dislocation theory. The foregoing short argumentation in favour of this theory and particularly the field theory of dislocation density, as formulated in the next sections needs further development, primarily in two directions. First, earthquake phenomena should be described in terms of irreversible thermodynamics. Secondly, a real nonlinear stress-strain characteristic of the material has to be taken into account.

Thermoelasticity equations comprise four equations with deformation components and a thermal field or density of entropy (Biot, 1956), which are to be solved simultaneously. In a simplified approach one can assume a given thermal field and then solve the equations for displacements. Of special interest for plane problems is the theorem by N.I. Muskhelishvili (1953): a thermal field which satisfies the harmonic equation leads in general to a stress field which may correspond to multivalued displacement functions. In other words, thermal stresses are in general equivalent to dislocation stresses. Careful interpretation of this theorem is important in earthquake problems (Teisseyre, 1963).

Thus, certain thermal fields, particularly thermal convection currents, correspond to dislocation stresses even if there are no real displacement discontinuities. But these thermal stresses could be removed by a real dislocation field of opposite character. The release mechanism would therefore again be described by stress annihilation due to annihilation of a dislocation pair—one, apparent, related to the thermal field, and the other, real, but of opposite character.

The second problem which should be given careful attention concerns realistic evaluation of stress-strain characteristics in

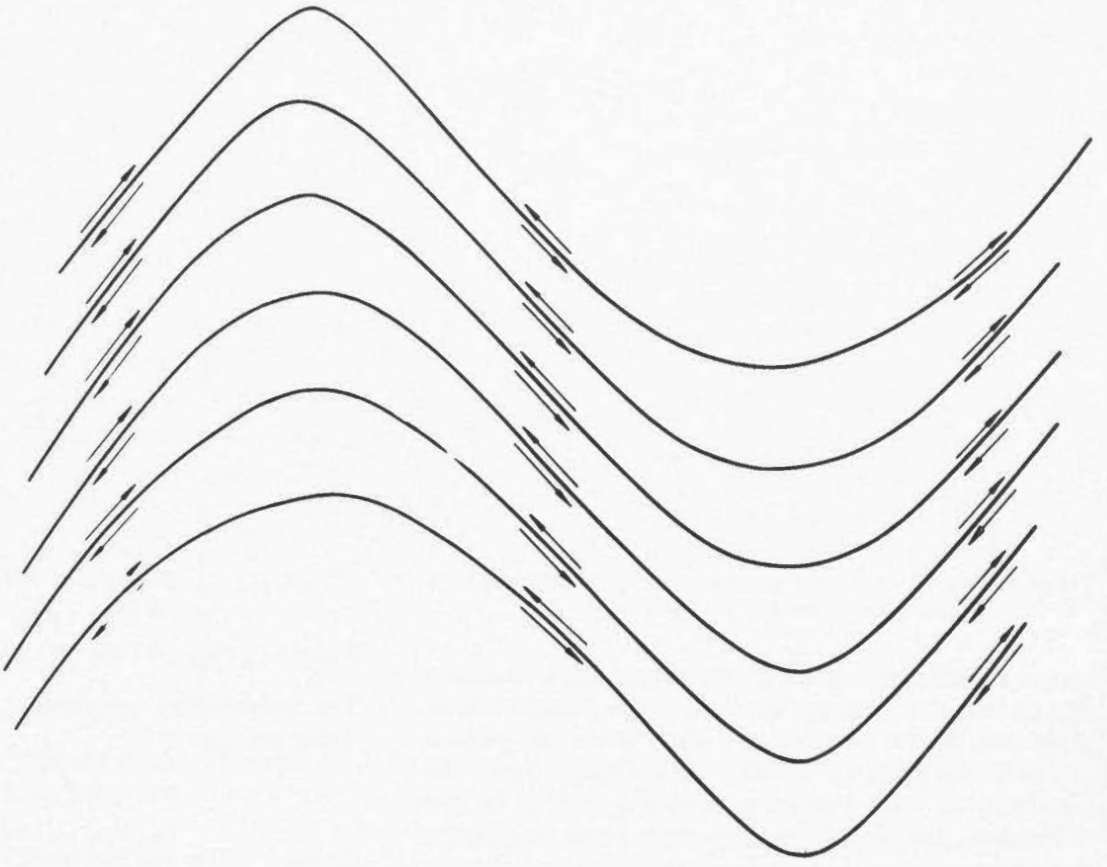

Figure 5. Fold deformation – dislocation distribution along layerlet boundaries.

focal processes. Even very general considerations lead to important conclusions regarding energy release in earthquake processes (Alpan and Teisseyre, 1966; Burridge and Knopoff, 1966). Apparent elastic moduli in the strain-release process determine the final deformation pattern as a function of distance from the earthquake fault. Therefore it would be essential to obtain for the focal process problem more realistic solutions of the dislocation field in a nonlinear medium.

Dislocation Density and its Relation to a Deformation State

Continuous dislocation distribution, or simply the field of dislocation density (Kondo, 1955a, 1955b; Kondo and Yuki, 1958; Bilby, *et al.*, 1955), seems in general to be the most powerful tool for describing a stress-strain pattern and combining the internal interactions of accumulated energy in a unified theory. The realistic picture of stress distribution and associated deformations can be obtained using the dislocation density. A proper distribution of dislocation density can approximate almost any stress system – for example, that due to cracks.

A deformation state is usually described by a displacement vector u_i, but, according to the general theorem (Kondo, 1955a, 1955b; Kondo and Yuki, 1958), a real deformed medium can be brought back to the ideal (stressless) state by means of the distortion tensor u_{ik} (nine components). This has only in special cases the potentials: $u_{ik} = \partial u_i/\partial x_k$. Thus the general deformation is described by the distortion u_{ik} which is related to the dislocation density by the rotation operator $\alpha_{mi} = \epsilon_{mks}\ (\partial u_{ik}/\partial x_s)$.

Similarly, as in the case of a dislocation, we can apply here the dynamic theory, coming thus to the field theory of internal processes in the Earth's interior. Stress self-interactions are also covered by the latter. Fold deformation (Figure 5) in a thin-layerlets structure has been discussed by R. Teisseyre (1966). Considerations on dislocation density flow in the Earth's interior (Teisseyre, 1967) raise some geophysical implications for the hypocentral plane problem in regions of troughs and ridges. It is worth noting that any singularities of the dislocation density field bring us back to the crack or dislocation theory of earthquakes.

However, the problem arises whether dislocations as large-scale units (in contrast to dislocations in crystals) really do exist in the Earth's interior or whether they should be regarded only as models of internal stress singularity. The mechanism of dislocation generation in a cross-zone was discussed in a paper (Teisseyre, 1961a). A cross-zone with fine boundary structure (e.g., crossing bands of thin layerlets) could generate dislocations with a Burgers vector equal to the individual distance between adjacent layerlets. This distance could serve

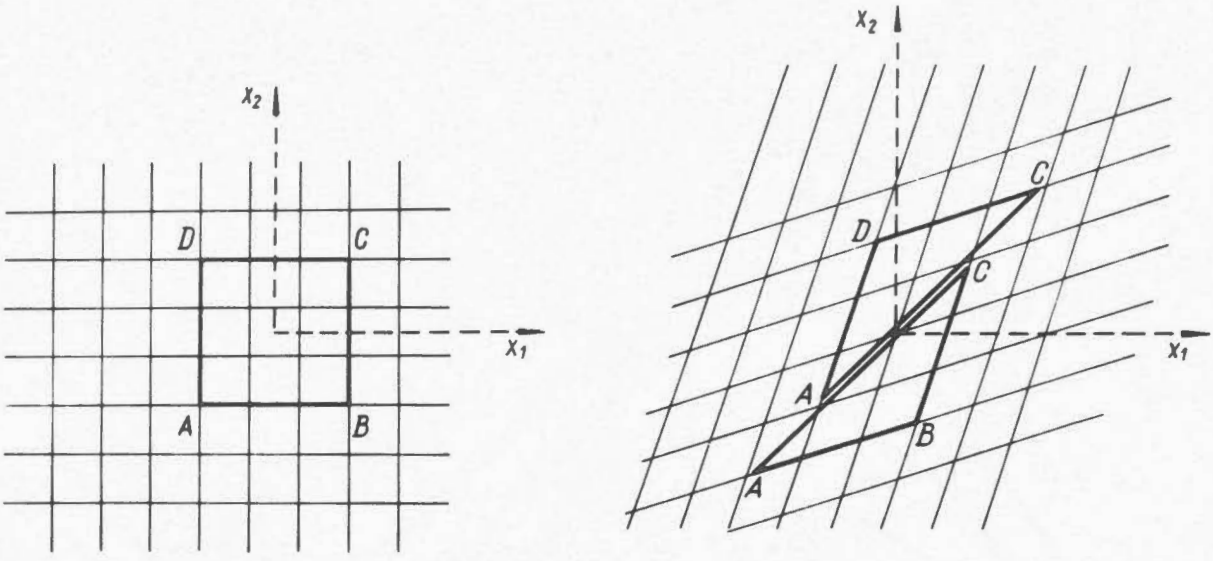

Figure 6. Shearing mechanism at cross-zone; appearance of gaps AA, CC in a formerly closed circuit ABCD.

here as a quantization factor for the Burgers vector of dislocation. Indeed, if we consider some dislocation elements located along some planes, we come to a plane interaction problem (forces of the order $1/r$ between the dislocation lines). The irregularity of their distribution favours generation of new dislocations. The problem corresponds to some extent to an irregular atomic lattice. A similar analogy is found when we consider generally some stress-concentration units. Their interaction pattern of type $1/r$ shows a large-scale analogy to an irregular plane lattice in which the stress-accumulation units correspond to some kind of centres in a superlattice.

Further, we would like to consider the dislocation distribution in a cross-zone at uniform shearing stresses. A shearing deformation in a cross-stratified medium can be treated as a plane problem with some dislocation density related to a displacement of discontinuous character along the laminar boundaries.

Assuming pure shear deformation in the $x_1 \cdot x_2$ plane to be given by e_{12} = constant, we have two distortion components u_{12} and u_{21} connected with this deformation by the relation

$$e_{12} = 1/2(u_{12} + u_{21}) = u_{(12)}.$$

These components must satisfy the equilibrium equations (Teisseyre, 1966). For the case $u_{ss} = u_{11} + u_{22} = 0$, one gets

$$u_{11,1} + u_{(12),2} = 0\,,\; u_{22,2} + u_{(12),1} = 0$$

$$1/2\,[u_{12} - u_{21}]_{,ss} = u_{[12],ss} = 0\;,\; s = 1,2.$$

These equations are satisfied when putting

$$u_{12} = k + mx_1 + nx_2,$$
$$u_{11} = -1/2(n + n')x_1 + 1/2(m + m')x_2$$
$$u_{21} = k' + m'x_1 + n'x_2,$$
$$u_{22} = 1/2(n + n')x_1 - 1/2(m + m')x_2$$

with $e_{12} = u_{(12)} = 1/2(k + k') + 1/2(m + m')x_1 + 1/2(n + n')x_2$

The nonvanishing components of the dislocation density tensor are given by

$$\alpha_{13} = u_{11,2} - u_{12,1} = 1/2(m' - m)$$
$$\alpha_{23} = u_{21,2} - u_{22,1} = 1/2(n' - n)$$

According to the general formula of the dislocation theory, the residual displacement due to non-closure of the contour *ABCD* (Figure 6) after deformation is given by

$$b_1 = \iint_{ABCD} \alpha_{13} dx_1 dx_2 = 1/2(m' - m)S$$
$$b_2 = \iint_{ABCD} \alpha_{23} dx_1 dx_2 = 1/2(n' - n)S$$

where S is the surface of *ABCD*. (The ends of the contour closed prior to deformation suffer certain displacements due to distortional deformation.) Demanding the Burgers vector to lie in the direction of maximum shear, we put $b_1 = b_2 = b/\sqrt{2}$. Hence $m' - m = n' - n = \sqrt{2}\, b/S$. For pure elastic deformation we have to put $m' = m = n' = n = 0$. Then the distortion elements can be derived from the displacement vector $u_{ik} = u_{i,k}$ with $u_1 = kx_2$ and $u_2 = k'x_1$, where the term k corresponds to elastic shear deformation.

Thus we see that dislocation density in a cross-layered zone is in this case equivalent to one, or to a number of, finite dislocations with the compound Burgers vector $\vec{b}$ $(b_1, b_2, 0)$. The structure of a cross-zone consisting of bands of layerlets favours the appearance of some finite dislocation under conditions of shearing deformation. It would seem that particular values of the Burgers vector are related to particular layer thicknesses. In this sense we suppose that a fine boundary structure could play the role of a quantization factor, but the arguments in favour of this hypothesis are still inadequate.

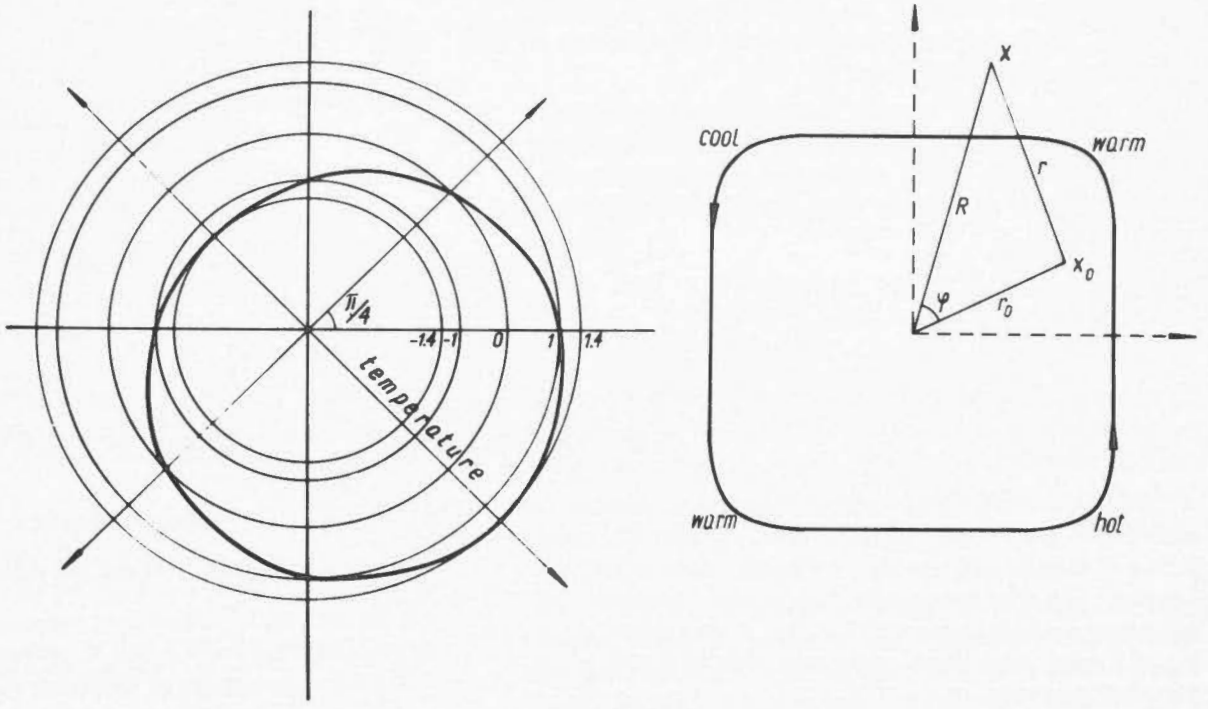

Figure 7. Angular temperature distribution in a convection cell.

Dislocation Density as Related to the Thermal Convection Field

The problem of thermal convection was so far discussed mainly from the viewpoint of convection cells, their hydrothermal properties and their distribution in the mantle. Convection theories are, of course, closely related to the hypothesis of tectonic development, while quantitative analysis of energy and stress distribution was treated only in the classical way.

In our present considerations, stress analysis is discussed with the assumption that relationships exist between thermal convection and dislocation density and its changes. Some results regarding the dislocation density field and dislocation flow, as applied to seismological and tectonic problems, were given in earlier papers (Teisseyre, 1966, 1967). A relationship between thermal stresses and the dislocation field was established by Muskhelishvili (1953) and discussed in connection with problems of earthquake origin and mechanism by the author (Teisseyre, 1963). An attempt to combine those findings in terms of dislocation density distribution as related to the thermal convection field is made in the following.

Let us first summarize some results given in our paper on the thermal field as applied to the problem of earthquake origin. Assume that the temperature distribution $T(x,y)$ is given by some regular function $T_0(x,y)$ and a part $T_1(x,y)$ which could represent a kind of singular thermal convection. Then we can write

$$T(x,y) = T_0(x,y) + T_1(x,y)$$
$$T_1 = \sum_k (\gamma_k x_k + \omega_k y_k) / r_k^2 \qquad (1)$$

where $x_k = x - x_k^0$; $y_k = y - y_k^0$; x_k^0 , y_k^0 are coordinates of singular convection centres; and γ_k , ω_k are coefficients defining these convections. The sum in Equation (1) represents the distribution of the convection centres. Each centre is connected with a discontinuity of displacement u,v where

$$\Delta_k(u + iv) = \frac{\pi\beta}{\lambda+\mu}(-\omega_k + i\gamma_k) \, , \; \beta = (\lambda + \frac{2}{3}\mu)\alpha.$$

Thus, according to the discussion given in the paper cited above (Teisseyre, 1963), each convection cell is equivalent to a dislocation with the Burgers vector $\vec{b}$ given by

$$b_x = \Delta u = -\frac{\pi\beta}{\lambda+\mu}\omega \; , \; b_y = \Delta v = \frac{\pi\beta}{\lambda+\mu}\gamma. \qquad (2)$$

The singular convection defined above does not fit, however, the temperature model of convection cells in the Earth's interior. The required convection model could be constructed by taking an appropriate distribution of the singular convections (x_k^0 , y_k^0) :

$$T_1 = \int\int \frac{\delta(r_0)\{(x-x_0)-(y-y_0)\}}{r^2} dx_0 dy_0 \qquad (3)$$

where $r^2 = (x - x_0)^2 + (y - y_0)^2$. We have passed to a continuous distribution of singular convection centres, choosing as convection coefficients the functions

$$\gamma = \delta(r_0)dx_0dy_0 \quad , \quad \omega = -\delta(r_0)dx_0dy_0$$

Each particular cell represents the angular temperature distribution, which for $r = 1$ is drawn schematically on the left side of Figure 7. This temperature distribution corresponds to

a convection cell defined in the classical way as an upward movement of hot and downward movement of cold masses as shown on the right side of Figure 7.

The same holds for the total field of temperature since in Equation (3) only the coefficient $\delta(r_0)$ enters. The coefficient $\delta(r_0)$, defining the radial distribution of convection cells, could be assumed as shown in Figure 8 and given in Equations (4):

$$\begin{aligned} &\text{for } r_0 < R_0 : && \delta(r_0) = 0 \\ &\text{for } R_0 \leqslant r_0 \leqslant R_1 : && \delta(r_0) = \delta \\ &\text{for } r_0 > R_1 : && \delta(r_0) = 0 \end{aligned} \tag{4}$$

R_0 and R_1 are certain distances which together with δ define the geometry of the convection cell. The values R_0 and R_1 could be identified with the inner and outer convection radii.

In Equation (3), which defines a convection model by its temperature distribution, we have used a continuous distribution of singular cells instead of a discrete distribution as in Equation (1). Correspondingly, we should determine the dislocation density tensor α_{mi} , in lieu of the Burgers vector b_m of a single dislocation, which was given in Equation (2). We would then have

$$\alpha_{xz} = \frac{\pi\beta}{\lambda+\mu}\delta(r_0) \ , \ \alpha_{yz} = \frac{\pi\beta}{\lambda+\mu}\delta(r_0) \tag{5}$$

where α_{xz} , α_{yz} represent the dislocation density as given by the number of dislocation lines intersecting a surface element with the normal in the z-direction. α_{xz} corresponds to the Burgers vector b_x , and α_{yz} to b_y . The stress field of a thermal convection is thus equivalent to a density field of dislocations.

We should at last compute the radial temperature distribution of the convection model given by Equations (4). From Equation (3) we get (see Figure 7)

$$T_1 = \int_0^{\infty}\int_0^{2\pi} \frac{\delta(r_0)\ \{\ (x-x_0)-(y-y_0)\ \}}{R^2 + r_0^2 - 2Rr_0\cos\phi}\, r_0 d\phi dr_0$$

We can further transform this integral to the form

$$T_1 = \frac{x-y}{R}\int_0^{\infty}\int_0^{2\pi} \delta(r_0)\ \frac{R - r_0\cos\phi}{R^2 + r_0^2 - 2Rr_0\cos\phi}\, r_0 d\phi dr_0$$

The last equation can be written as follows:

$$\begin{aligned} T_1 &= \frac{x-y}{R}\int_0^{\infty} \delta(r_0)\Phi r_0 dr_0 \ , \\ \text{with } \Phi &= \int_0^{2\pi} \frac{R - r_0\cos\phi}{R^2 + r_0^2 - 2Rr_0\cos\phi}\, d\phi \end{aligned} \tag{6}$$

Now we shall compute Φ , first for the case $a = \frac{r_0}{R} < 1$.

$$\Phi = \frac{1}{R}\int_0^{2\pi} \frac{1 - a\cos\phi}{1 + a^2 - 2a\cos\phi}\, d\phi = \frac{2\pi}{R}$$

For the case $\frac{R}{r_0} < 1$, we get analogously $\Phi = 0$.

Returning to Equations (6) and (4), we obtain for $R > R_1$, $(r_0 \leqslant R_1)$:

$$T_1 = \frac{x-y}{R}\,\frac{2\pi}{R}\int_{R_0}^{R_1} \delta\, r_0 dr_0 = \frac{x-y}{R}\,\delta\pi\,\frac{(R_1^2 - R_0^2)}{R} \tag{7}$$

For $R_0 < R < R_1$ we get:

$$T_1 = \frac{x-y}{R}\,\frac{2\pi}{R}\int_{R_0}^{R} \delta\, r_0 dr_0 = \frac{x-y}{R}\,\delta\pi\,\frac{(R^2 - R_0^2)}{R} \tag{8}$$

For $R \leqslant R_0$ we get

$$T_1 = 0$$

Thus Equation (7) represents the distribution of temperature outside the convection region, and Equation (8) that inside it. The corresponding radial distribution is given on the right side of Figure 8; the diagram on the left side represents the cell distribution, Equation (4), tantamount to dislocation density, Equation (5). Equation (5) defines also the direction of the Burgers vectors indicated on Figure 9.

Considering now two neighbouring thermal convection cells with equal circulation, we get a stress distribution equivalent to a dislocation density as marked by a few dislocation sections on Figure 9. Let us consider a dislocation pair, $A'B'$, in the

Figure 8. Radial distribution of cell density and corresponding radial distribution of temperature in a convection unit.

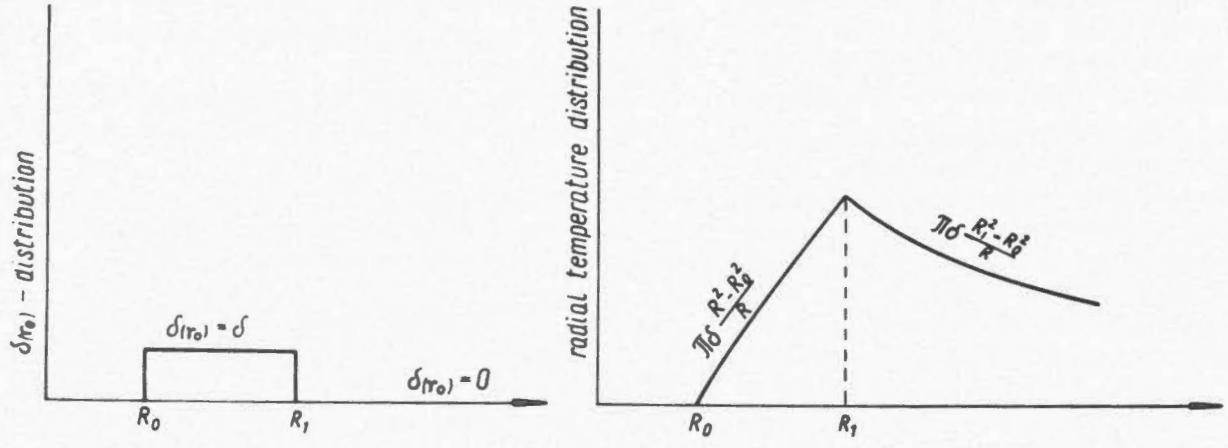

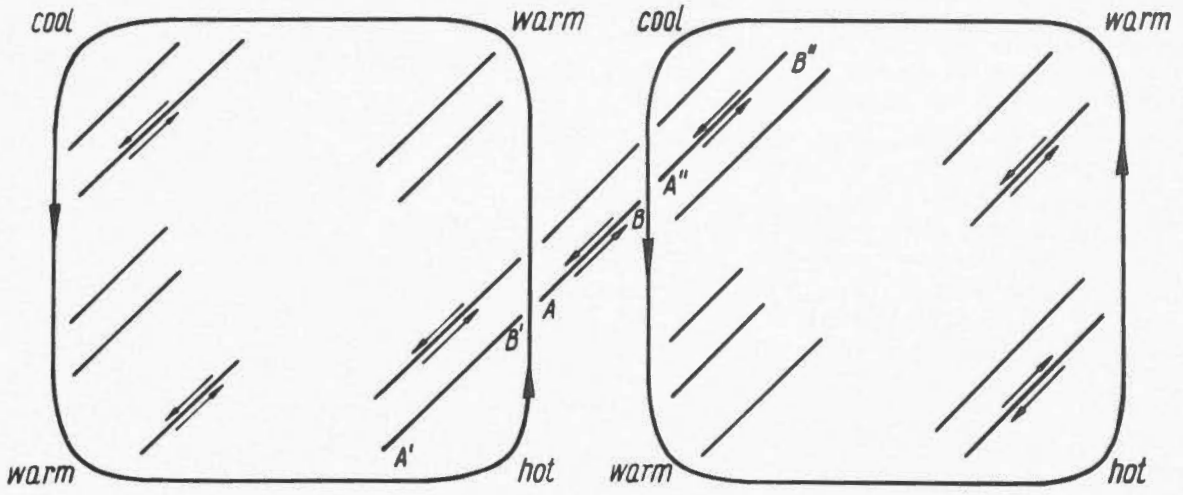

Figure 9. Equivalent (to thermal stresses) dislocation density and energy release mechanism between neighbouring convection units.

left cell and $A''B''$ in the right cell. Both dislocations are apparent, but the equivalent stresses due to the thermal field really do exist. Dislocations B' and A'' have opposite signs and therefore can mutually annihilate by the joining process. This, however, can be also realized by the creation of a real dislocation pair AB of the same characteristics as $A'B'$ and $A''B''$. Thus the stress field of thermal convections could decrease when the real slips occur in the region between neighbouring cells. This mechanism is, considering stresses, quite equivalent to a pair creation AB or annihilation $B'A''$ as in a simple dislocation mechanism (Figure 2).

In the usual case we consider two convection cells with opposite circulations, that is, with common (upward or downward) sense of movement in their adjacent parts. In the present case, the respective stress pattern is more complicated. However, similar arguments can be used when considering the joining process, with thermal stresses and dislocation occurrences as counterparts.

Dislocation Flow along a Hypocentral Plane System

The basic idea of the dislocation theory of earthquakes lies in an interaction problem between energy concentration units. Dynamic development of a strain pattern in the Earth's interior needs to allow units of energy accumulation to be able to slowly move and adjust themselves to the actual stress pattern. Thus, it is here assumed that separate dislocations can move and in this way their self-energy is dragged along.

In this meaning one can consider a dislocation flow as describing the processes of energy which drag along some active planes. In this approach one can further take into account any changes of dislocation density due to generation of dislocations in some internal zones as well as annihilation of dislocations in the processes of energy release. Earthquake zones, that is, zones of energy release, can be along the same hypocentral plane more or less displaced in relation to the zones, where dislocations are formed. A dislocation flow joins here these counterparts in an unique physical process. The assumed existence of a dislocation flow could be also directly related to the large-scale thermal convections.

The general pattern of dislocation flow can be obtained by considering boundary conditions for dislocation density flow in a layered medium (Teisseyre, 1967). According to results presented in the quoted paper, the following system of equations governs the processes of dislocation flow I_{kmn}. In the case of a screw dislocation flow, Equations (9) and (10) below follow from Equations (35) in the quoted paper.

$$(C_0/I^0_{221}) \sum_{i=1}^{n} \dot{\beta}^{(i)}_{32} = 1-(\tan\alpha_0/\tan\alpha_n) \tag{9}$$

$$(C_0/2I^0_{221})\ (dp_{32}/dt) = \mu_n-\mu_0-\mu_n(C_0/I^0_{221}) \sum_{i=1}^{n} \dot{\beta}^{(i)}_{32} \tag{10}$$

In the case of an edge dislocation flow, Equations (11) to (13) follow from Equations (42) in the paper mentioned.

$$(C_0/I^0_{323}) \sum_{i=1}^{n} \dot{\beta}^{(i)}_{31} = \{\mu_0(1+\cot^2\alpha_0)/\mu_n(1+\cot^2\alpha_n)\}-1 \tag{11}$$

$$(-C_0/2I^0_{323})\ (dp_{31}/dt) = \mu_n-\mu_0+\mu_n\,(C_0/I^0_{323}) \sum_{i=1}^{n} \dot{\beta}^{(i)}_{31} \tag{12}$$

$$\frac{C_0}{2I^0_{323}}\frac{dp_{33}}{dt} = \mu_0\cot\alpha_0\,\{A^{1/2}(\frac{\mu_n}{\mu_0}\sec^2\alpha_0-\frac{\mu_n^2}{\mu_0^2}A\tan^2\alpha_0)^{1/2}-1\} \tag{13}$$

with $A = 1 + (C_0/I^0_{323}) \sum_{i=1}^{n} \dot{\beta}^{(i)}_{31}$

$\dot{\beta}^{(i)}_{31}$, $\dot{\beta}^{(i)}_{32}$ are the time rates of dislocation density changes in relation to a separate layer i; $\sum_{i=1}^{n} \dot{\beta}^{(i)}_{3k}$ represents the respective

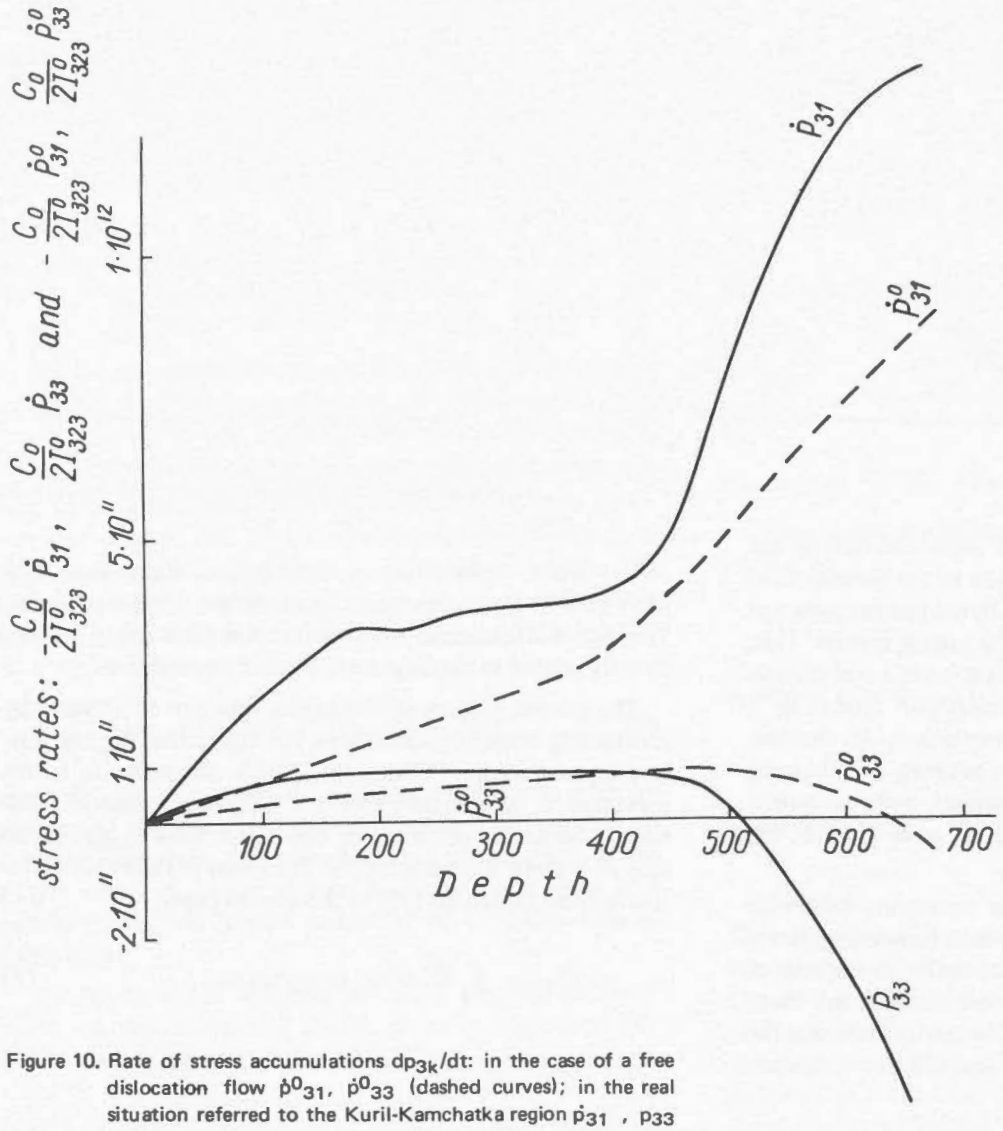

Figure 10. Rate of stress accumulations dp_{3k}/dt: in the case of a free dislocation flow $\dot{p}^0_{31}$, $\dot{p}^0_{33}$ (dashed curves); in the real situation referred to the Kuril-Kamchatka region $\dot{p}_{31}$, p_{33} (solid curves).

sum over n layers. The time rate $\dot{\beta}^{(i)}_{3k}$ is understood as the difference of generation rate and annihilation of dislocations.

The case $\dot{\beta}^{(i)}_{3k} = 0$ represents a free dislocation flow; here the generation rate of dislocations is at the same place compensated by annihilation processes. In the case of screw dislocations, the resulting plane of dislocation flow has constant inclination α , but in the case of edge dislocation, the respective plane bends as is shown on Figure 11. The stress rates $\frac{dp_{3k}}{dt}$ are given on Figure 10 by dashed lines (Teisseyre, 1967).

In a general case with $\dot{\beta}_{3k} \neq 0$, there can be achieved a comparison of the theoretical results with the form of a hypocentral plane and the release of earthquake energy at different depths along that plane. The case of a screw dislocation flow would correspond to a horizontal displacement along a fault, for example, the San Andreas. The case of an edge dislocation flow corresponds to a dip-slip displacement, and thus displacement normal to the trend of the structure is observed. This is, according to Hodgson (1962) and also Balakina (1962), the case of the west Pacific system of arcuate structures. For the Kuril-Kamchatka trench, for example, the tentative form of the hypocentral plane is given on Figure 11, as follows from the distribution of foci (Gadomska and Teisseyre, 1968). The corresponding angles of inclination as a function of depth $\alpha(z)$ allow us to compute $\sum_{i=1}^{n} \dot{\beta}^{(i)}_{31}$ and $\dot{\beta}^{(i)}_{31}$ itself (Equation 11). The stress rates $(-C_0/2I^0_{323})(dp_{31}/dt)$ and $(C_0/2I^0_{323})(dp_{33}/dt)$ are computed after Equations (12) and (13). These results are presented on Figure 10. Worth noting is the increase of $\dot{p}_{31}$ with depth, suggesting that very deep processes highly influence the earthquake occurrences. Below the depth of 500 km the values of $(C_0/2I^0_{323})\dot{p}_{33}$ become less than zero.

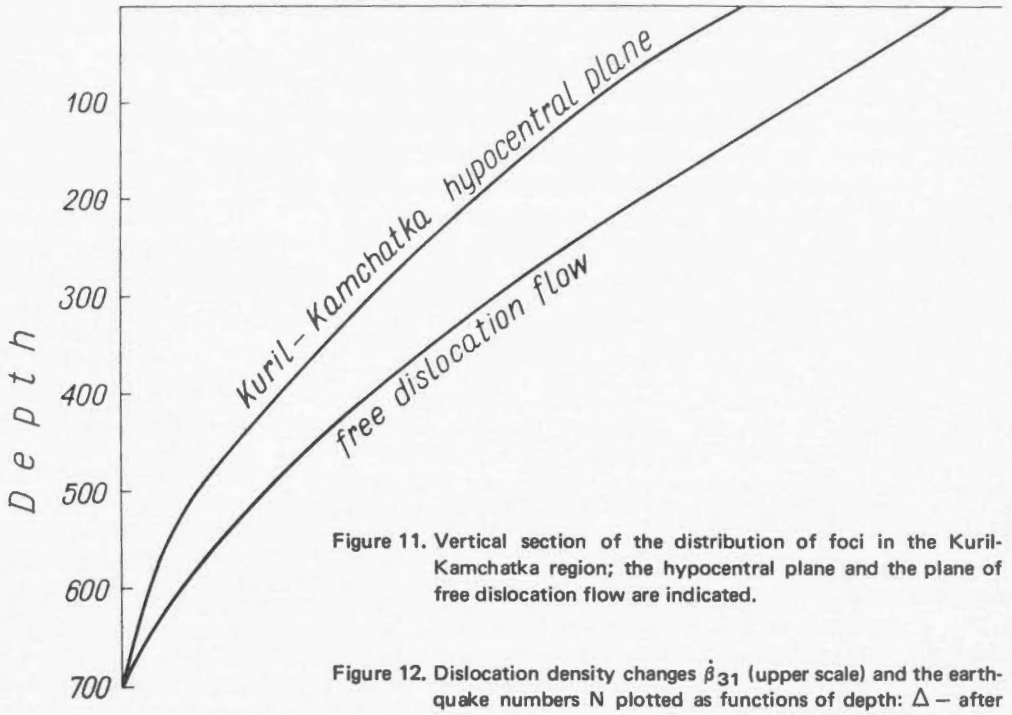

Figure 11. Vertical section of the distribution of foci in the Kuril-Kamchatka region; the hypocentral plane and the plane of free dislocation flow are indicated.

Figure 12. Dislocation density changes $\dot{\beta}_{31}$ (upper scale) and the earthquake numbers N plotted as functions of depth: Δ – after Sykes (1966), ○ – after Gadomska and Teisseyre (1968).

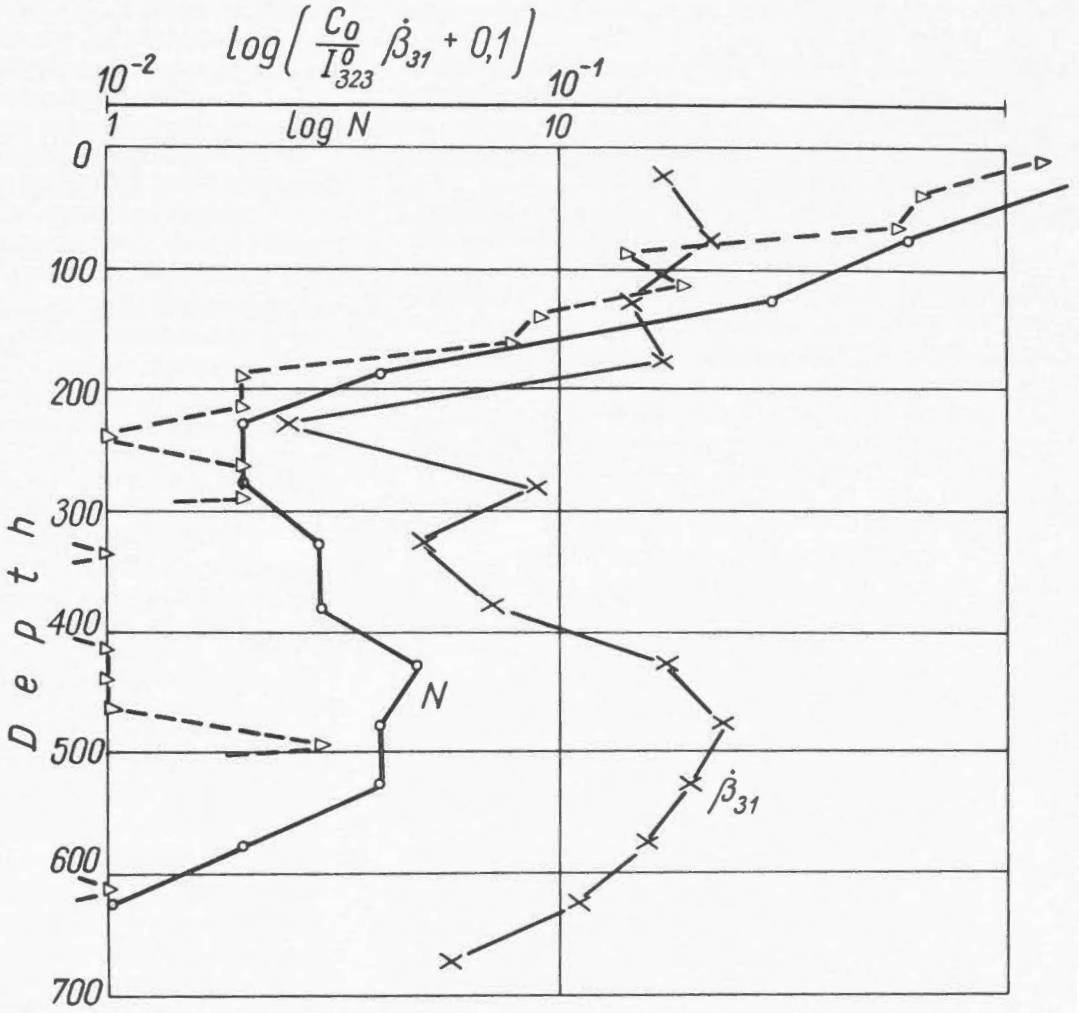

This fact can be probably interpreted only as related to the change of direction of the dislocation flow. Thus, probably the dislocation current in the range 0 – 500 km would meet at that depth the countercurrent existing in the range 500 – 700 km depth. This fact can be related to the earthquake activity increase as follows from Figure 12 giving log N plotted as a function of depth. The numbers of earthquakes N in the Kuril-Kamchatka region for the 50 km intervals of depth (Gadomska and Teisseyre, 1968) and for the 25 km intervals (Sykes, 1966) are furthermore compared with the computed values $\hat{\beta}_{31}$. The result is presented on Figure 12.

References

Alpan, I., and R. Teisseyre, 1966. The energy balance in faults. *Bull. Inter. Inst. Seis. and Earth. Eng.*, 3, 53-69.

Balakina, L.M., 1962. Overall regularities in the directions of the principal stresses acting at the foci of earthquakes of the Pacific Ocean seismic belt. *Akad. Nauk SSSR, Izv. ser. geofiz.* 11, 1471-1483; in the Eng. ed. 918-926

Ben-Menahem, A., 1961. Radiation of seismic surface waves from finite moving sources, *Bull. Seism. Soc. Am.* 51, 401-435.

Bilby, B.A., R. Boullough, and E. Smith, 1955. Continuous distributions of dislocations: a new application of the methods of non-Riemannian geometry. *Proc. Roy. Soc. Lond., A*, 231, 263-273.

Biot, M.A., 1956. Thermoelasticity and irreversible thermodynamics. *J. Appl. Phys.* 27, 240-253.

Burridge, R., and L. Knopoff, 1966. The effect of initial stress or residual stress on elastic energy calculations. *Bull. Seism. Soc. Am.*, 56, 421-424.

Chinnery, M.A., 1961. The deformation of the ground around surface faults. *Bull. Seism. Soc. Am.*, 51, 355-372.

Droste, S., and R. Teisseyre, 1959. The mechanism of earthquakes according to dislocation theory. *Sci. Rep. Tôhoku Univ., Ser. 5, Geoph.*, 11, 55-71.

Eshelby, J.D., F.C. Frank, and F.R.N. Nabarro, 1951. The equilibrium of linear arrays of dislocations. *Phil. Mag.*, 42, 351-364.

Gadomska, B., and R. Teisseyre, 1968. Energy release distribution in Tonga-Kermadec and Kuril-Kamchatka regions and the hypothesis of dislocation flow (in preparation).

Griffith, A.A., 1921. The phenomenon of rupture and flow in solids. *Phil. Trans. Roy. Soc. Lond., A*, 221, 163-198.

Hodgson, J.H., 1962. Movements in the earth's crust as indicated by earthquakes. In: *Continental Drift*, S.K. Runcorn (ed.), Academic Press, New York, 67-102.

Housner, G.W., 1955. Properties of strong ground motion earthquakes. *Bull. Seism. Soc. Am.*, 45, 197-218.

Kasahara, K., and R. Teisseyre, 1966. A dislocation model of earthquake swarms. *Bull. Earthq. Res. Inst.*, 44, 793-810.

Kondo, K., 1955a. Geometry of elastic deformation and incompatibility. *RAAG Memoirs, Div. C.*, 1, 361-373.

Kondo, K., 1955b. Non-Riemannian geometry of imperfect crystals from a macroscopic viewpoint. *RAAG Memoirs, Div. D.*, 1, 458-469.

Kondo, K., and M. Yuki 1958. On the current viewpoints of non-Riemannian plasticity theory. *RAAG Memoirs, Div. D.*, 2, 202-226.

Miyamura, S., S. Omote, R. Teisseyre and E. Vesanen, 1965. Multiple shocks and earthquake series pattern. *Bull. Inter. Inst. Seis. and Earth. Eng.*, 2, 71-92.

Mogi, K., 1963a. The fracture of a semi-infinite body caused by an inner stress origin and its relation to the earthquake phenomena (Second paper). *Bull. Earthq. Res. Inst.*, 41, 595-614.

Mogi, K., 1963b. Some discussions of aftershocks, foreshocks and earthquake swarms – the fracture of a semi-infinite body caused by an inner stress origin and its relation to the earthquake phenomena (Third paper). *Bull. Earthq. Res. Inst.*, 41, 615-658.

Muskhelishvili, N.I., 1953. *Some Basic Problems of the Mathematical Theory of Elasticity*, P. Noordhoff, Groningen, Holland, 704 p.

Nabarro, F.R.N., 1951. The synthesis of elastic dislocation fields. *Phil. Mag.*, 42, 1224-1231.

Savage, J.C., 1965. The effect of rupture velocity upon seismic first motions. *Bull. Seism. Soc. Am.*, 55, 263-275.

Steketee, J.A., 1958. Some geophysical applications of the elasticity theory of dislocations. *Can. J. Phys.*, 36, 1168-1198.

Sykes, L.R., 1966. The seismicity and deep structure of island arcs. *J. Geophys. Res.*, 71, 2981-3006.

Teisseyre, R., 1961a. Dynamic and time relations of the dislocation theory of earthquakes. *Acta Geophys. Polon.*, 9, 3-58.

Teisseyre, R., 1961b. A dislocation theory of the earthquake processes. *Bull. Ac. Pol. Sci., Ser. math., astro., phys.*, 9, 423-428.

Teisseyre, R., 1963. Thermomechanical model of the earthquake origin and process. *Acta Geophys. Polon.*, 11, 229-234.

Teisseyre, R., 1964. Dislocation systems and their interaction in shock sequence. *Acta Geophys. Polon.*, 12, 23-36.

Teisseyre, R., 1966. Density field of dislocations and fold deformation problem. *Bull. Earthq. Res. Inst.*, 44, 153-165.

Teisseyre, R., 1967. Dislocation flow through a layered earth structure. *Bull. Earthq. Res. Inst.*, 45, 359-374.

Tsuboi, C., 1958. On seismic activities in and near Japan. In: *Contributions in Geophysics* H. Benioff, *et al.* (eds.), Pergamon Press, New York, 87-112.

Vvedenskaya, A.V., 1956. The determination of displacement fields in earthquakes by means of dislocation theory. *Akad. Nauk SSSR, Izv. ser. geofiz.*, 3, 277-284.

Vvedenskaya, A.V., 1958. On the displacements on a surface of rupture accompanied by sliding. *Akad. Nauk SSSR, Izv. ser. geofiz.*, 2, 175-183; in the Eng. ed. 102-105.

Vvedenskaya, A.V., 1959. The displacement field associated with discontinuities in an elastic medium. *Akad. Nauk SSSR, Izv. ser. geofiz.*, 4, 516-526; in the Eng. ed. 357-362.

Vvedenskaya, A.V., 1965. Investigation of the dependence of the displacements in body waves on the extension and rate of propagation of the dislocation. *Akad. Nauk SSSR, Izv. Fizika Zemli*, 1, 3-11; in the Eng. ed. 1-5.

Weertman, J., 1965. Relationship between displacements on a free surface and the stress on a fault. *Bull. Seism. Soc. Am.*, 55, 945-953.

THEORETICAL FAULT MODELS

Michael A. Chinnery

Department of Geological Sciences
Brown University
Providence, R.I., U.S.A.

ABSTRACT: A number of theoretical models which may be applied to the study of fault mechanics are reviewed, with particular emphasis on the boundary conditions assumed for the surfaces of the crack. The displacements and stresses which arise on the boundaries of the crack under the action of an applied shear stress are derived for each model. Particular consideration is given to the model which includes a frictional stress that increases linearly with depth. As an application of these models, the stress drops associated with some real faults are calculated in several ways using a variety of fault parameters. The calculated stress drops for vertical strike slip faults show a very small spread, and generally lie within the range of 30 to 60 bars. Similar calculations for dip slip faults have a much larger spread, probably because of inadequate field data. A discussion of the usefulness of more complex fault models is included.

RÉSUMÉ: L'auteur passe en revue un certain nombre de modèles théoriques pouvant servir à l'étude du mécanisme des failles, mettant particulièrement en relief les conditions de limite admise pour les surfaces de la fissure. La détermination des déplacements et des contraintes subis par les bords de la fissure sous l'action d'un effort de cisaillement est alors effectuée pour chaque modèle. Le modèle qui englobe une contrainte de friction augmentant linéairement en profondeur fait l'objet d'une attention particulière. En se servant de ces modèles, les baisses de contraintes dans des failles réelles sont calculées de plusieurs façons avec divers paramètres de faille. Il est démontré que les baisses de contraintes calculées dans le cas de failles verticales à glissement transversal présentent une très faible dispersion; elles se situent généralement entre 30 et 60 bars. L'application de calculs analogues à des failles à rejet vertical révèle une plus grande dispersion due probablement à l'inexactitude des données relevées sur le terrain. Suit l'étude de l'utilité de modèles de failles plus complexes.

Introduction

The purpose of this paper is to review those theoretical approaches to fracture that have application to the study of faulting in the earth's crust. A great many papers have been published on the mechanics of cracks and holes in elastic media, beginning with the classic work of Inglis (1913) and Griffith (1921), and the mathematical foundations for many of the more sophisticated models were set up even earlier by the Italian school of mathematicians, notably by Volterra (1907). In addition to the amount of work that has been carried out, the situation is further confused by the variety of contexts in which the theoretical models have been applied, and also by the number of different journals in which the various models are described.

To illustrate this diversity, we can compare the approaches to fracture of the engineer, the metallurgist and the geologist. In engineering studies a crack is often regarded as a model of a flaw in a mechanical structure, which, under the action of certain applied stresses (often tensile), may become a potential source of failure. Within a crystal lattice, the crack becomes a model of a dislocation. In this case the metallurgist is concerned less with failure and more with the nature of the crystal lattice and the interatomic bond. To the geologist, the crack is a model of a fault and he is often concerned with the sudden fault movements that accompany earthquakes. Unfortunately, these different approaches have led to a series of different concepts and mathematical treatments that have tended to obscure the underlying similarity of the problems involved.

The largest volume of information is to be found in the engineering literature (for a recent review, see for example, Paris and Sih, 1965). Much of this work has been devoted to the two-dimensional situation, corresponding to a crack or a hole in a thin plate. The edges of the crack are usually assumed to act as free surfaces, and in the case of thin cracks, even the frictional stresses between the faces of the crack are assumed negligible. The application of this model to faulting in the earth's crust is clearly rather dubious, because of the large compressive stresses present within the earth. In spite of this, there have been a number of studies of fault mechanics which have been based on this model.

The approach of the crystal physicist has diverged from that of the engineer with the introduction of the concept of the dislocation line. This concept arises in the study of discontinuous media such as a crystal-lattice, and its direct application to a continuous elastic solid is not obvious. More recently, the theory has been expanded to include the possibility of continuous distributions of dislocation lines. Using this idea many of the results of crystal dislocation theory may now be applied directly to an elastic medium. There are, however, still some serious problems of communication involved; for example, the crystal physicist will often specify a dislocation distribution function rather than a displacement vector.

An important contribution to the theory of fracture in an elastic solid arose in the work of Steketee (1958a), who reformulated the earlier work of Volterra (1907) into a form directly applicable to the general problem of a three-dimensional crack in an elastic medium, with a general interaction

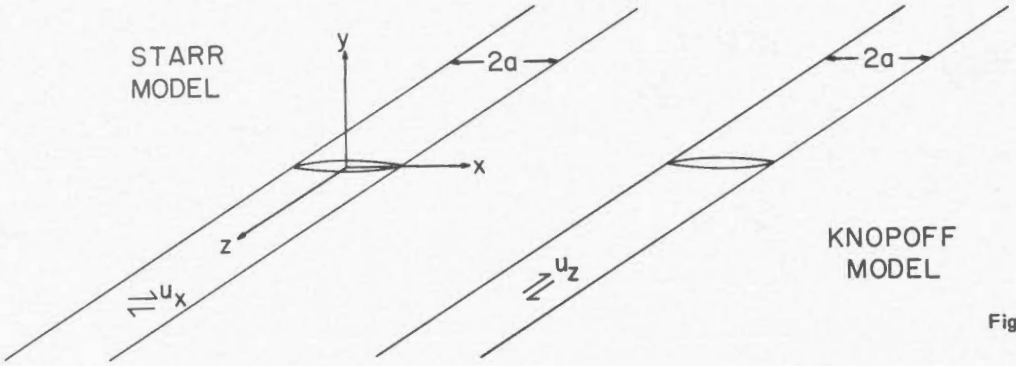

Figure 1. Diagrammatic representation of the two-dimensional crack models of Starr (1928) and Knopoff (1958).

between the faces of the crack. Steketee distinguished his theory from that of crystal physics by calling it the elasticity theory of dislocation. In principle his model is based on the same foundations as that of crystal dislocation theory, but instead of the dislocation line, Steketee introduced clearly the idea of a dislocation surface. In spite of some rather formidable analytical difficulties, Steketee's theory has opened the way to a variety of investigations concerned with three-dimensional cracks and faults within an elastic medium.

The models which we shall discuss in the following sections are those which are most commonly applied to the analysis of faulting. Although the original authors may have considered other cases, we shall be concerned with the analysis of a closed crack in an elastic medium subjected to a shear stress. Also, where possible, we shall make the crack intersect the surface of a semi-infinite medium, and include the boundary condition of zero stress, together with a frictional stress due to gravitational pressure which increases with depth. We shall be particularly concerned with the boundary conditions which are assumed for the surface of the crack.

We shall only consider the simplest types of fault model, such as the vertical strike slip fault in a semi-infinite elastic medium, though the mathematical techniques are available for studying more complex models (including dipping faults, nonelastic earth properties, etc.). Our reason for this is important. As we shall see, the field observations, with which the model predictions must be compared, are few and uncertain. In many cases, the introduction of new parameters into the simple problem is enough to make a unique solution impossible. In the geological literature, this point has not received the attention that it deserves.

As an example of the application of these models, we shall examine the change in stress which accompanies the formation of a fault, the so-called 'stress drop'. It was shown several years ago (Chinnery, 1964) that the stress drop calculated on a simple model was between one and two orders of magnitude less than the commonly accepted strength of crustal rocks. Since that time, more sophisticated methods of analysis have become available, and many more faults have been investigated. The present study has been prompted by a recent paper by Brune and Allen (1967), who calculated the stress drop for a number of observed faults, and concluded that the large spread in their results indicated a "wide variation in the character of ruptures that occur in surface faulting." In the last section of this paper, we shall re-examine this conclusion in the light of a more thorough review of the fault models concerned.

Two-dimensional Crack Models

As examples of the analysis of an infinitely long crack situated within an elastic medium, where the edges of the crack are assumed to act as free surfaces, we shall consider two cases. The first was described by Starr (1928) and the second by Knopoff (1958). The geometry of the models and the orientation of the coordinate axes which will be used throughout this paper, are shown diagrammatically in Figure 1. In each case the faces of the crack are in contact, that is, the crack has no thickness in the y direction.

Starr (1928) considered the deformation of a two-dimensional elliptical crack under the action of a shear stress $S = \tau_{xy}$, applied at infinity. This causes a displacement of the sides of the crack in the x direction, which varies as a function of x. The results which are quoted below are obtained from Starr's model by setting the minor axis of his ellipse equal to zero. The variation in displacement across the crack is then found to be

$$U(x) = \frac{Sa}{2}\frac{(\lambda+2\mu)}{\mu(\lambda+\mu)}\left(1-\frac{x^2}{a^2}\right)^{1/2} \quad \text{for } |x| \leqslant a \qquad (1)$$

where a is the half width of the crack, and λ and μ are Lamé's elastic constants. This displacement variation is shown at the top of Figure 2. The maximum offset occurs at the centre of the crack; if $\lambda = \mu$ it is given by

$$U_m = 2U(0) = \frac{3}{2}\frac{Sa}{\mu} \qquad (2)$$

Since in the absence of the crack the stress at the origin would be S, and after the insertion of the crack the stress (because of the boundary condition on the crack surface) is zero, the change in stress due to the occurrence of the movement $U(x)$ is given by

$$\Delta\tau = S = \frac{2}{3}\frac{U_m \mu}{a} \tag{3}$$

However, at points adjacent to the crack the initial shear stress will not necessarily be relieved. In fact, Starr's theory shows that the shear stress along the x axis is given by

$$\begin{aligned} \tau_{xy} &= 0 && \text{for } |x| \leqslant a \\ \tau_{xy} &= \frac{Sx}{(x^2-a^2)^{1/2}} && \text{for } |x| \geqslant a \end{aligned} \tag{4}$$

The stress near the tip of the crack becomes extremely large.

It is useful to rewrite these results in a slightly different form. The effect of the displacement $U(x)$ given by Equation (1) is to produce a stress of magnitude $-S$ on the faces of the crack. We can therefore define a stress $\tau(x)$ which is the result of imposing $U(x)$ on a crack in an unstressed medium. Then:

$$\begin{aligned} \tau(x) &= -S && \text{for } |x| \leqslant a \\ \tau(x) &= S\left[\frac{x}{(x^2-a^2)^{1/2}} - 1\right] && \text{for } |x| \geqslant a \end{aligned} \tag{5}$$

This stress variation is shown at the bottom of Figure 2. We shall use these symbols $U(x)$ and $\tau(x)$ in the same way throughout this paper. We can regard the quantity S as being defined by Equation (2).

The general problem for the displacements and stresses at any point throughout the medium may be solved (for example) by the methods of Muskhelishvili (1953) in one of two ways. The displacements may be specified along the x axis as:

$$\begin{aligned} U &= U(x) && \text{for } |x| \leqslant a \\ U &= 0 && \text{for } |x| \geqslant a \end{aligned} \tag{6}$$

or the crack may be regarded as a mixed boundary value problem where:

$$\begin{aligned} \tau &= \tau(x) && \text{for } |x| \leqslant a \\ U &= 0 && \text{for } |x| \leqslant a \end{aligned} \tag{7}$$

These two approaches are equivalent, and there is, as we shall see, a relation between $U(x)$ and $\tau(x)$. The presence or absence of the applied stress S is, of course, of no consequence to the analysis of the problem, since we are dealing with linear elasticity.

The crack model described by Knopoff (1958) is very similar to that of Starr, except that the applied stress $S = \tau_{yz}$, and the resulting displacement is parallel to the length of the crack, i.e., the z axis. The displacements and stresses at the crack are then given by

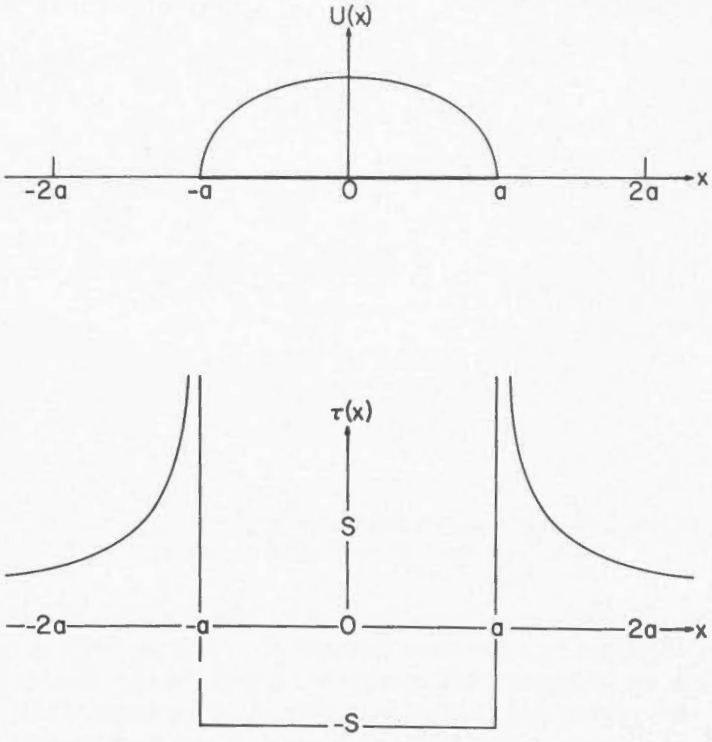

Figure 2. The displacements and stresses along the x axis for the models shown in Figure 1. In Starr's model $U = U_x$ and $\tau = \tau_{xy}$. In Knopoff's model $U = U_z$ and $\tau = \tau_{yz}$.

$$\begin{aligned} U(x) &= \frac{Sa}{\mu}\left(1-\frac{x^2}{a^2}\right)^{1/2} && \text{for } |x| \leqslant a \\ \tau(x) &= -S && \text{for } |x| \leqslant a \\ \tau(x) &= S\left[\frac{x}{(x^2-a^2)^{1/2}} - 1\right] && \text{for } |x| \geqslant a \end{aligned} \tag{8}$$

The functional form of $U(x)$ and $\tau(x)$ are the same as in Starr's model, and correspond to the diagrams in Figure 2. Once again, the stresses at the tip of the crack are very large. The maximum offset and stress drop on Knopoff's model are then

$$\begin{aligned} U_m &= \frac{2Sa}{\mu} \\ \Delta\tau = S &= \frac{1}{2}\frac{U_m \mu}{a} \end{aligned} \tag{9}$$

Since $\tau_{xy} = 0$ on $x = 0$, we may use Knopoff's analysis to investigate a vertical strike slip fault of infinite extent (see Figure 3.). The x axis points into the earth, and $\tau(x)$ is the stress change at the fault associated with a fault movement which varies with depth according to $U(x)$. Physically, the infinite stress at the lower edge of the fault model suggests that the fault will tend to propagate downwards. (Note that Starr's model cannot be used in the same way to model a dip slip fault, since τ_{xy} is not equal to zero at all points on the plane $x = 0$).

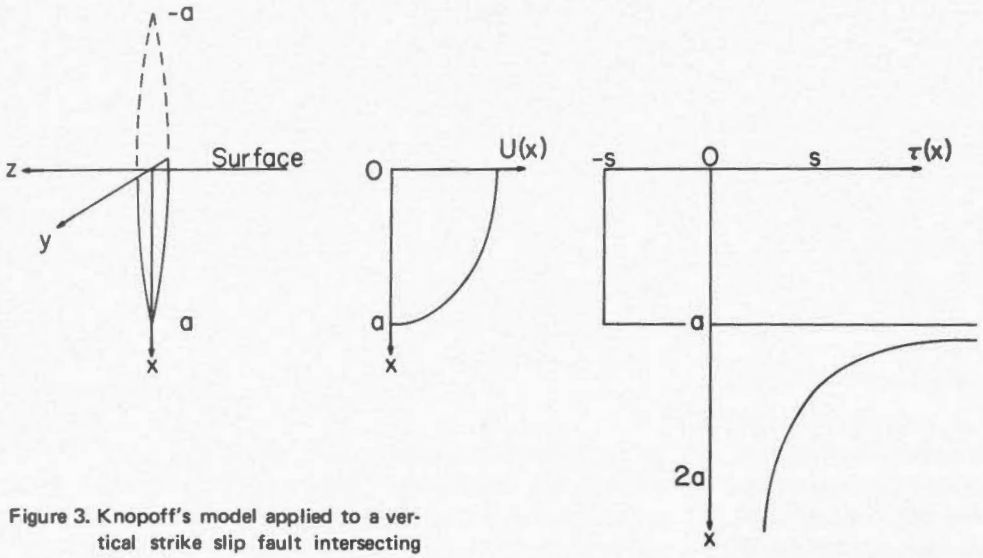

Figure 3. Knopoff's model applied to a vertical strike slip fault intersecting the surface.

The basic fault model described by Starr and Knopoff can be critized for a number of reasons. One of the most important is the assumption that the edges of the crack are free. Many of the original crack models were designed for the study of tension cracks or holes within a material. Where the edges of a crack are held apart, the assumption is probably reasonable. However, in a material in compression, such as the earth, this is not so. Analytically, the simple model assumes that τ_{xy}, τ_{yy} and τ_{yz} are zero on the crack surface.

Within the earth, or within any material in compression, the faces of the crack must be in contact, and stress may be transmitted across them. Thus, τ_{xy}, τ_{yy} and τ_{yz} will generally not be zero, and we must only require that the stresses are continuous across the crack surfaces after failure. Mathematically, we must view the edges of the crack as being 'welded' together after the failure has occurred. Within the earth, for example, the value of τ_{yy}, because of gravitational compression is likely to exceed any of the shear stresses involved, at a depth of only a few kilometers.

This leads us to consider a new model, in which the stresses are continuous across the edges of the crack, and are specified on the crack surface. In the simplest case, we may suppose that movement on the fault is opposed by a constant frictional stress S_f, which could be, for example, the normal pressure on the crack surfaces (τ_{yy}) multiplied by a frictional coefficient n. If we assume S_f is constant, and that the external applied stress is S, the stress drop due to the movement is constant, and is given by

$$\Delta\tau = S - S_f \tag{10}$$

We have therefore to solve the problem of a crack in which the shear stress is specified on the surface of the crack to have the form

$$\begin{aligned} \tau(x) &= -\Delta\tau \qquad \text{for } |x| \leqslant a \\ U(x) &= 0 \qquad\quad \text{for } |x| \geqslant a \end{aligned} \tag{11}$$

The solution for this problem can be deduced immediately from the models of Starr or Knopoff, or they can be obtained from Muskhelishvili (1953). We find exactly the same forms for the displacements and stresses involved as those given in Equations (1), (5) and (8) (depending on the orientation of the applied stress), with S replaced by $S - S_f$. Once again, the stresses at the tip of the crack become infinite. Clearly, the new model adds very little to the earlier models.

The presence of the infinite stress associated with the tip of the crack is physically very unreasonable. There seem to be two ways to view this problem. In most of the engineering literature the infinite stress seems to be accepted. The argument is that, in the vicinity of this region, the considerations of continuum elasticity do not apply, and plastic effects will dominate. Thus the singularity can be excluded from the region under consideration.

An alternative approach assumes that the presence of an infinite stress indicates that the fault is in an unstable state, and that it will propagate until it reaches some position where the stress becomes finite at the tip. Such a case is considered in some detail in the next section. With this point of view in mind, we reach the interesting conclusion that neither the stress nor the displacement on the fault plane can be constant across the fault plane. The major difficulty now is to formulate a theory which will suggest how either the stress or the displacement varies on the fault plane so as to remove the singularity in stress. The results of the next section suggest a solution to this problem which may be of very general application.

The Vertical Fault with Linearly Increasing Friction

Considering the vast literature concerned with the simple crack models described above, it is surprising that so little effort has been expended on other possible crack models. Problems in which the stress or the displacement on the crack

vary in a more complex way than the simple models have been described by Kasahara (1957), Weertman (1964, 1965), Berg (1967), Walsh (1968), and Chinnery and Petrak (1968). The first four authors mentioned considered the vertical strike slip fault of infinite horizontal length, which simplified the theory to a problem in plain strain.

Kasahara (1957) gives the solution for the problem of a fault where the stress on the fault plane is specified by the series

$$\tau_{yz} = \sum_m \sum_n F_{mn} \cos my \cos nz \tag{12}$$

Unfortunately, the only case he evaluated using this technique was τ_{yz} = *constant*, which, as we have seen, is a very trivial problem. This example, however, does suggest that the convergence of the method may be quite slow.

Weertman, Berg and Walsh considered the more specific and extremely interesting problem of a fault in the presence of a frictional stress which increases linearly with depth. We shall discuss the results of Weertman (1964), though the later papers consider the significance of the model in more detail.

In Weertman's analysis, the fault is modelled as a continuous distribution of dislocation lines. This distribution is described by a function $B(x)$, where $B(x)\,dx$ represents the total length of the Burgers vectors of the infinitesimal dislocations situated between x and $x+dx$. $B(x)$ is related to the displacement $U(x)$ by

$$U(x) = \int_0^x B(x)\,dx \tag{13}$$

If the stress $\tau(x)$ is specified on the fault plane, the dislocation distribution is given by

$$B(x) = -\frac{2\alpha}{\mu\pi} \int \frac{\tau(\xi)\,d\xi}{x-\xi} \tag{14}$$

where $\alpha = 1$ for screw dislocations (Knopoff's case), and $\alpha = 1-\upsilon$ for edge dislocations (Starr's case), and where υ = Poisson's ratio.

Weertman evaluates this equation for the case where the stress acting on the fault plane has the form $S - S_f$. S is the (constant) externally applied shear stress, and S_f, the frictional stress, is presumed to increase linearly with depth as $S_f = kx$. Using the complex variable methods of Muskhelishvili (1953), he then finds that breakage will occur from the surface to a depth of b, where

$$b = \frac{\pi S}{2k} \tag{15}$$

and where the displacements and stresses on the x axis are given by

$$B(x) = \frac{4kx}{\pi\mu} \log \left[\frac{b + (b^2-x^2)^{1/2}}{x} \right] \qquad \text{for } 0 \leqslant x \leqslant b$$

$$U(x) = \frac{k}{\pi\mu} \left[b(b^2-x^2)^{1/2} - x^2 \log \left\{ \frac{b + (b^2-x^2)^{1/2}}{x} \right\} \right] \qquad \text{for } 0 \leqslant x \leqslant b \tag{16}$$

and

$$\tau(x) = S\left[\frac{x}{b}\frac{\pi}{2} - 1\right] \qquad \text{for } 0 \leqslant x \leqslant b$$

$$\tau(x) = S\left[\frac{x}{b}\sin^{-1}\frac{b}{x} - 1\right] \qquad \text{for } x \geqslant b \tag{17}$$

$U(x)$ and $\tau(x)$ are plotted as functions of depth in Figure 4. Because the slope of the displacement depth curve approaches zero at $x = b$, the stress singularity is removed. The depth b, given by Equation (15), is an 'equilibrium' depth (Walsh, 1968). If the actual depth of faulting is different from this value, the stress singularity reappears, and we must conclude that the fault is in an unstable state.

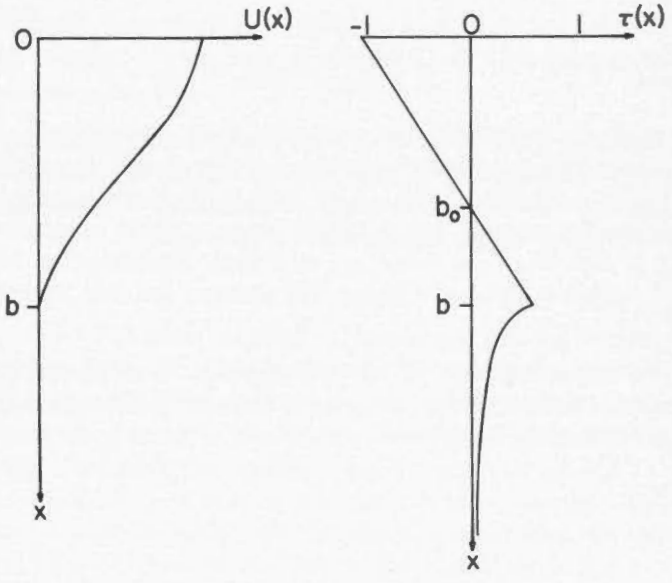

Figure 4. The displacements and stresses on the fault plane for the model of Weertman (1964), in which there is a frictional stress that increases linearly with depth. The stress is measured in units of $S-S_{f_0}$ (see text).

It is interesting to note that the fault extends beyond the point at which the applied stress equals the frictional stress, $x = b_0$. For here

$$S = S_f = kb_0 \quad \text{or} \quad b_0 = S/k \tag{18}$$

The final depth of movement b is therefore equal to $\pi b_0/2$.

If there is any component of the frictional stress that is constant, say S_{f_0}, then, as Walsh (1968) points out, the above formulas still apply, but S should be replaced by $S-S_{f_0}$ Note, however, that if $k = 0$, so that the stresses acting on the fault plane do not change with depth, $b = \infty$. As we have seen earlier,

this case always results in an infinite stress at the crack tip, and we must expect the crack to propagate downward indefinitely.

The maximum value of the offset on the fault occurs at $x = 0$, where

$$U_m = \frac{2kb^2}{\pi\mu} = \frac{b\ (S - S_{f_0})}{\mu} \tag{19}$$

The stress drop on the fault plane is a function of depth, and is a maximum at the surface $x = 0$, where

$$\Delta\tau = S - S_{f_0} = \frac{U_m \mu}{b} \tag{20}$$

Following Weertman (1964), we suppose that the frictional stress in the crust of the earth may be approximated by the simple law

$$S_f = kx = n\rho g x$$

so that

$$k = n\rho g \tag{21}$$

and

$$S - S_{f_0} = \frac{2n\rho g b}{\pi}$$

where n is a coefficient of friction, ρ is an average density and g is the acceleration of gravity. It is intriguing to notice that Equations (20) and (21) imply a relationship between the maximum offset U_m and the depth of faulting b:

$$U_m = \frac{2n\rho g}{\pi\mu} b^2 \tag{22}$$

One interesting way to use this equation is to substitute suitable parameters for a long fault, such as the San Andreas, to estimate the 'coefficient of friction' n. If we set $\rho \simeq \pi$ gms/c.c., $\mu \simeq 3 \times 10^{11}$ c.g.s., $U_m \simeq 5$ metres, and $b \simeq 15$ km (see Table 2), we find $n \simeq 0.03$. This value is very much lower than the coefficients of sliding friction measured in the laboratory (e.g., Brace, 1960), which usually lie between 0.5 and 1.0. This elementary calculation clearly throws some doubt on the applicability of Weertman's model to a typical fault movement.

A convincing explanation for this difficulty has been given by Berg (1967). He considers what happens *after* the fault movement described above, if the externally applied stress S is slowly increasing. Presumably, once the initial movement is completed, there will be a partial healing of the fault surfaces, and no more movement will occur until the increment in stress δS is large enough to overcome this 'cohesive strength'. At this point, movement will occur over the fault plane, and the fault will propagate to a new equilibrium depth $b + \delta b$. If δU is the accompanying fault offset at the surface, we can relate δS, δb and δU as follows:

$$\delta b = \frac{\pi}{2n\rho g}\,\delta S$$

$$\delta U = \frac{2b}{\mu}\,\delta S$$

The stress drop at the surface is clearly δS, where

$$\delta S = \frac{1}{2}\frac{\mu \delta U}{b}$$

If we set $n \simeq 1$, $\delta S \simeq 40$ bars, and $b \simeq 15$ km (see Table 2) we find that the fault movement δU is 4 metres, and the depth increment δb is 1/10 km. These values are very reasonable. The value of $S - S_{f_0}$ corresponding to a depth of 15 km can be obtained from Equation (21), and is found to be 3000 bars. This is remarkably close to the commonly accepted strength of crustal rocks.

Berg's model strongly suggests, therefore, that faulting should not be regarded as occurring only under the influence of an applied stress S at infinity. Instead, each fault movement is an accommodation to a change in the applied stress, and the stresses in the neighborhood of the fault are composed of the initial stress S, the incremental change δS, and the residual stresses built up from previous movements. Furthermore, the observed stress drop gives a measure of the cohesive strength of the brecciated material between the faces of the fault, and may vary considerably from one place to another. Clearly there is no relation between stress drop and applied stress, and Berg (1967) has rightly criticized Chinnery (1964) for suggesting such a relationship.

It is interesting to note that in the adjustment from one equilibrium state at depth b to the next at depth $b + \delta b$, the change in stress on the fault plane is simply δS from the surface down to the depth b. In the small additional interval δb, the change is more complicated, and is such as to ensure the absence of the stress singularity at the tip. However δb is very small, and to all intents the change is constant with depth, and this suggests that Knopoff's model may in fact give a very good representation of the displacements and stresses associated with a given movement.

One serious failing of the Weertman-Berg model is that it neglects the possibility of permanent deformation, particularly at depth. The time interval between successive movements on the same section of a fault is probably measurable in centuries. It is not likely that the earth can maintain the high applied stress near the lower edge of the fault for this length of time without some adjustment taking place. It may be that aftershocks, which often seem to occur in just this region, are indications of a redistribution and reduction of this stress by movement on local weaknesses. This in turn suggests that the calculated depth increment δb may have very little meaning in practice.

To put this problem another way, Equation (22) suggests that for a given depth of faulting there is a corresponding total offset at the surface. Using the parameters given above, a fault depth of 15 km should result from a total surface offset of 3/10 km. Worse still, if there is a surface offset of 100 km on the San Andreas fault, it should have penetrated to a depth of 250 km! The absurdity of this result does not imply that the Weertman-Berg model is invalid; it only points out that the

earth does not behave elastically on a geological time scale, and the model may be a good approximation for two successive fault movements. It will be interesting, however, to investigate refinements of the model that include the possibility of plastic deformation.

To consider faults whose length is finite, the theory must be extended to handle a three-dimensional crack surface. Models of this kind are discussed in the following section.

Three-dimensional Models

The simplest three-dimensional crack model is obtained by rotating the elliptical crack of Inglis (1913) or Starr (1928) about a minor axis to form the ellipsoidal or 'penny-shaped' crack. The deformation of such a crack by an applied stress has been considered by Sneddon (1946) and Sack (1946), who discussed the effect of a tensile stress, and by Eshelby (1957) and Keylis-Borok (1959), who included the effect of a shear stress. If the crack has a radius a, lies in the plane $y=0$, and is subjected to $S=\tau_{xy}$ (compare Figure 1), the displacements along the x axis are given by

$$U(x)=\frac{4aS}{\pi\mu}\frac{(\lambda+2\mu)}{(3\lambda+4\mu)}\left(1-\frac{x^2}{a^2}\right)^{1/2} \quad \text{for } 0\leqslant|x|\leqslant a \tag{23}$$

The maximum offset at the centre of the crack U_m and the stress drop $\Delta\tau$ are given by (for $\lambda=\mu$)

$$U_m=\frac{24aS}{7\pi\mu} \tag{24}$$

$$\Delta\tau=S=\frac{7\pi}{24}\frac{U_m\mu}{a} \tag{25}$$

(This result was quoted erroneously by Brune and Allen (1967)). The displacement $U(x)$ has the same form as in Starr's model (Figure 2) and as may be expected, $\tau(x)$ becomes infinitely large at the tip of the crack.

The foundations for a much more comprehensive theory were laid down by Volterra (1907). This theory is based on the concept of a dislocation surface, which is a surface of discontinuity in displacement. The process of formation of such a surface can be imagined as follows. A cut is made over an arbitrary surface within an elastic solid, the two sides of the cut are deformed relative to one another, and then the sides of the crack are welded back together in their new positions. Because of this 'welding' process, the stresses are continuous across the dislocation surface.

There have been several attempts to use this theory, including, for example, the work of Nabarro (1952) and Vvedenskaya (1959). However, it was left for Steketee (1958a) to express this theory in its most useful form. He was the first to show clearly that a dislocation surface can be regarded as a distribution of sources, called 'nuclei of strain'. These nuclei have been discussed frequently since their introduction by Volterra (1907) and Love (1944).

Steketee's theory can be summarized by the following formula, which relates the displacement u at an arbitrary point P due to a discontinuity Δu over an arbitrary surface Σ in an infinite elastic medium.

$$u_k(P)=\frac{1}{8\pi\mu}\iint_{\Sigma}\Delta u_i\,\tau_{ij}^{k}\,\nu_j\,d\Sigma \tag{26}$$

where μ is the rigidity, ν_j are the direction cosines of the normal to the element $d\Sigma$, and the τ_{ij}^{k} are a set of Green's functions. Shear fracture on a plane involves those Green's functions with $i\neq j$, while more general dislocation surfaces involve all six functions ($ij=ji$).

In a semi-infinite medium, analogous to the equivalent problem in potential theory, the boundary condition at the free surface can be included in the Green's function:

$$U_k(P)=\frac{1}{8\pi\mu}\iint_{\Sigma}\Delta u_i\,\omega_{ij}^{k}\,\nu_j\,d\Sigma \tag{27}$$

The analytical forms for the τ_{ij}^{k} and ω_{12}^{k} have been derived by Steketee (1958a), and Maruyama (1964) has quoted the remaining functions.

Steketee only considered 'Volterra' dislocations, in which the Δu_i has the form of a rigid body displacement. This corresponds, in the simplest case, to Δu_i being constant over Σ. Maruyama (1964) showed that the same formulas will apply for a 'Somigliana' dislocation, in which Δu_i varies over Σ, though the Δu_i must satisfy certain continuity conditions.

From Equations (26) and (27), assuming that the integrals can be evaluated either analytically or numerically, we may determine the displacements throughout the medium. From these we may derive the stresses at any point, by using the generalized form of Hooke's law,

$$\tau_{ij}=\lambda\,\delta_{ij}\,u_{k,k}+\mu\,(u_{i,j}+u_{j,i}) \tag{28}$$

then,
$$\tau_{ij}(P)=\frac{1}{8\pi\mu}\iint_{\Sigma}\Delta u_i\,G_{ij}^{kl}\,\nu_j\,d\Sigma \tag{29}$$

where
$$G_{ij}^{kl}=\lambda\,\delta_{kl}\,\tau_{ij}^{m,m}+\mu\left(\tau_{ij}^{k,l}+\tau_{ij}^{l,k}\right)$$

From these expressions, though some care is necessary, the stresses on the fault plane may be obtained.

Applications of this model have been described by Steketee (1958b), Chinnery (various papers, see references), Maruyama (1964), Press (1965), Savage and Hastie (1966) and Hastie (1966). In all of these cases the surface Σ is taken to be a plane, and the Δu_i correspond to a shear type movement. Also, in all but the most recent work (Chinnery and Petrak, 1968), the movement Δu_i has been assumed to be constant over the surface, thus permitting an analytical solution. For convenience, we shall mention here only the simplest cases, where Σ is a rectangular surface either in an infinite elastic medium,

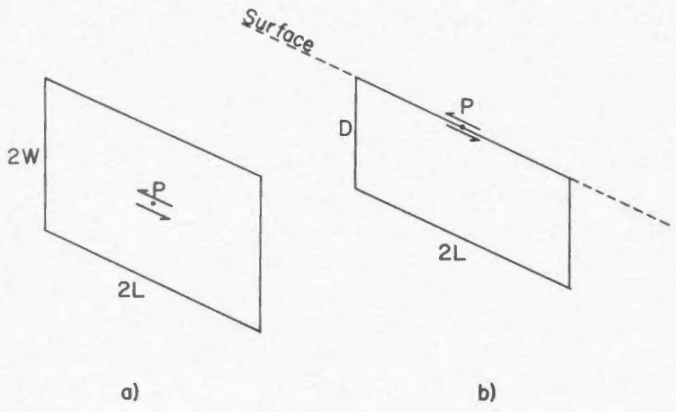

Figure 5. Three-dimensional fault models. (a) A rectangular surface within an infinite medium, with displacement parallel to the dimension $2L$. (b) A vertical rectangular strike slip fault.

as a model of a fault at depth, or near the surface of a semi-infinite medium, as a model of a vertical strike slip fault (see Figure 5).

The case $\Delta u = constant$ makes the edge of the dislocation surface singular where the displacement is indeterminate and the stress is infinite. This model may be criticized therefore in much the same way that we criticized earlier models of Starr and Knopoff. However, because the model results in some fairly simple analytical expressions, it is a useful one, and we shall consider how the results of this model should be modified to approximate more complex types of movement.

If the displacement Δu is constant, the associated stress change will vary over the dislocation surface. Therefore, to define a stress drop, a point of reference must be selected. In the case of the rectangular dislocation in an infinite elastic medium (Figure 5a), the stress drop at the centre of the dislocation is given by

$$\Delta\tau = \frac{U\mu}{3\pi} \frac{LW}{(L^2+W^2)^{1/2}} \left[\frac{4}{L^2} + \frac{3}{W^2}\right] \qquad (30)$$

In the case of the vertical strike slip fault intersecting the surface, as shown in Figure 5b, the stress drop at the midpoint P of the surface trace is given by Chinnery (1964):

$$\Delta\tau = \frac{U\mu}{2\pi}\left[\frac{3}{L} + \frac{2L}{pD} - \frac{L\,(3p+4D)}{p(p+D)^2}\right] \qquad (31)$$

where $p^2 = L^2 + D^2$

One useful aspect of the models that we have described up to this point, is their use in the estimation of the depth to which a surface fault extends. Kasahara (1957), Byerly and DeNoyer (1958) and Chinnery (1961) have shown how measurements of the displacements of the ground surface in the neighborhood of a fault trace may be used for this purpose, for vertical strike slip faults. Savage and Hastie (1966) have applied a similar model to dip slip faults. Weertman (1965) and Walsh (1968) have suggested that observations of surface strain may be more sensitive to variations of displacements with depth, but no observations of this kind are available at present. Each model predicts, for a given fault geometry, a rate of fall-off of surface displacement with distance from the fault trace. Having assumed a given model and, in the case of the three-dimensional fault, having assumed a length (see Figure 5), it is easy to compare observed surface displacements with the theoretical predictions. The depth estimated in this way varies considerably according to the model that is used, and generally is smallest for the model in which the displacement is assumed constant with depth, and is largest when the displacement falls off quite slowly with depth as in Figure 4. (The latter case is discussed in some detail in Petrak (1965)). Walsh (1968) notes that the depth obtained using Weertman's model may be more than twice the depth obtained from Chinnery's model.

In addition to an estimate of the depth of faulting, the three-dimensional models described above require an estimate for the length of faulting $2L$, which is usually presumed to be equal to the length of the surface trace of the fault. This parameter turns out in practice to be much more difficult to observe than it may seem at first sight. Faults often extend into unmapped or inaccessible regions, and even when the fault lies in a well known area, it is often difficult to locate the exact ends of a given movement on the fault.

There remain two parameters which must be assigned values in any of the fault models considered. These are the rigidity μ, and the fault offset U_m. The rigidity is usually assumed to have a value of about 3×10^{11} c.g.s. units, though this value may often be in error by up to 50%. The displacement U_m is even harder to ascertain, since in most instances there is a considerable variation in displacement along the trace of a fault. Certainly, the displacement must decrease to zero near the end of the fault trace (see Chinnery and Petrak, 1968), and the value needed for the models is the maximum displacement. Brune and Allen (1967) get around this problem by multiplying the average displacement on the fault trace by 4/3. However, it is clear that all of the parameters involved in the construction of a theoretical fault model are uncertain to some degree, and this must be borne in mind in assessing the comparison between theory and observation.

The situation is even worse in the case of dip slip faults, or faults which do not have any surface expression (see Fig. 5a). For example, a vertical dip slip fault with the orientation of the surface shown in Fig. 5b would relieve the stress component τ_{xy}. However, this component of stress must be zero at all times on the free surface of the earth, and we must therefore conclude that a vertical dip slip fault, even though it has a surface expression, must have arisen from stresses within the crust of the earth. The surface expression of such a fault must therefore be regarded as a secondary feature, and it is somewhat doubtful whether measurements of the associated displacements of the ground surface are truly representative of the conditions on the fault plane. It is also doubtful in this

TABLE 1

The Geometrical Factor η for Several Models

Author	Model	A	η
Starr (1928)	Two-dimensional fault in infinite medium. Displacement parallel to width (Figure 1)	a	2/3
Eshelby (1957)	Circular fault, radius a, in infinite medium	a	0.92
Knopoff (1958)	Two-dimensional fault in infinite medium. Displacement parallel to length (Figure 1)	a	1/2
Knopoff (1958)	Two-dimensional vertical strike slip fault (Figure 3)	a	1/2
Weertman (1964)	Two-dimensional vertical strike slip fault (Figure 4)	b	1.00
Berg (1967)	Two-dimensional vertical strike slip fault	b	1/2
Chinnery (1964)	Rectangular vertical strike slip fault (Figure 5b)	D	0.32 (for $L \geqslant D$)
			0.54 (for $L=D$)
This paper	Rectangular fault in infinite medium. Displacement parallel to dimension L. (Figure 5a)	W	0.32 (for $L \geqslant W$)
		L or W	0.53 (for $L=W$)
		L	0.42 (for $L \leqslant W$)

case whether the applied stress S may be assumed to act at infinity. In the discussions that follow we shall, therefore, treat dip slip faults as if they occurred away from the surface of the earth, that is, we shall use the model shown in Figure 5a. Inevitably we shall find that estimates for the geometry of such faults and the displacement on the faults are subject to more error than in the case of vertical strike slip faults that intersect the surface.

In the next section we shall apply the results from several models to the computation of the stress drop involved in a number of real faults. Clearly, these will be order of magnitude estimates only.

Calculated Stress Drops for Some Real Faults

The stress drop that accompanies faulting has been discussed by Aki (1967) and Brune and Allen (1967) in terms of the simple formula

$$\Delta\tau = \eta \frac{U_m \mu}{A} \tag{32}$$

where μ is the rigidity, U_m is the maximum value of the offset, A is a dimension and η is a numerical factor which summarizes the geometry of the fault zone. The model considered by Knopoff (1958) shows that the surface of the earth acts somewhat like a mirror for a vertical strike slip fault. It is reasonable, therefore, to define A as follows:

A = the depth D, for vertical strike slip faults (Figure 5b)

A = one half of the smallest dimension, in the case of buried faults (Figure 5a)

Using this definition of A, the values of η corresponding to the various models that we have considered, are shown in Table 1. In view of the other uncertainties involved, it is clear

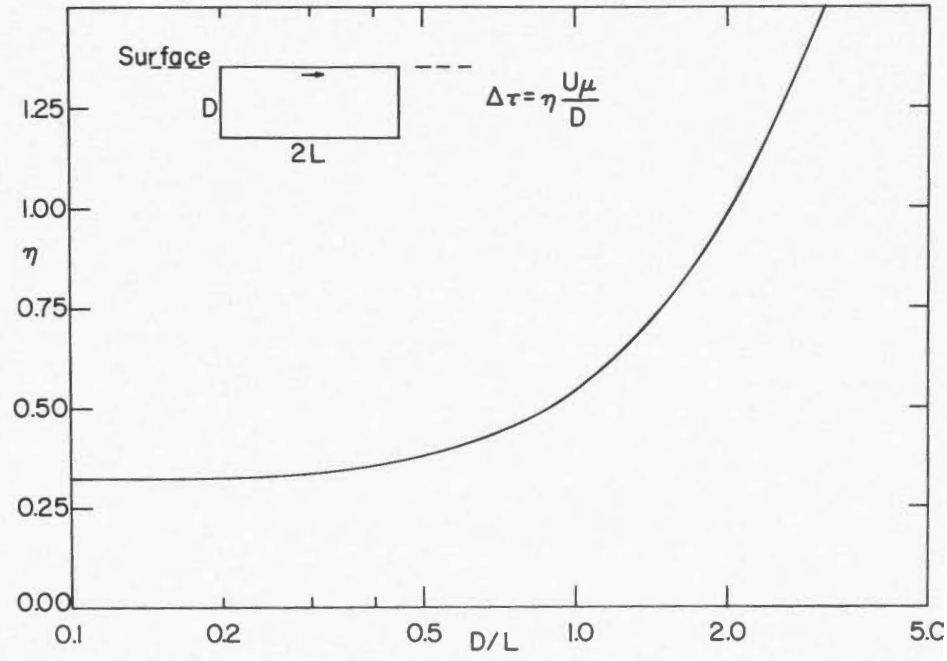

Figure 6. Variation of the geometrical factor η with fault dimensions for a vertical strike slip fault with constant displacement.

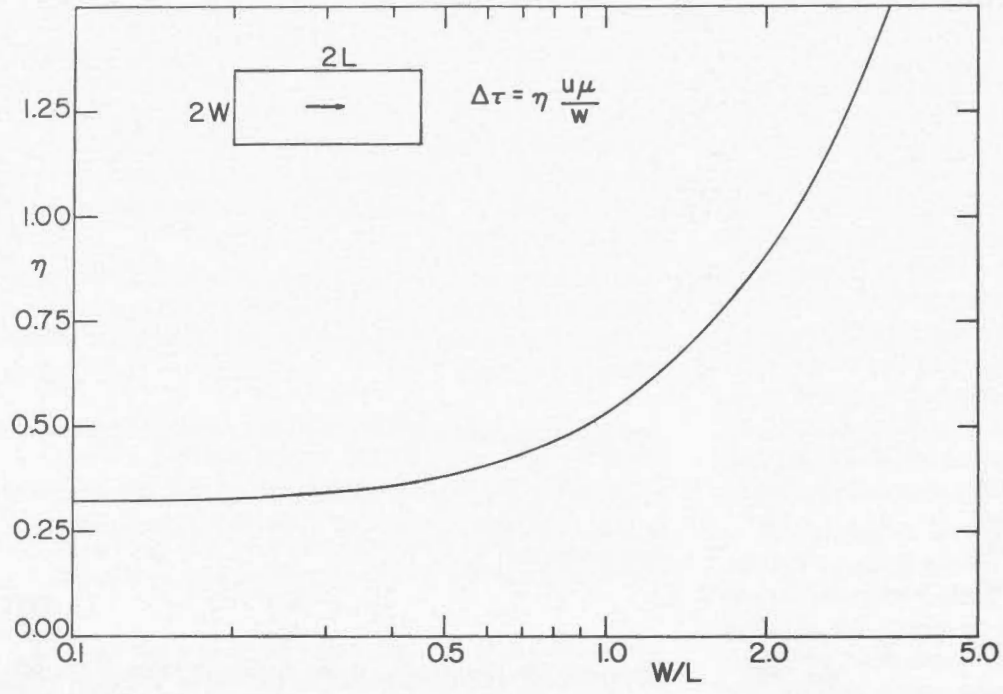

Figure 7. Variation of the geometrical factor η with fault dimensions for a buried rectangular fault surface, with displacement parallel to largest dimension.

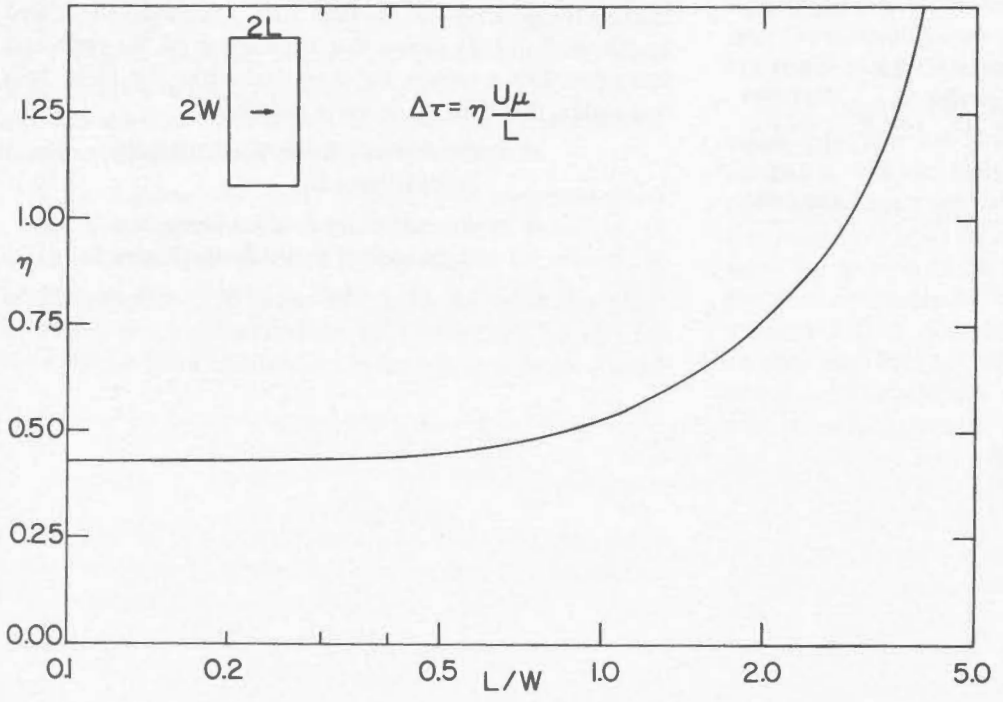

Figure 8. Variation of the geometrical factor η with fault dimensions for a buried rectangular fault surface, with displacement parallel to shortest dimension.

that $\eta = 1/2$ is a value which will apply to almost any geometrical situation. The values of η corresponding to the three-dimensional models shown in Figure 5 are plotted as a function of source dimensions in Figures 6, 7 and 8. The differences between these curves, which are obtained from Equations (30) and (31), are comparatively small. It is clear that η assumes its largest values when the source is approximately square.

The determination of the appropriate dimension A in Equation (32) presents, as we have seen, a number of difficulties. However, the models which tend to give the smallest values of A (i.e., the constant displacement models) also have the smallest value of η. Hence it turns out that if both A and η are derived on the basis of the same model, the stress drops calculated on different models are very similar. For example, although Weertman's model gives depth for vertical strike slip faulting often twice those obtained on the constant displacement model, the stress drops calculated in the two cases differ only by 25%. Again, this magnitude of error is entirely acceptable in estimates of this kind.

TABLE 2

Stress Drops for Some Strike Slip Faults

Date	Earthquake	Magnitude	Length $2L$ (km)	Depth D (km)	Movement U (m)	Reference	η	Stress drop (bars)
1906	San Francisco	8.3	435	3.2	4.0	Knopoff (1958)	0.50	188
			440	6	5.0	Kasahara (1958)	0.50	125
			450	10	4.9	Byerly and DeNoyer (1958)	0.32*	47
			440	5*	5.0	Chinnery (1961)	0.32*	96
			450	12**	4.9	Petrak (1965)	1.00**	122
1927	Tango	7.5	30	15	3.0	Kasahara (1958)	0.50	30
			30	15*	3.4	Chinnery (1961)	0.54*	37
			40	10*	3.4	Chinnery (1961)	0.38*	39
			40	25	3.4	Petrak (1965)	0.65	27
			18	20	3.4	Petrak (1965)	1.08	55
1930	North Izu	7.0	15	8	4.0	Kasahara (1958)	0.50	75
			24	12*	3.8	Chinnery (1961)	0.54*	51
			24	26	3.8	Petrak (1965)	1.05	46
1940	Imperial Valley	7.1	70	8	4.2	Kasahara (1958)	0.50	79
			70	6*	4.2	Chinnery (1961)	0.33*	69
			70	13**	4.2	Petrak (1965)	1.00**	96
			80	12**	4.2	Petrak (1965)	1.00**	106
			60	10	1.7(?)	Brune and Allen (1967)	0.34*	17(?)
1953	Turkey	7.2	50	15	4.3	Brune and Allen (1967)	0.41*	35
1954	Fairview Peak	7.1	60	15	3.0	Kasahara (1958)	0.50	30
			80	23	3.0	Byerly and DeNoyer (1958)	0.40*	16
	(strike slip component)		45	16*	3.0	Chinnery (1961)	0.44*	25
			60	10*	3.0	Chinnery (1961)	0.34*	31
			60	26**	3.0	Petrak (1965)	1.00**	34
			80	15**	3.0	Petrak (1965)	1.00**	60
			24	6	2.0	Savage and Hastie (1966)	0.38*	38
			48	6	2.0	Savage and Hastie (1966)	0.33*	33
1956	San Miguel	6.8	19	5	0.85	Brune and Allen (1967)	0.37*	19
1957	Mongolia	8.3	280	20	4.7	Brune and Allen (1967)	0.32*	23
1966	Parkfield	5.5	38	12	0.05	Aki (1967)	0.43*	0.5
1966	Imperial	3.6	10	1.4	0.01	Brune and Allen (1967)	0.34*	0.7

*Calculated using the constant displacement model. **Calculated using Weertman's model.

The stress drops calculated in this way for a number of real faults are shown in Tables 2 and 3. Table 2 shows the results for strike slip faults, most of which are approximately vertical. The references in this table refer to papers that have quoted the source parameters used, and often where the depth of faulting has been estimated. The sources of the original field observations are mentioned in these references. The variations in the parameters $2L$ and U show clearly the difficulty in making accurate measurements in the neighborhood of fault zones, and the quoted values of U are usually some kind of average of observed fault displacements, and may well be in error up to 50%. Because of this, and the variation in the different models which may be applied, it is not surprising to see the large variety of depths which have been calculated for these various faults.

In view of this variation in parameters used, the general consistency of the calculated stress drops is remarkable. If we omit a few of the extreme stress drops, which can usually be attributed to an inadequate study of the field observations, the stress drops for the earthquakes in the magnitude range 6.8 to 8.3 lie mostly between 30 and 60 bars. There is no apparent correlation between the 'average' stress drop and the magnitude of the accompanying earthquake.

The two low-magnitude events at the end of Table 2 appear to be associated with stress drops that are about an order of magnitude lower than the others. Clearly, if the models we have described are applicable, this indicates an unusually low cohesive strength, which could arise for a number of reasons. This could explain the discrepancy between the observed fault lengths for these two cases and previous attempts to construct

TABLE 3

Stress Drops for Some Dip Slip Faults
(Length is defined as the fault dimension parallel to the slip)

Date	Earthquake	Magnitude	Width $2W$(km)	Length $2L$(km)	Movement U (m)	Reference	η	Stress drop (bars)
1952	Kern County	7.8	50	20	0.6	Brune and Allen (1967)	0.44	8
1954	Fairview Peak	7.1	24	6	2.2	Savage and Hastie (1966)	0.43	95
			48	6	2.2	Savage and Hastie (1966)	0.43	95
	(dip slip component)		60	10	2.2	Chinnery (1961)	0.43	57
1959	Montana	7.1	30	15	13.3	Brune and Allen (1967)	0.45	239
			30	15	10	Savage and Hastie (1966)	0.45	180
1964	Niigata	7.5	100	20	4.0	Aki (1967)	0.43	52
1964	Alaska	8.5	700	150	10	Press (1965)	0.43	17
			600	200	10	Savage and Hastie (1966)	0.44	13

a relationship between fault length and magnitude (see Brune and Allen, 1967, Figure 6).

The equivalent data for some dip slip faults are shown in Table 3. For the reasons outlined in the previous section, we have disregarded the boundary condition at the surface of the earth, and have used the constant displacement model of a fault within an infinite medium (Figure 5a). There is, in most of these instances, considerable doubt about the fault parameters which are quoted. Often the movement on these faults is both strike slip and dip slip, and there is some doubt about the validity of using a dip slip fault model for their interpretation. Also, the fault movement must be deduced from surface evidence, and this may not be representative of the movement at depth. These difficulties are almost certainly the reason for the wide variety of calculated stress drops. On the basis of present data on this type of faulting, it is extremely doubtful that one can conclude, as Brune and Allen (1967) have done, that these calculated stress drops indicate a variety of different fault mechanisms. It is much more likely that the results in Table 3 simply indicate the uncertainty in observations combined with the oversimplified assumptions of the models used.

Concluding Remarks

The objective of this paper has been to relate and compare a number of the different theoretical models that have been applied to faulting. Because we have been most concerned with the physical basis for the models, we have considered them only in their simplest form and have omitted most of the additional complexities which have been mentioned by many of these authors. In addition we have not included the large amount of work which may be applied, in one way or another, to the study of tension cracks and dyke formation, where the edges of a crack are being forced apart.

We have, however, discussed all the basic models which may be applied to the problem of shear-fracture in the presence of a compressive stress. Because of this, many of the arguments presented in the earlier part of this paper have a direct application to a variety of fields. In particular, the implications of the model of Weertman (1964) may throw some new light on a number of problems in crack propagation.

The variety of models available for the study of fault mechanics is reasonably complete. The two-dimensional models cover most of the simple possibilities, and Weertman (1964) and Walsh (1968) have outlined the techniques for handling more complex problems. It may be necessary to specify a more complex stress distribution on the surfaces of a fault than that considered by these authors, but the form of this stress distribution will have to be obtained from a detailed study of the processes occurring very close to the fault face.

Although there are some analytical difficulties, the three-dimensional crack models can be viewed as distributions of nuclei of strain, and, since the fields of these nuclei are now known in a variety of situations, the effect of many different kinds of faults on their surroundings may be determined simply by integrating over the appropriate surface. The theory discussed by Steketee (1958a) specifies in effect the displacement over a fault plane. As we have seen, it may be more useful physically to specify the stress acting across the face of a fault, and some improvements in the basic theory are needed to adequately include the effect of friction on the fault plane.

However, in the present author's opinion, there is a definite limit to the amount of complexity that should be included in models designed for the study of faulting. The reason for this, as we have mentioned, is the general lack of adequate field data. The usefulness of any theory must be judged on its ability to predict new results, which may then be compared with observation. At the present time field data do not have the resolution to be able to distinguish between different theories which involve large numbers of variables. The complexity of the geology in the neighbourhood of most active faults suggests that it may be a long time before there is a significant improvement in this situation.

Acknowledgement

This research has been supported by National Science Foundation Grant GA-708.

References

Aki, K., 1967. Scaling law of seismic spectrum. *J. Geophys. Res.* 72, 1217-1231.

Berg, C.A., 1967. A note on the mechanics of seismic faulting. *Geophys. J.*, 14, 89-99.

Brace, W.F., 1960. An extension of the Griffith theory of fracture to rocks. *J. Geophys. Res.*, 65, 3477-3480.

Brace, W.F., and J.D. Byerlee, 1966. Stick-slip as a mechanism for earthquakes. *Science*, 153, 990-992.

Brune, J.N., and C.R. Allen, 1967. A low-stress-drop, low-magnitude earthquake with surface faulting: the Imperial, California, earthquake of March 4, 1966. *Bull. Seism. Soc. Am.*, 57, 501-514.

Byerly, P., and J. DeNoyer, 1958. Energy in earthquakes as computed from geodetic observations. In: *Contributions in Geophysics in Honor of Beno Gutenberg*, H. Benioff, *et al.* (eds.), New York, Pergamon Press, pp. 17-35.

Chinnery, M.A., 1961. The deformation of the ground around surface faults. *Bull. Seism. Soc. Am.*, 51, 355-372.

Chinnery, M.A., 1963. The stress changes that accompany strike-slip faulting. *Bull. Seism. Soc. Am.*, 53, 921-932.

Chinnery, M.A., 1964. The strength of the earth's crust under horizontal shear stress. *J. Geophys. Res.*, 69, 2085-2089.

Chinnery, M.A., 1965. The vertical displacements associated with transcurrent faulting. *J. Geophys. Res.*, 70, 4627-4632.

Chinnery, M.A., 1966a. Secondary faulting I: theoretical aspects. *Can. J. Earth Sci.*, 3, 163-174.

Chinnery, M.A., 1966b. Secondary faulting II: geological aspects. *Can. J. Earth Sci.*, 3, 175-190.

Chinnery, M.A., and J.A. Petrak, 1968. The dislocation fault model with a variable discontinuity. *Tectonophysics* (in press).

Eshelby, J.D., 1957. The determination of the elastic field of an ellipsoidal inclusion, and related problems. *Proc. Roy. Soc. Lond.*, A, 241, 376-396.

Griffith, A.A., 1921. The phenomena of rupture and flow in solids. *Phil. Trans. Roy. Soc. Lond.*, A, 221, 163-198.

Hastie, L. M., 1966. Surface deformation associated with strike-slip faulting (abstract). *Earthq. Notes*, 37, no. 4, 17.

Inglis, C.E., 1913. Stresses in a plate due to the presence of cracks and sharp corners. *Trans. Inst. Nav. Arch.*, 55, 219-230.

Kasahara, K., 1957. The nature of seismic origins as inferred from seismological and geodetic observations (1). *Bull. Earthq. Res. Inst.*, 35, 473-532.

Kasahara, K., 1958. Physical conditions of earthquake faults as deduced from geodetic data. *Bull. Earthq. Res. Inst.*, 36, 455-464.

Keylis-Borok, V.I., 1959. On estimation of the displacement in an earthquake source and of source dimensions. *Annali Geofis.*, 12, 205-214.

Knopoff, L., 1958. Energy release in earthquakes. *Geophys. J.*, 1, 44-52.

Love, A.E.H., 1944. *The Mathematical Theory of Elasticity*, 4th. ed., New York, Dover Publ., 643 p.

Maruyama, T., 1964. Statical elastic dislocations in an infinite and semi-infinite medium. *Bull. Earthq. Res. Inst.*, 42, 289-368.

Muskhelishvili, N.I., 1953. *Some Basic Problems of the Mathematical Theory of Elasticity*, Groningen, Holland, P. Noordhoff, 704 p.

Nabarro, F.R.N., 1952. The mathematical theory of stationary dislocations. *Adv. in Physics*, 1, 269-394.

Paris, P.C., and G.C. Sih, 1965. Stress analysis of cracks. In: *Symposium on Fracture Toughness Testing and Applications*, A.S.T.M. Spec. Tech. Publ., No. 381, 30-83.

Petrak, J.A., 1965. *Some theoretical implications of strike-slip faulting.* M.A. thesis, University of British Columbia, Vancouver.

Press, F., 1965. Displacements, strains, and tilts at teleseismic distances. *J. Geophys. Res.*, 70, 2395-2412.

Press, F., 1967. Dimensions of the source region for small shallow earthquakes. In: *Proceedings of VESIAC Conference on Shallow Source Mechanisms*, VESIAC Report 7885-1-X, pp. 155-163.

Sack, R.A., 1946. Extension of Griffith's theory of rupture to three dimensions. *Proc. Phys. Soc. Lond.*, 58, 729-736.

Savage, J.C., and L.M. Hastie, 1966. Surface deformation associated with dip-slip faulting. *J. Geophys. Res.*, 71, 4897-4904.

Sneddon, I.N., 1946. The distribution of stress in the neighbourhood of a crack in an elastic solid. *Proc. Roy. Soc. Lond.*, A, 187, 229-260.

Starr, A.T., 1928. Slip in a crystal and rupture in a solid due to shear. *Proc. Camb. Phil. Soc.*, 24, 489-500.

Steketee, J.A., 1958a. On Volterra's dislocations in a semi-infinite elastic medium. *Can. J. Phys.*, 36, 192-205.

Steketee, J.A., 1958b. Some geophysical applications of the elasticity theory of dislocations. *Can. J. Phys.*, 36, 1168-1198.

Volterra, V., 1907. Sur l'équilibre des corps élastiques multiplement connexes. *Ann. Sci. École Norm. Supér.*, Paris, 24, 401-517.

Vvedenskaya, A.V., 1959. The displacement field associated with discontinuities in an elastic medium. *Akad. Nauk Izv. ser. Geofiz.*, 4, 516-526; in the Eng. ed. 357-362.

Walsh, J.B., 1968. Mechanics of strike-slip faulting with friction. *J. Geophys. Res.*, 73, 761-776.

Weertman, J., 1964. Continuum distribution of dislocations on faults with finite friction. *Bull. Seism. Soc. Am.*, 54, 1035-1058.

Weertman, J., 1965. Relationship between displacements on a free surface and the stress on a fault. *Bull. Seism. Soc. Am.*, 55, 945-953.

A PHYSICAL BASIS FOR EARTHQUAKE STATISTICS

L. Knopoff and C.-Y. King

Institute of Geophysics and Planetary Physics
University of California
Los Angeles, California, U.S.A.

R. Burridge

Department of Applied Mathematics and Theoretical Physics
Cambridge University
Cambridge, England

ABSTRACT: A postulate is made that friction between the walls of a fault structure governs the seismicity along the fault. Sequences of shocks generated in a laboratory and a numerical model with friction as an important parameter are found to show statistical features similar to those of naturally occurring earthquakes. Similarities between model and natural events are found in the magnitude-frequency relationship, in the causal connection between the time sequences of shocks, in the time sequences of aftershocks, in the scaled velocity of propagation of rupture and in the interrelationship between shock magnitude and rupture parameters. The application of observations made on the model also leads to reasonable conclusions about the dependence of seismic energy and focal stress drop upon magnitude.

RÉSUMÉ: Il est admis que la friction des lèvres d'une faille détermine la séismicité le long de cette faille. L'étude de séries de secousses produites en laboratoire, et celles d'un modèle numérique ayant la friction comme l'un des paramètres de base, met en relief des caractéristiques statistiques analogues à celles des séismes naturels. Ces similitudes entre les modèles et les séismes portent sur la relation magnitude-fréquence, sur le rapport causal entre les successions des intervalles entre secousses, sur les successions des intervalles entre répliques, sur l'échelonnement de la vitesse de propagation de la rupture, et sur le rapport entre la magnitude de la secousse et les paramètres de la rupture. Grâce aux observations faites sur le modèle, il est permis d'admettre que l'énergie séismique et la baisse de contrainte au foyer dépendent de la magnitude.

Friction as a Mechanism for Inhibiting Slip

In this paper we investigate the role of friction between the walls of a pre-existing earthquake fault and couple it with some of the properties of the static stress distribution around dislocations in solids. We shall show that these two factors can account, in a qualitative sense, for many of the observations of the statistics of earthquake occurrence and, in some part, account for them in a quantitative manner as well.

The general notions of the physical relations are relatively simple: two blocks of solid matter are held together across a fault by compressional stresses. When the normal shearing stresses exceed the fracture strength of the contact between the two blocks, rupture is initiated and the two blocks move to a new position relative to one another with an accompanying drop in stress along the fault.

We consider a long fault. The occurrence of a dislocation of the type described above generally takes place over only a fraction of the total length of the fault. Thus stress concentrations are introduced at the ends of the ruptured section. Over a period of time, because of the continuing occurrence of many shocks, the stress distribution along the fault takes on an extremely irregular pattern. A multitude of shocks, each with differing energy release and with differing lengths of the ruptured parts, now occur because the fault behaves mainly like a heterogeneous medium. Over a sufficiently long period of time, some form of steady-state or quasi-steady-state distribution of these stresses can be described with some steady-state statistical structure. Corresponding to these stresses, one should obtain a steady-state distribution of earthquake events for frequency of occurrence, energies, stresses, lengths of the ruptured sections, etc.

The model described above can be criticized for picturing the interaction between the walls as one of dry friction between the two blocks. Below a depth of only a few km in the earth, the hydrostatic pressures are sufficiently large that rupture of this type cannot take place. A way out of this difficulty is obtained if we note that the fracture strength of rocks is significantly reduced because of environmental water pressure, whether the water be interstitial or chemically bound as water of hydration. The role of water will not be further explored here; it need only be mentioned that the weakening of the rocks by the presence of water permits the application of the present model of earthquake occurrence under shear deformations to events perhaps as deep as 100 km. This point is discussed by Raleigh (1967) and by Griggs and Baker (1968).

A Laboratory Model

To investigate the consequences of the postulate that friction governs the statistical observations of seismicity, Burridge and Knopoff (1967) have proposed two models

amenable to quantitative study. In the first of these, a laboratory model has been constructed which permits direct observation of the events in question. Imagine a linear chain of alternating masses and springs, with the masses resting on a horizontal tabletop. Dry friction occurs naturally between the masses and the tabletop; experimentally, we can parameterize, and hence establish the uniformity or lack thereof, the spring constants, masses and frictional coefficients. The last mass in the chain is free; arguments can be offered which indicate that this end condition may be preferable to one in which the last mass is connected to a rigid wall, if one wishes to simulate naturally occurring phenomena. The leading spring is connected by a thread to a motor which pulls slowly upon the thread at a constant rate.

Consider now the sequence of events that takes place. The leading spring stretches under the influence of the driving thread until the differential tension between the first and second springs exceeds the breaking shear strength of the contact of the first mass with the tabletop. The first mass will then hop over to a new position. The stress in the first spring is reduced by the shock, while that in the second spring is correspondingly increased. Immediately after the shock has taken place, the system of masses is once again at rest and the leading spring once again begins to stretch under the tectonic drive. Again, when the differential stress exceeds the critical value, the first mass moves abruptly, thereby transferring a bit more stress energy to the second spring.

When a number of such shocks have taken place in which only the first mass moves, a considerable amount of stored energy or stretch in the second spring will have been built up. When, finally, the first mass is once again triggered into motion, the abrupt increase of stress in the second spring increases the differential stress between the second and third springs beyond the critical value for the second mass, so that the second mass now moves as well. Thus we can say that the motion of the first mass has triggered the second mass into motion. The length of the rupture is now greater than in the case in which only one mass moves. Considerably more energy has been released in the shock than in the case in which only one mass moves. It also follows, by a relatively simple extension, that there will be many shocks in which only one mass moves, fewer shocks in which only two masses move, and so on.

Thus one gets the notion of a charging-cycle in which energy is loaded into the chain through the mechanism of small shocks. If one starts with a chain which has relatively little potential energy in the form of stretch of the springs stored in it, the succession of small- and intermediate-sized shocks can serve to increase the amount of energy stored in the chain. Thus, one role of the shocks is to transfer energy rapidly from one part of the chain to the other. A typical graph of the energy as a function of time is shown in Figure 1. The potential energy stored in the chain increases, but is interrupted by sudden small drops in the potential energy because of energy released in the shocks. The energy balance of the configuration is as follows: the energy derived from the tectonic drive, namely the motor in this case, is converted into (a) energy stored as potential energy along the chain, transferred there rapidly through the mechanism of small- and intermediate-sized shocks, (b) energy dissipated in the form of seismic energy radiated, and (c) heat developed in friction during the motion. Further, this model simulates well the notion of stress concentrations introduced at the termini of the rupturing segments.

When the entire chain has been stretched to its maximum so that no more potential energy can be stored without a shock taking place, the next small motion of the leading mass triggers the entire chain into motion and a catastrophic event

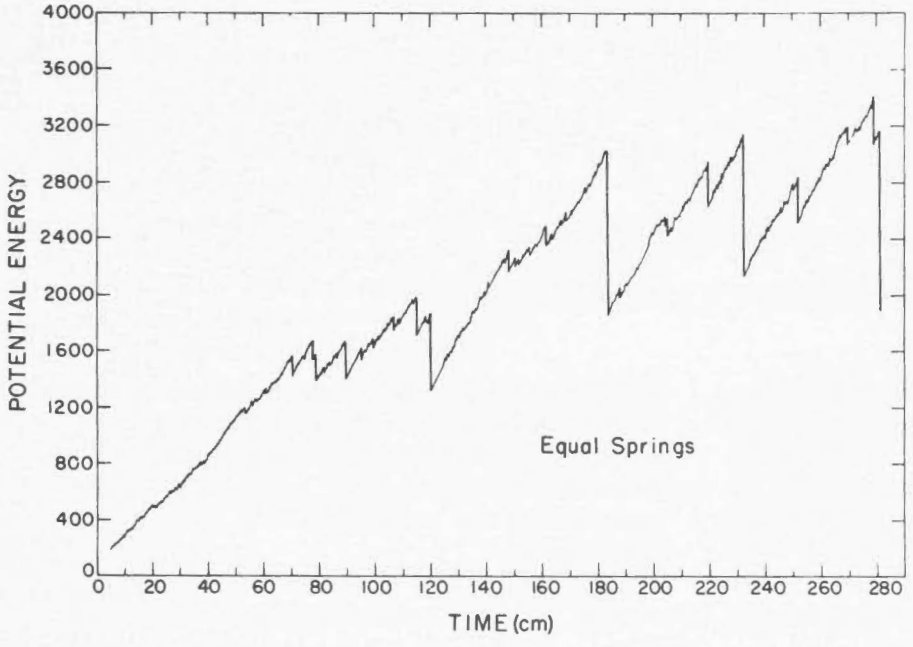

Figure 1. Potential energy as a function of time for the laboratory model.

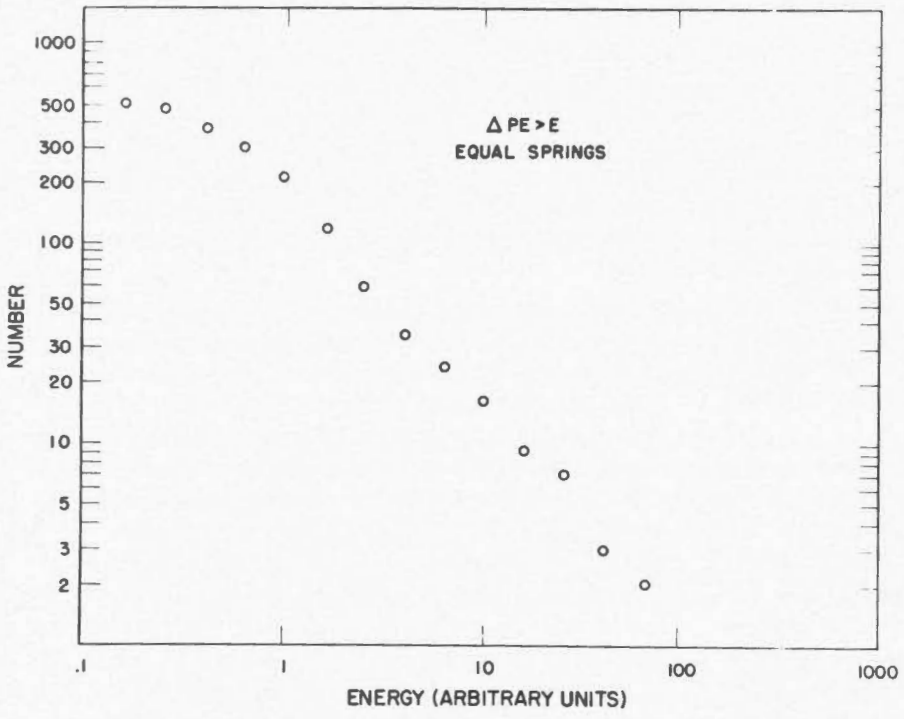

Figure 2. Cumulative frequency diagram of log N vs log E for the laboratory model.

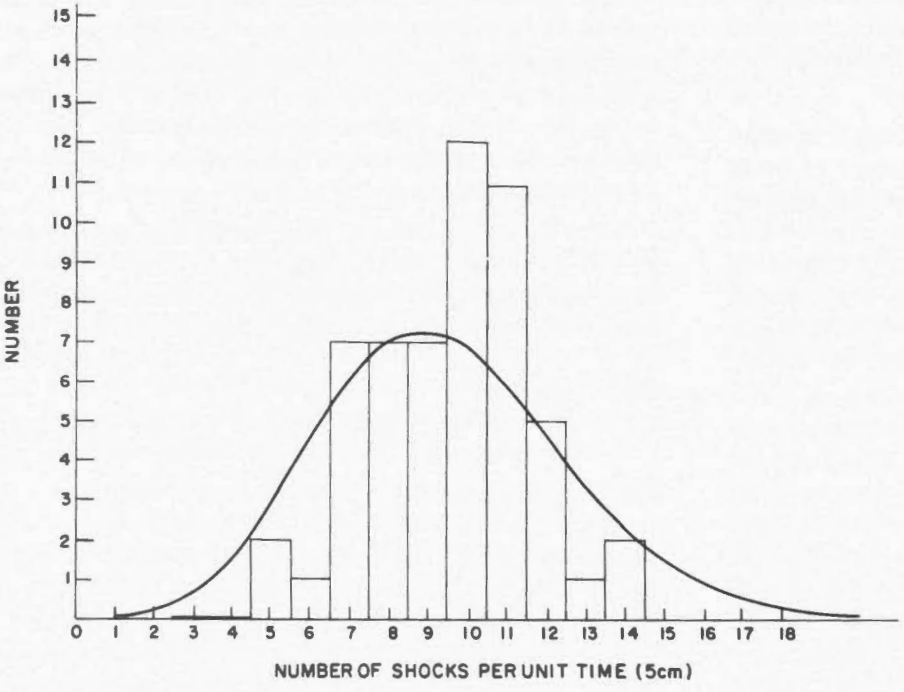

Figure 3. Histogram for frequency of occurrence of laboratory events. Continuous curve is the corresponding Poisson distribution.

occurs on the chain, in which a large part of the stored energy is released. The consequences of this event are much like the release of a stretched rubber band. The chain suddenly shortens, often with reflections of wave motions along the chain, and comes to rest in a state with significantly lower potential energy. Never does the chain lose completely all of the stored potential energy; a residual potential energy always remains following a catastrophe of this type. Following a first catastrophe, the potential energy in the chain is found to be bounded by some upper threshold, just prior to the largest shock, and a lower threshold of potential energy immediately following a catastrophic shock. These thresholds are upper and lower bounds; the actual energies in the chain never reach these extremes.

A simple counting procedure of the frequency of seismic events gives a log N vs. log E graph which is linear with a

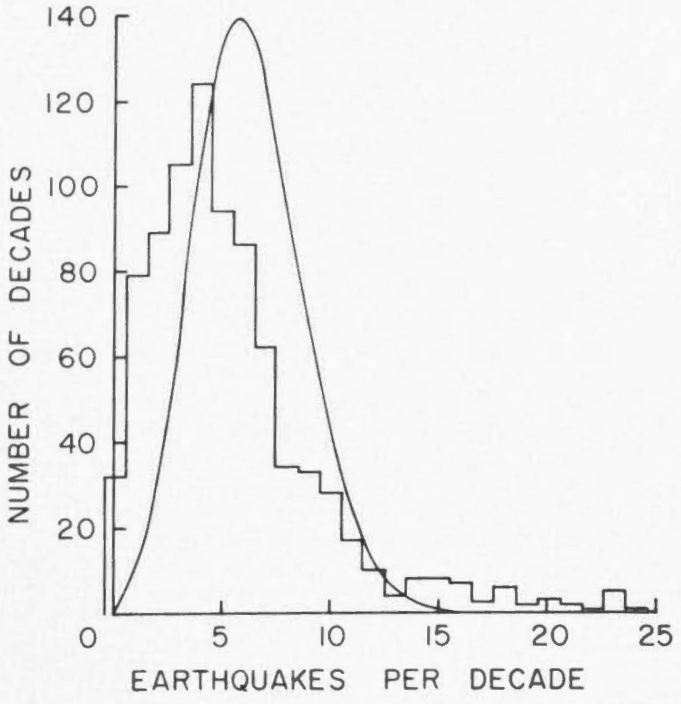

Figure 4. Histogram for frequency of occurrence of southern California earthquakes 1934-1958, $M \geq 3.0$. Continuous curve is the corresponding Poisson distribution.

$$\log \eta E = \log E_S = a + \beta M \qquad (2)$$

where η is the seismic efficiency and E_s is the seismic energy radiated. If log η is, at most, a linear function of M, the results obtained in these experiments and those observed in nature become formally consistent.

The causal connection between events can be tested. In Figure 3, it is seen that the sequence of laboratory events does not fit a Poisson distribution at all well. Naturally occurring events also do not fit a Poisson distribution (Aki, 1956; Knopoff, 1964; Ferraes, 1967) although the two biases, for the laboratory events and for the naturally occurring ones, are significantly different (Figure 4).

A Numerical Model

A second model involves numerical integration of the equations of motion of the masses during the seismic event itself, once again for a one-dimensional chain. The advantages of the numerical solution over the laboratory model are self-evident; numerical integration permits parameterization of the model. In neither the numerical nor the laboratory model is it certain that the models or materials chosen for the frictional contact simulate the properties of the friction in naturally occurring earthquake faults.

Figure 5. Friction function used in the integration of the differential equations of motion.

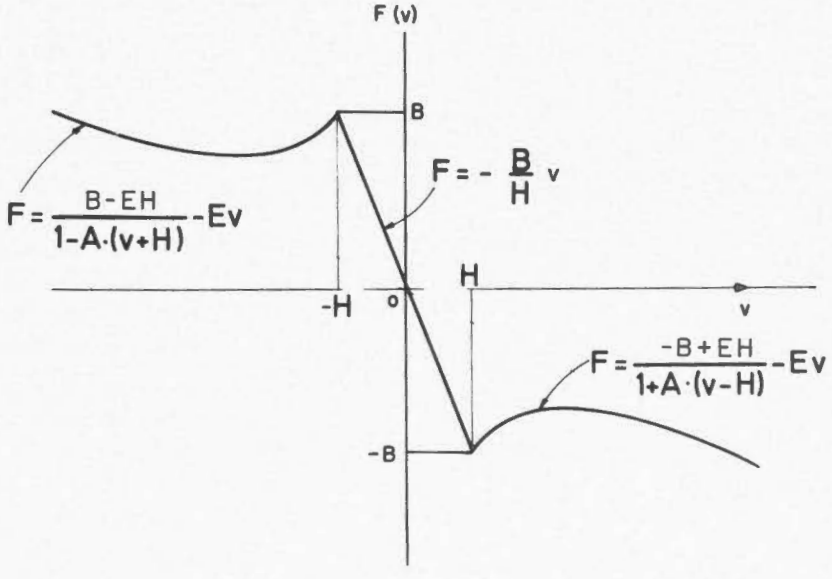

FRICTION AS A FUNCTION OF RELATIVE VELOCITY

negative slope (Figure 2). This is a cumulative frequency diagram. We have plotted the total number of shocks N with potential energy release greater than a certain potential energy E. This result is, of course, quite similar to the usual relationship for natural earthquakes.

$$\log N = a - bM \qquad (1)$$

Let one assume the usual magnitude-energy relationship

Despite these uncertainties, the design of a friction function for use in the integration of differential equations can be done with certain properties in mind. The function chosen is shown in Figure 5, together with the parameters used in the specification of the various parts of the function. This function has several features:

1. The linear part through the origin indicates that the frictional stresses are of the Newtonian viscous type, at least in

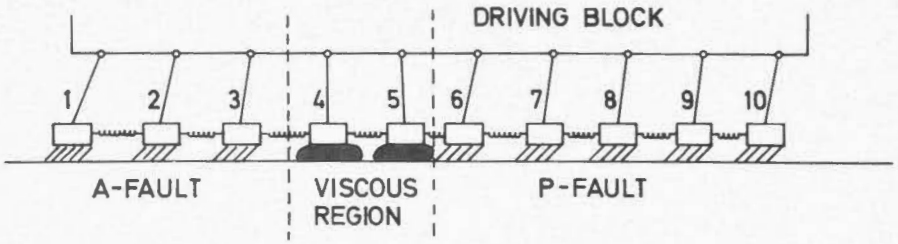

Figure 6. Schematic diagram of a numerical model. The model is divided into a longer principal part (P) and a shorter auxiliary part (A). B values are generally greater on the P segment than on the A segment.

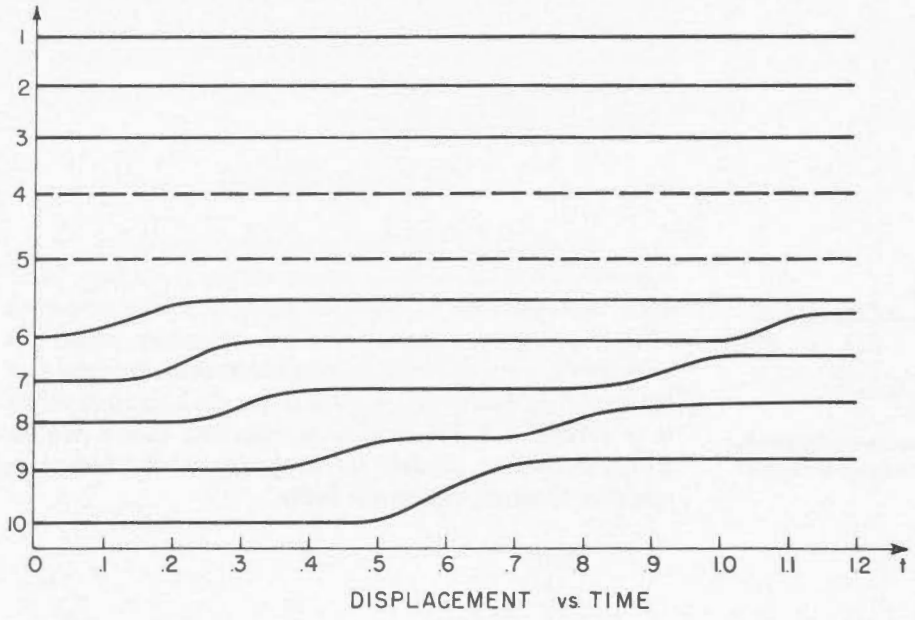

Figure 7 (above and below). Detailed motion of the lattice as a function of time on the model of Figure 6. Only particles 4 and 5 move during the interval of about 4×10^4 units of time. This motion is followed by an aftershock.

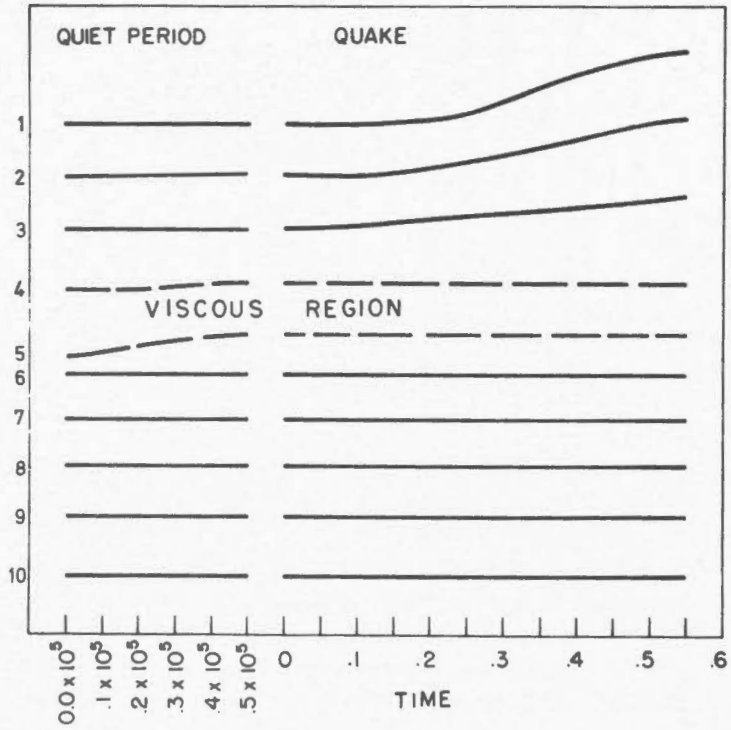

this range of velocities.

2. The contact has a finite breaking strength, indicated by the parameter B. When a stress equal to B is reached, rupture is initiated, the motion taking place against the instability because of the sudden decrease in frictional force. This is the quantitative statement of the usual notion that the dynamic friction is less than the static friction between solids.

3. The effect of seismic radiation is taken into account by letting the function be proportional to velocity asymptotically for large velocities.

In one calculation, for a model illustrated schematically in Figure 6, each of ten masses may be imagined to be resting, coupled through friction of the type described above, on a stationary block. The masses are interconnected by springs in the usual way. However, in this case, the tectonic drive is obtained from a block moving with slow, steady velocity and coupled to each of the masses by a set of leaf, or flat, springs. In this way, each of the masses is separately driven by the tectonic drive instead of by the method of drive used in the laboratory model in which only the leading spring is excited directly. For the model described in Figure 6, two of the masses are coupled to the stationary block through a Newtonian viscous fluid. The elements resting on the viscous fluid separate two parts of the chain; the masses in the outer parts of the chain have a coupling which is of the more typical dry

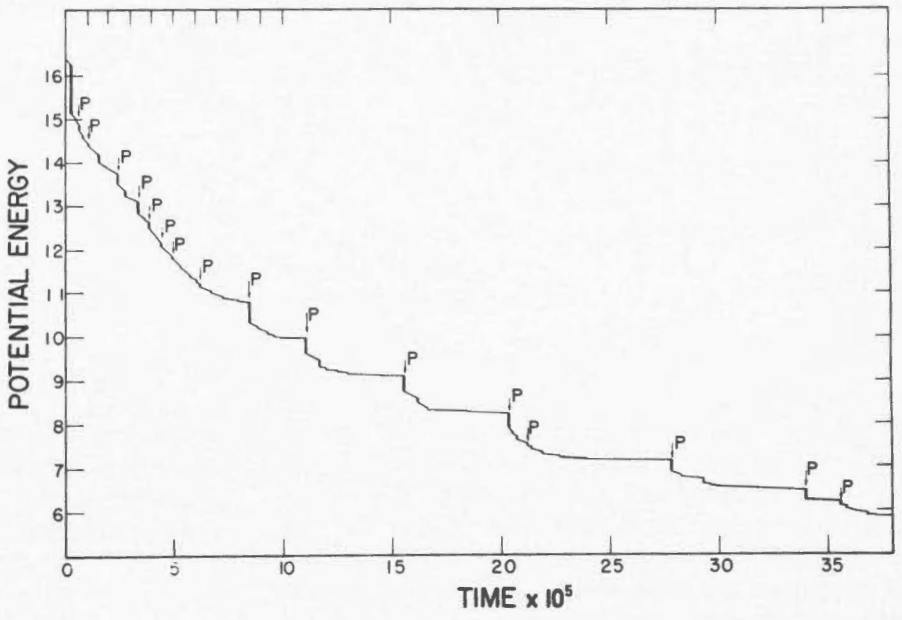

Figure 8. Potential energy as a function of time for the aftershock sequence, starting with the shock of Figure 7. Shocks occurring in the *P*-segment are identified.

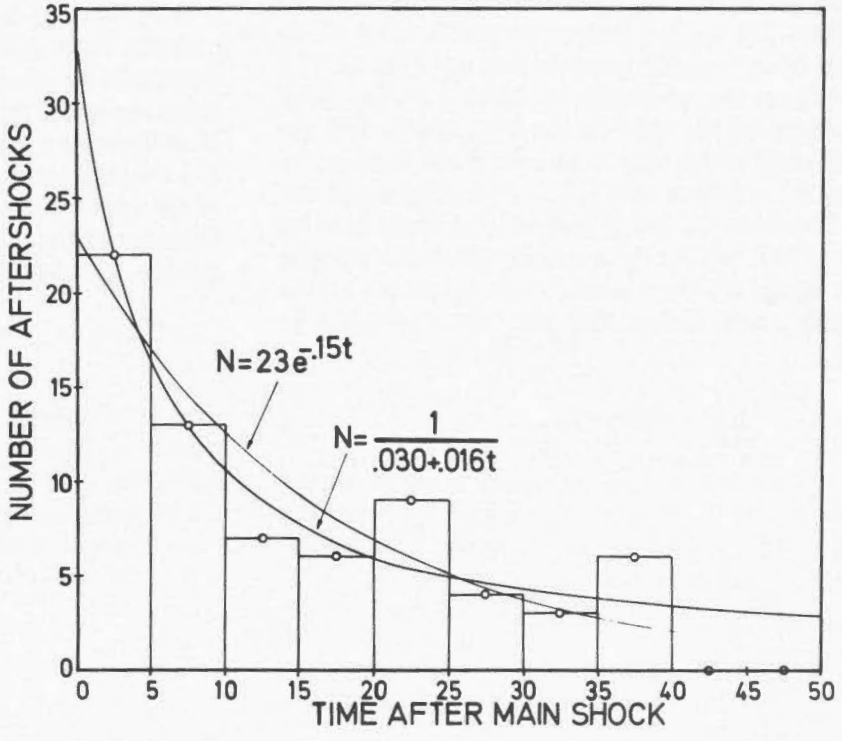

Figure 9. Histogram for number of aftershocks as a function of time. Smooth curves are fits of Omori and exponential types.

friction type. The viscous coupling is simply obtained parametrically by letting the value of B become very large and the slope of the linear segment through the origin become small, in comparison with the parameters for the nonviscous elements.

For a particular choice of parameters, a large event was initiated at the sixth mass. As a consequence of the detailed calculation of the displacements of the masses as functions of time (Figure 7), a finite velocity of rupture along the longer segment, followed by a reflection, was observed. The reflection takes place from the inhomogeneity at the end of the chain. The masses in the longer segment of the chain come to rest after a short time. The spring between masses 5 and 6 is compressed and masses 4 and 5 begin to slide against this compression with the relaxation time of the viscous elements; this motion in turn causes a compression of the spring between masses 3 and 4. After a substantial time interval, adjusted by a suitable choice of parameters, an aftershock takes place in the shorter segment of the chain. Indeed, for this particular sequence of events, 69 aftershocks were generated numerically, some of them taking place on the shorter segment of the chain. Potential energy in the system is lost, not only during

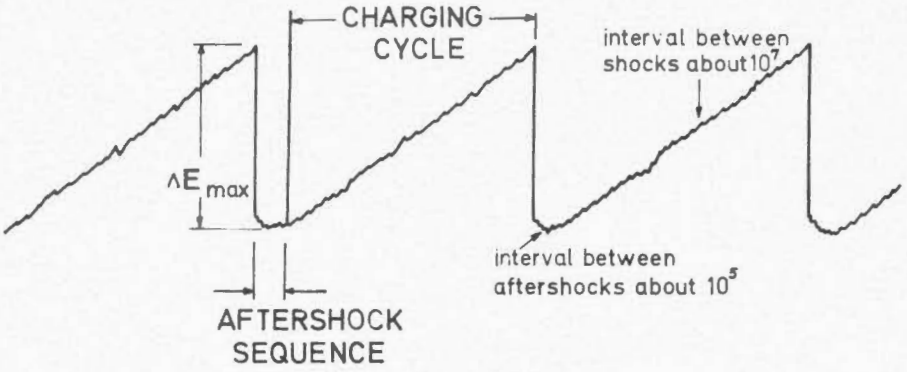

Figure 10. Schematic diagram of potential energy in the system as a function of time.

the initial large shock and the aftershocks, but also by dissipation through the viscous elements in the time intervals between shocks. Some nesting of aftershocks is observed, especially late in the aftershock series (Figure 8). The aftershock distribution as a function of time is found to fit an Omori distribution reasonably well, a condition also found in naturally occurring earthquakes (Figure 9).

A typical quasisteady sequence of events thus takes the following form. The usual charging cycle is observed in which small shocks occur in greater numbers than larger shocks. The smaller shocks are the mechanism by which more and more potential energy may be stored in the linear springs until the catastrophic event occurs with its associated aftershocks. The total energy in the system continues to drop in the aftershock sequence. Following the last aftershock, the chain is in its lowest energy state and the entire chain enters upon a charging cycle once again; the time interval between shocks of the charging cycle is much longer than that between aftershocks (Figure 10).

Stress Drop

A further result obtained by the numerical model was the observation that the efficiency η of conversion of potential energy into energy radiated in shocks occurring during the charging part of the cycle is essentially independent of the amount of potential energy released during the shock (Figure 11). We may use this result by coupling it with some observations taken from dislocation theory concerning the static energy release in a shock to give information concerning stress drop in shocks (King and Knopoff, 1968a).

The seismic energy release in a dislocation is given by the formula

$$E_S = g\mu L D^2 \eta f(\gamma) \tag{3}$$

where g is a factor of the order of unity which takes into account the Poisson's ratio of the medium, the geometry of the fault surface and the type of dislocation (edge, screw, etc.); L is some linear dimension of the fracture surface usually taken to be the length of the fracture surface for large faults and D is the relative displacement between the two blocks; μ is the shear modulus; $f(\gamma)$ is a function of the dimensionless ratio of the shear stress on the fault after the shock to that before the shock; hence, $(1-\gamma)$ is the fractional stress drop. Burridge and Knopoff (1966) have shown that

$$f(\gamma) = \frac{1+\gamma}{1-\gamma} \tag{4}$$

if the stress drop is uniform over the entire fault surface. μ probably does not vary by as much as a half-order of magnitude for crustal shocks. From the above discussion, it seems reasonable to assume that $\log g\eta\mu$ for a real earthquake is, at worst, a weak function of the magnitude of the shock and the parameters describing the geometry and environment of the fault. We take $\log g\eta\mu$ to be a constant. Thus, taking the logarithm of Equation (3) and applying the energy-magnitude relation, Equation (2), we get

$$\beta(M-M_0) = \log LD^2 + \log f(\gamma) \tag{5}$$

with M_0 a constant. A graph of magnitude vs. $\log LD^2$ for a number of large shallow shocks, for which the rupture trace parameters L and D have been observed at the surface, yields a substantially linear relationship. However, the slope of this curve (Figure 12) indicates that we must postulate a relationship of the type

$$\log f(\gamma) = \delta + \epsilon M \tag{6}$$

to account for the difference between the observed slope and the theoretical value β^{-1}. If we apply Equation (4), we get

$$\gamma = \tanh\left(C_0 (M_1 - M)\right) \tag{7}$$

with C_0 and M_1 constants. These results indicate that the fractional stress drop is a function of the magnitude and hence of the energy released. Fitting to the field observations of (L,D) for real shocks, total stress drop takes place at about $M_1 = 9$.

The above observations can be tested on the laboratory model because the stretch in the leading spring is a measure of the applied stress (King and Knopoff, 1968b). Figure 13 is a graph of the fractional stress drop as a function of the

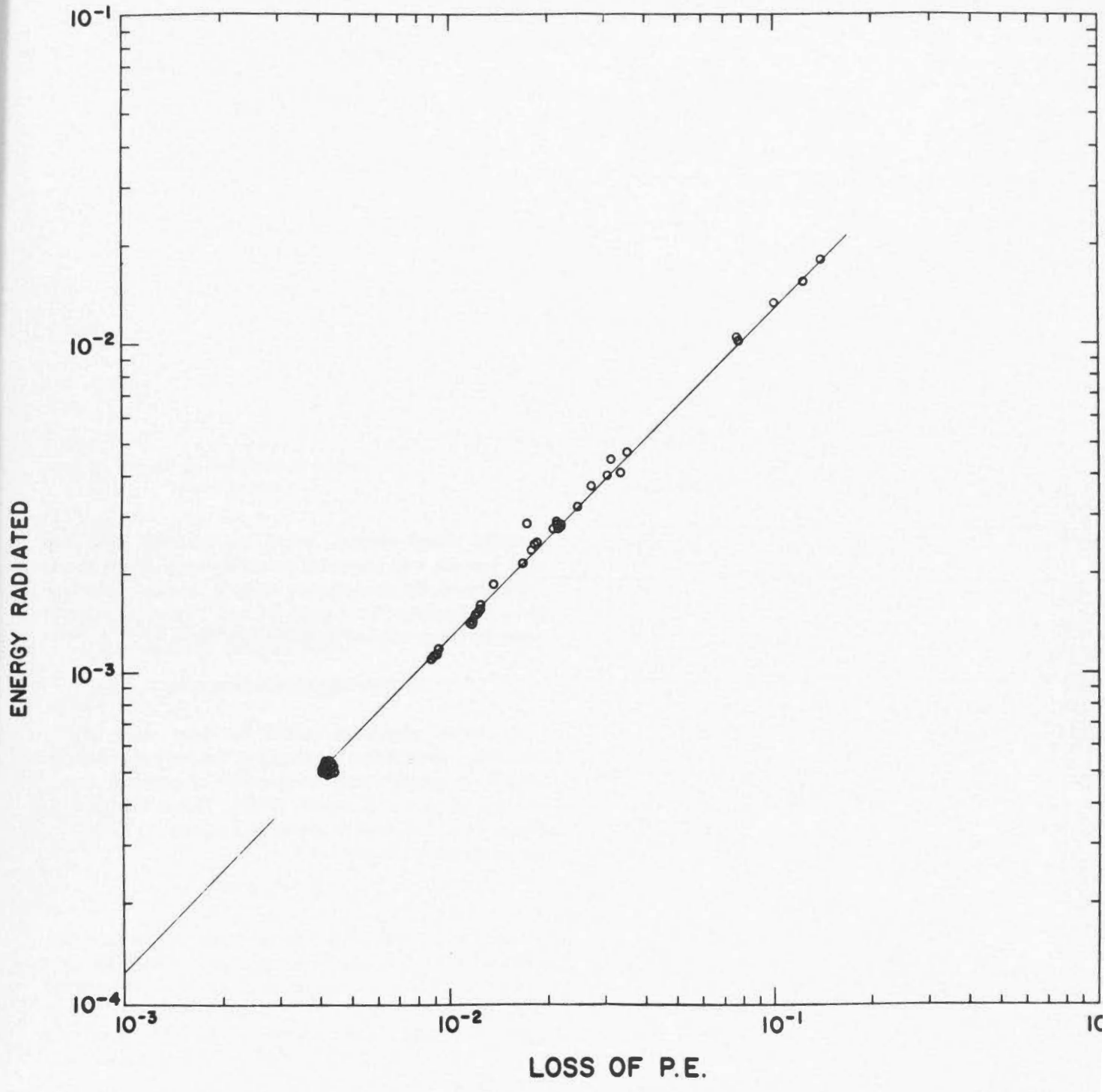

Figure 11. Peak kinetic energy and total kinetic energy as a function of potential energy release in shocks in the charging cycle.

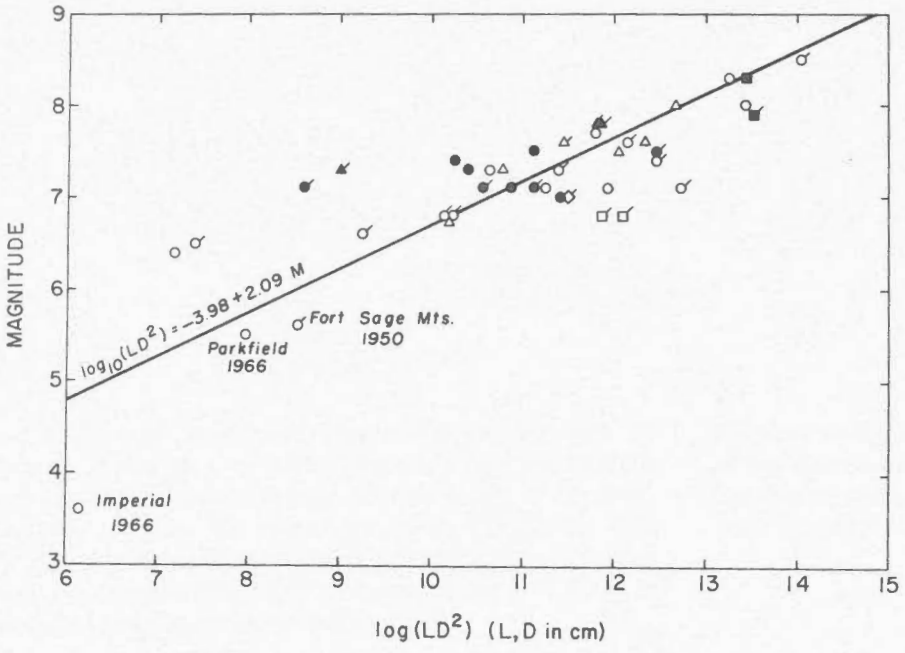

Figure 12. Magnitude vs. log LD^2 for large shallow shocks.

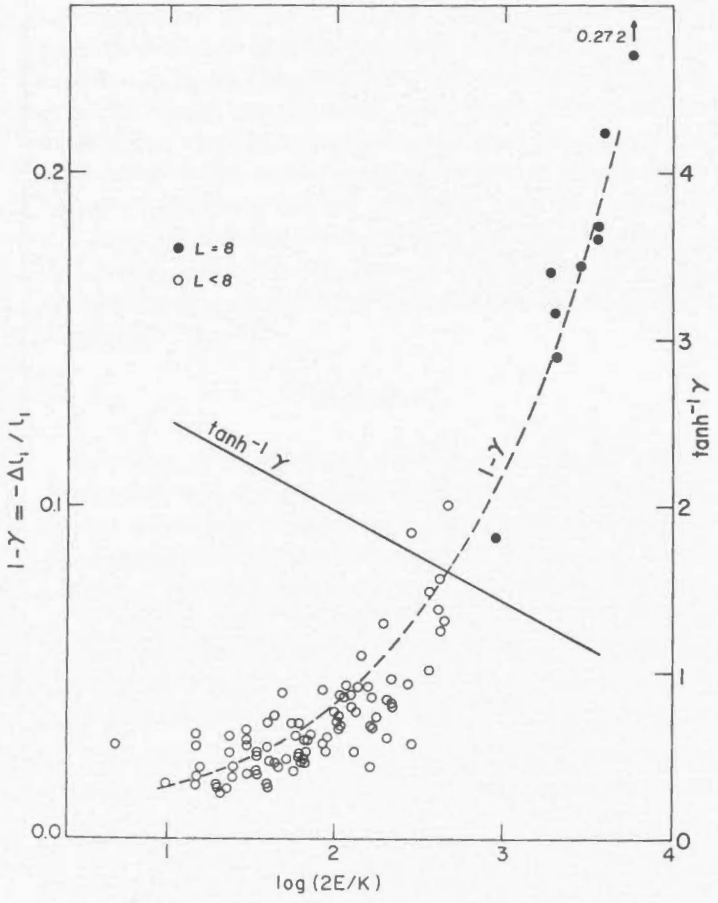

Figure 13. Fractional stress drop as a function of potential energy released on the laboratory model. The solid curve is the result of the computation $\tanh^{-1}\gamma$ on the smoothed (dashed) curve through the data points.

potential energy released. Indeed, the fractional stress drop does increase with increasing potential energy of the shock. Furthermore, the data strongly imply a formula of the type given in Equation (7): a graph of $\tanh^{-1}\gamma$ vs. logarithm of potential energy released is substantially linear.

Energy-Magnitude Formula

A further observation which has been made on the laboratory model is that the average of the pre- and post-shock stresses is approximately independent of potential energy released (King and Knopoff, 1968b). This is illustrated in Figure 14. If this result is applied to Equation (5), a relatively simple calculation shows that

$$\log LD = C_1 + \beta M \qquad (8)$$

with C_1 a constant. This may be tested by the same data obtained from observations of rupture parameters for large shocks and, indeed, a graph of log LD vs M is approximately linear once again (Figure 15). This leads to a value of β in the energy-magnitude relation of about 1.7 for large shocks (King and Knopoff, 1969).

Summary

We have introduced the postulate that friction along faults is the indirect generator of a significant amount of seismic statistical information. No assertion can be made that this model is unique. It is very likely that, in the future, other constructions will also generate a quantity of similar statistical information. However, our model is certainly a plausible one.

Having assumed that a suitably chosen model of friction is appropriate for the generation of statistical seismic focal

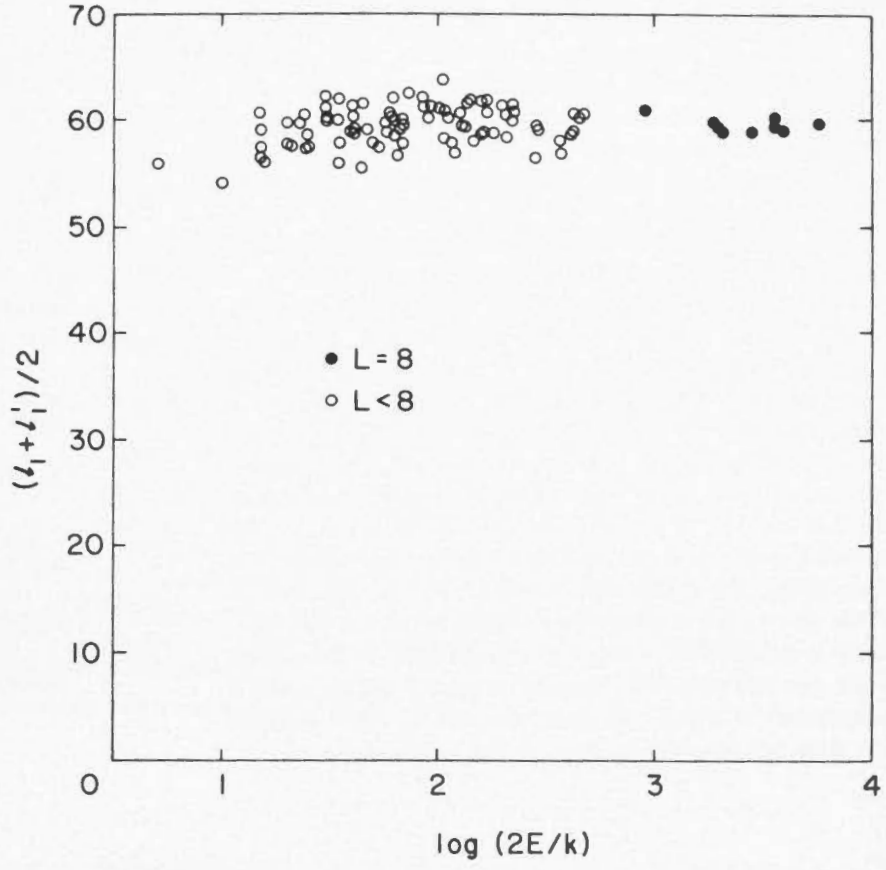

Figure 14. Average of pre- and post-shock stresses on the laboratory model.

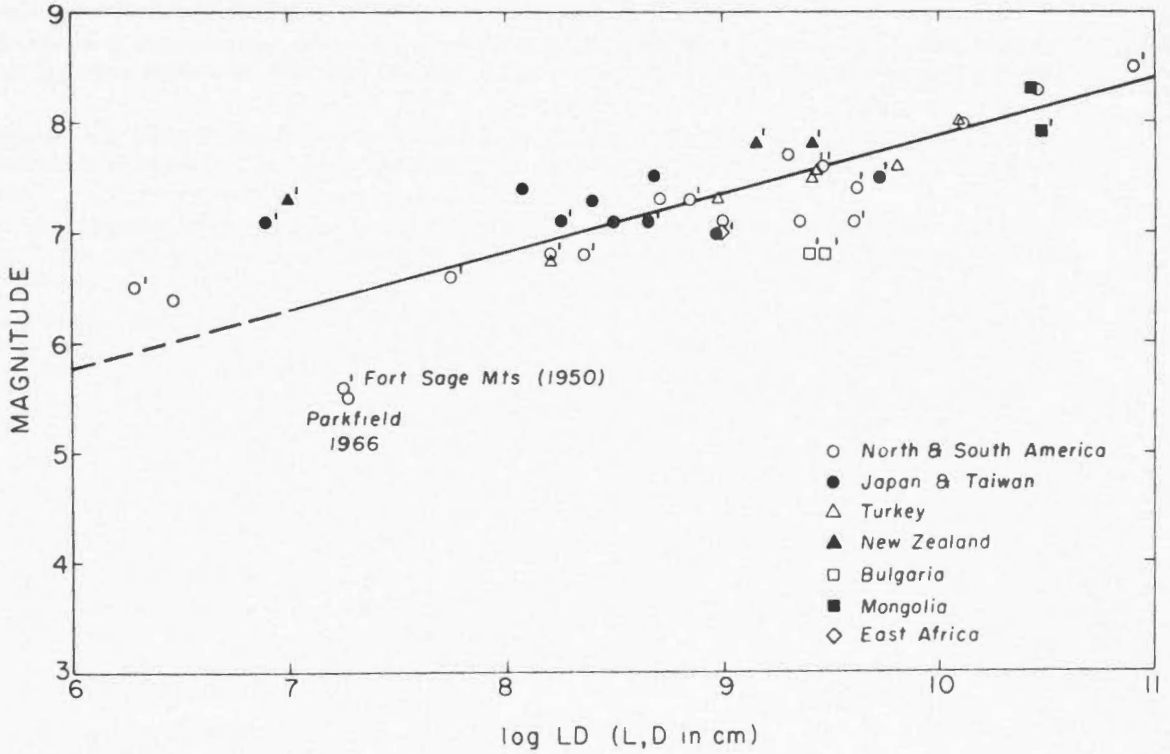

Figure 15. Magnitude vs. log *LD* for large shallow shocks.

phenomena, we have found that for our models (a) the energy-frequency relationship is similar in form to that observed for naturally occurring shocks, (b) the time sequences of shocks are causally connected, as they are in nature, (c) aftershocks can be produced which have time sequences similar to those observed in nature, (d) rupture phenomena are found to take place, with scaled rupture velocities comparable to those observed in nature (Burridge and Knopoff, 1967), and (e) the interrelations between shock magnitude and rupture parameters, such as the length of the fracture surface and the relative displacement of the two blocks, is remarkably similar to that observed in nature (King and Knopoff, 1968b). In addition, the application of several results obtained from the models leads to conclusions which seem reasonable: (a) that the fractional stress drop is a strong function of shock magnitude, especially for large shocks, and (b) that at least one coefficient in the energy-magnitude relationship for large shocks can be determined using these observations. These latter conclusions are a direct consequence of the observation that the seismic efficiency on the numerical model is independent of shock magnitude and that the average of the pre- and post-shock stresses on the laboratory model is independent of shock magnitude; we have no direct evidence that these two observations hold for real earthquakes.

References

Aki, K., 1956. Some problems in statistical seismology. *Zisin*, 8, 205-228.

Burridge, R., and L. Knopoff, 1966. The effect of initial stress or residue stress on elastic energy calculations. *Bull. Seism. Soc. Am.*, 56, 421-424.

Burridge, R., and L. Knopoff, 1967. Model and theoretical seismicity. *Bull. Seism. Soc. Am.*, 57, 341-371.

Ferraes, S.G., 1967. Test of Poisson process for earthquakes in Mexico City. *J. Geophys. Res.*, 72, 3741-3742.

Griggs, D.T., and D.W. Baker, 1968. Origin of deep-focus earthquakes. In: *Properties of Matter*, New York, John Wiley (in press).

King, C.-Y., and L. Knopoff, 1968a. Stress drop in earthquakes. *Bull. Seism. Soc. Am.*, 58, 249-257.

King, C.-Y., and L. Knopoff, 1968b). Model seismicity: rupture parameters, stress and energy relations. *J. Geophys. Res.*, 73, 1399-1406.

King, C.-Y., and L. Knopoff, 1969. A magnitude-energy relation for large earthquakes. *Bull. Seism. Soc. Am.*, 59, 269-273.

Knopoff, L., 1964. The statistics of earthquakes in southern California. *Bull. Seism. Soc. Am.*, 54, 1871-1873.

Raleigh, C.B., 1967. Tectonic implications of serpentinite weakening. *Geophys. J.*, 14, 113-118.

EARTHQUAKE MECHANISMS

D.T. Griggs

Institute of Geophysics and Planetary Physics
University of California
Los Angeles, California, U.S.A.

ABSTRACT: A family of earthquake mechanisms is proposed to account for those earthquakes which exhibit the symptoms of sudden shear stress drop associated with shearing displacement:

1. Fracture or stick-slip frictional sliding, in which the resistance to shearing displacement, after loss of cohesion, is dry friction. This mechanism is restricted to the upper few kilometres of the earth's crust.

2. Fracture or stick-slip frictional sliding in rocks with high pressure of connate water, in which the frictional resistance to shearing displacement is decreased by the high water pressure. This mechanism is probably restricted to the sedimentary rocks.

3. Fracture or stick-slip frictional sliding facilitated by high fluid pressure resulting from dehydration or dissociation. This mechanism can operate at any depth to which hydrous minerals can survive, perhaps 100 km.

4. Shear instability resulting from the self-heating of deformation and its localization due to the thermal activation of creep. This mechanism can operate at any depth where the appropriate magnitudes of shear stress, strain rate and activation energies occur. This is believed to be the primary mechanism of intermediate and deep-focus earthquakes.

The first two mechanisms have been investigated by many, notably W.F. Brace and collaborators. The third mechanism has been elucidated by the experiments of Heard, Raleigh and Paterson. The last mechanism is the subject of investigation in our laboratory and its experimental and theoretical basis will be shown.

The application of the second mechanism to the Denver earthquakes will be discussed.

RÉSUMÉ: La série suivante des mécanismes de tremblements de terre permet d'expliquer les séismes caractérisés par une baisse brusque de la contrainte de cisaillement provenant d'un déplacement de cisaillement:

1. La fracture ou le glissement avec friction tour à tour dans lequel la résistance au cisaillement, après la perte de cohésion, est la friction statique. Ce mécanisme ne s'applique, en profondeur, qu'aux premiers kilomètres de la croûte terrestre.

2. La fracture ou le glissement avec friction tour à tour dans des roches avec une forte pression d'eau innée qui entraîne la diminution de la résistance par friction au cisaillement. Ce mécanisme ne s'applique probablement qu'aux roches sédimentaires.

3. La fracture ou le glissement avec friction tour à tour facilité par une pression fluide élevée due à la déshydratation ou à la dissociation. Ce mécanisme peut agir en aussi grande profondeur que celle où peuvent subsister les minéraux aqueux, peut-être jusqu'à 100 km.

4. L'instabilité du cisaillement résultant de l'auto-réchauffement de la déformation et sa localisation due à l'activation thermique du fluage. Ce mécanisme peut agir aussi profondément que peut exister les magnitudes nécessaires de la contrainte de cisaillement, du taux de tension, et des énergies d'activation. Il s'agirait du mécanisme d'origine des séismes dont les foyers sont à profondeur intermédiaire ou profonde.

De nombreux chercheurs ont étudié les deux premiers mécanismes, notamment W.F. Brace et ses collaborateurs. Les expériences de Heard, Raleigh et Paterson ont permis d'expliquer le troisième de ces mécanismes. Quant au dernier, c'est un sujet à l'étude dans notre laboratoire; ses données de base expérimentales et théoriques sont exposées ici.

Cet exposé se termine par une étude de l'application du deuxième mécanisme aux séismes de Denver.